Green hydrogen production from offshore wind power

A reliability-centric approach to an integrated techno-economic system performance evaluation

Bart van 't Geloof

Delft University of Technology

TU Delft

Green hydrogen production from offshore wind power

A reliability-centric approach to an integrated techno-economic system performance evaluation

by

Bart van 't Geloof

Thesis committee:	Prof. dr. ir. E.L.V. Goetheer	TU Delft	Supervisor, Chair
	Ir. O. Manmohan Sane	Shell	Supervisor
	Prof. dr. ir. W. de Jong	TU Delft	Committee member
	Dr. ir. M. Ramdin	TU Delft	Committee member

Project duration:	March, 2023 - January, 2024
Study:	Master, Sustainable Energy Technology
Faculty:	Faculty of Electrical Engineering, Mathematics and Computer Science
University:	Delft University of Technology, The Netherlands

TU Delft

Acknowledgements

The master thesis presented here evaluates systems enabling offshore hydrogen production. This technology is pivotal in the energy transition and the future of green energy. In this thesis, I aim to assess these systems, ranging from a single system to multiple systems, including a frequently overlooked aspect in the literature: the reliability of these systems. Through this thesis, I endeavour to offer the reader insightful perspectives gained during the nine months of research.

I would not have reached this point without guidance throughout this project. First, I extend my gratitude to Earl Goetheer, who, as the supervisor and chair of the committee, provided excellent guidance. Your enthusiasm, energy and interest made the entire project immensely enjoyable, for which I am deeply thankful. Omkar Manmohan Sane, as the Shell supervisor, ensured smooth progress of the project. Your guidance struck the perfect balance between assistance and allowing me to learn lessons independently, giving me the sense of having learned more than just about this subject. Additionally, I would like to thank Frank Geuzebroek for his mentorship at Shell and the engaging discussions, the entire Shell Green Hydrogen team, and the countless others from both Shell and TU Delft who contributed to this final product. I also extend my regard to my friends and family for their support, which has been a source of motivation and reflection throughout this journey. Lastly, I extend my sincere appreciation to Wiebren de Jong and Mahinder Ramdin for their participation on the committee and for lending their expertise in the evaluation of this thesis.

With these concluding words, my time at TU Delft draws to a close. During this period, I have experienced and learnt a great deal, and I look back on this chapter with great fondness. Writing this thesis has been a rewarding experience, and I hope that you, as a reader of it, finds equal enrichment.

Bart van 't Geloof
January 2024

Abstract

The escalating climate crisis underscores the urgency for an energy transition, necessitating a shift from traditional fossil fuel-based systems to sustainable solutions. This transition is pivotal not just in the realm of electrons, which power our electricity grids, but also in the world of molecular energy carriers, essential for a range of industrial applications. In this evolving energy landscape, hydrogen stands out for its potential to bridge these domains. As a versatile and clean energy carrier, hydrogen can play a significant role in decarbonizing sectors where direct electrification is challenging. Integrating renewable energy sources, specifically offshore wind, with hydrogen production leads us to the innovative concept of wind-to-hydrogen (W2H) systems. By harnessing the power of offshore wind to produce green hydrogen through electrolysis, W2H systems offer a promising approach to not only overcome the intermittency of wind energy but also to leverage its full potential in creating a sustainable and resilient energy infrastructure. These systems are increasingly at the forefront of renewable energy innovation and are witnessing substantial investment and interest from the public, private, and academic sectors. Despite the momentum and significant resources being channelled into their development and implementation, there are still critical aspects of their real-world performance and efficiency that remain uncharted, highlighting the need for ongoing, comprehensive research and exploration.

The objective of this study is to generate insights into the application of the reliability of a W2H system and its impact on the techno-economic performance. This involves examining the case of a single system to analyse on a micro-level the underlying conditions affecting performance, as well as exploring W2H farms to observe performance and the effects of changing conditions on a macro-level. To this end, MATLAB models have been utilised and developed to simulate various components of a system, such as wind turbines and electrolysers, focusing on aspects like hydrogen production and the number of breakdowns per year. The model creates insights into technical and economic parameters.

When modelling the performance of a single W2H system, it yields a hydrogen production of 847 t H_2 per year and a LCOH of €7.72/kg H_2. However, when Reliability, Availability, Maintainability (RAM) modelling is applied, an availability of 88.1% is achieved, resulting in a hydrogen yield that is 11.9% lower than the calculation assuming 100% availability. Consequently, the Levelised Cost of Hydrogen (LCOH) increases by 13.5% to €8.76/kg H_2. The inclusion of RAM modelling thus has a significant effect on the techno-economic performance. Nevertheless, the numerical result is heavily dependent on both operational and RAM variables, which under favourable conditions could be around €6/kg H_2. For W2H farms, it becomes clear that the conventional LCOH calculation is not suitable as it does not account for maintenance requirements. An alternative calculation results in a minimum LCOH of €8.35 for an offshore setting and €6.76 as an indicative figure for an onshore variant. The answer to the question of what the effects are when RAM is included resulting from this thesis is not so much numerical, given the situational nature of the results, but rather qualitative in that awareness of these effects and integrating them into case studies, likely increases the accuracy of LCOH estimations for green hydrogen production from W2H systems.

Contents

List of Figures

List of Tables

Nomenclature

Abbreviations

Abbreviation	Definition
A	Availability
AC	Alternating Current
AEL	Alkaline Electrolyser
AEM	Anion Exchange Membrane
ASE	Availability Standard Error
B2B	Back-to-Back
BOP	Balance of Plant
BP	Bipolar Plate
CAPEX	Capital Expenditures
CCS	Carbon Capture and Storage
DC	Direct Current
DECEX	Decommissioning Expenditures
EDI	Electrodeionisation
FLH	Full load hours
FMEA	Failure Mode and Effects Analysis
FR	Failure Rate
HVAC	High Voltage Alternating Current
HVDC	High Voltage Direct Current
HHV	Higher Heating Value
LCOE	Levelised Cost of Electricity
LCOH	Levelised Cost of Hydrogen
LHV	Lower Heating Value
MEA	Membrane Electrode Assembly
MTBF	Mean Time Between Failures
MTTF	Mean Time To Failure
MTTD	Mean Time To Diagnose
MTTR	Mean Time To Repair
MRL	Market Readiness Level
O&M	Operations and Maintenance
OPEX	Operational Expenditures
OREDA	Offshore and Onshore Reliability Data
P-F	Potential-Failure to Functional-Failure
PEM	Proton Exchange Membrane
PS	Planned Shutdown
R	Reliability
RAM	Reliability, Availability, and Maintainability
RBD	Reliability Block Diagram
RO	Reverse Osmosis
RR	Repair Rate
RSE	Reliability Standard Error
SMR	Steam Methane Reforming
SOEC	Solid Oxide Electrolysis Cell
SOV	Service Operation Vessel
TDS	Total Dissolved Solids
TRL	Technology Readiness Level

Abbreviation	Definition
UA	Unavailability
UR	Unreliability
W2H	Wind-to-Hydrogen
W2W	Walk-to-Work
WACC	Weighted Average Cost of Capital

Symbols

Symbol	Definition	Unit
A	Area	[m^2]
D	Diameter	[m]
E	Energy	[J]
F	Force	[N]
g	Gravitational constant	[m/s^2]
h	Height	[m]
I	Current	[A]
J	Current density	[A/cm^2]
L	Length	[m]
m	Mass	[kg]
P	Power	[W]
p	Pressure	[bar]
Q	Flow rate	[m^3/s]
R	Resistance	[Ω]
T	Temperature	[$^\circ$C]
t	Time	[s]
U	Voltage	[V]
V	Volume	[m^3]
v	Velocity	[m/s]
ζ	Conversion rate	[-]
η	Efficiency	[%]
ρ	Density	[kg/m^3]
σ	Conductivity	[S]
τ	Torque	[Nm]

1

Introduction

This chapter establishes the foundation of this thesis on the evaluation of offshore Wind-to-hydrogen (W2H) systems. In Section 1.1, the background information is elucidated. Section 1.2 describes the main research question and subdivides it into several sub-research questions. Additionally, the scope is delineated in this section. In Section 1.3, the methodology is detailed, and finally, Section 1.4 outlines the report.

1.1. Background information

Why W2H systems, or renewable energy systems in general, are necessary for our planet's future is a well-known question with a multifaceted answer. In the following paragraph, this question is answered, including a motivation as to why specifically W2H systems represent an intriguing opportunity in the search of the solution.

The necessity for an energy transition

The global crisis surrounding climate change is escalating. The need for a transition in our energy production and consumption is becoming increasingly urgent. Within the scientific community, it is generally accepted that human activities, primarily through the burning of fossil fuels, are accelerating climate change. This consensus is supported by the extensive reports from the Intergovernmental Panel on Climate Change (IPCC), which show that human-induced activities have been the dominant cause of the observed rise in global temperatures since the mid-20th century (IPCC, 2022).

To mitigate the effects of global warming or prevent more severe consequences, international agreements are being made. For example, in Paris in 2015, a framework for international cooperation was signed in which the 196 signatory countries aim to cap global warming at a level below 2°C above pre-industrial averages by 2050 (UN, 2015). This is not a symbolic goal; exceeding the two degrees is very likely to trigger disastrous environmental impacts, including intensified weather extremes, rising sea levels, and a dramatic loss of biodiversity (Rogelj et al., 2016).

Central to climate change is the role of carbon emissions, with the burning of fossil fuels being the primary contributor to these emissions, accounting for approximately 85% of all anthropogenic CO_2 emissions (IEA, 2022a). This scientific consensus has been emphasised by the latest commitments made during COP28 in Dubai, where it was acknowledged for the first time that phasing out fossil fuels towards a net-zero target by 2050 is essential (Erbach & Roniger, 2023).

Given our dependency on energy, a transition to sustainable forms is needed. Technologies like solar, wind, and hydroelectric power offer viable pathways to decarbonise the energy sector and are essential for meeting the objectives outlined in the Paris Agreement.

To effectively address this challenge, it is crucial to understand the types of energy that society relies upon; electrons and molecules.

The forms of energy

The energy landscape is divided into two categories: electrons and molecules. Electrons serve as the drivers for the generation and distribution of electricity. They can be generated through renewable sources such as solar and wind power, but also though nuclear power and combustion of fossil fuels such as coal and gas. The versatility of electrical energy is proven by its wide range of applications, from keeping the lights on in skyscrapers to powering electric vehicles. Conversely, molecules such as oil and gas function as carriers of chemical energy. These are primarily used in situations where the required energy is more specific in the form of e.g., energy density or chemical properties. They are mostly used in aviation, heavy industry and chemical manufacturing.

In pursuing decarbonisation, there has been significant advancement in generating green electricity. The mass production of solar panels and wind turbines, among other renewable sources, has contributed to their comprising approximately 28% of total power generation in 2021, aiming to reach 40% by 2027 (IEA, 2022c). In stark contrast, the molecular sector poses a more complex set of challenges. A negligible percentage of molecules is currently produced from renewable sources. As reported by the IEA, less than 1% of global hydrogen production is derived from renewable energy while a fraction of molecular energy requirements is fulfilled through hydrogen. This underscores the need to focus on the development and adoption of sustainable molecular energy carriers.

Hydrogen is an important part to the solution of this problem, with its high energy density and chemical versatility, offers a promising route to decarbonise hard-to-electrify sectors. However, it can serve multiple roles, from energy storage to overcome renewable energy source intermittence to electricity generation for transportation and grid regulation. Additionally, hydrogen can be converted into derivatives like ammonia and methanol with specific chemical properties for certain sectors, expanding its utility in agriculture and industry (IRENA, 2023). Throughout this entire research, when hydrogen is mentioned, it refers to the hydrogen molecule H_2 in its gaseous form , unless otherwise indicated.

There are many different ways to produce hydrogen (Wang et al., 2017). It is done via the use of fossil fuels, like Steam Methane Reforming (SMR) or coal gasification. But also by using renewable power to split water and even through the several biological processes. However, for now the two most prominent methods will be discussed.

Steam Methane Reforming (SMR) is the most used method for hydrogen production due to its economic viability and established industrial scale. The process involves the heating of methane with steam, usually with a catalyst involved. This reaction, referred to as the reforming reaction (1.1), in combination with the Water Gas Shift reaction (1.2), will produce hydrogen and carbon dioxide, as represented by the overall reaction (1.3).

$$\mathrm{CH_4}(g) + \mathrm{H_2}(g)\mathrm{O} \rightarrow \mathrm{CO}(g) + 3\mathrm{H_2}(g) \tag{1.1}$$

$$\mathrm{CO}(g) + \mathrm{H_2O}(g) \rightarrow \mathrm{CO_2}(g) + \mathrm{H_2}(g) \tag{1.2}$$

$$\mathrm{CH_4}(g) + 2\mathrm{H_2O}(g) \rightarrow \mathrm{CO_2}(g) + 4\mathrm{H_2}(g) \tag{1.3}$$

Thus, this form of hydrogen production generates carbon dioxide, meaning the hydrogen is not free of emissions. However, this grey hydrogen can be called blue hydrogen if Carbon Capture and Storage (CCS) is employed. CCS has the potential to capture between 71% to 92% of carbon dioxide emissions in SMR-based hydrogen production (van Cappellen et al., 2018), though it is constrained by the long-term availability of suitable storage sites such as depleted gas fields. Given these limitations, it becomes clear that pursuing alternative methods for producing hydrogen without carbon emissions is necessary. Currently, electrolysis appears to be the most promising technology for achieving this.

Electrolysis is the dissociation of water into hydrogen and oxygen (reaction 1.4), facilitated by an electric current supplied to a specialised device known as an electrolyser.

$$2\mathrm{H_2O}(l) \rightarrow 2\mathrm{H_2}(g) + \mathrm{O_2}(g) \tag{1.4}$$

Among the various electrolysis systems, Alkaline Electrolysers (AEL), Proton Exchange Membrane (PEM) Electrolysers, and Solid Oxide Electrolysis Cells (SOEC) are currently the most established or hold significant promise (Hu et al., 2022). Alkaline electrolysis, a well-established technology, employs an alkaline solution as the electrolyte but is characterised by its low operational efficiency and limited flexibility, yet it remains cost-effective and robust. In contrast, PEM electrolysis utilises a solid polymer electrolyte to conduct hydrogen protons and is distinguished by its compact design, high efficiency, and operational flexibility. However, the use of expensive noble metal catalysts renders it a costly option. SOEC technology operates at elevated temperatures, offering exceptional efficiency and flexibility, but its energy-intensive start-up requirements and complex infrastructure render it less favourable as technology. Currently, Alkaline and PEM technologies are implemented on a commercial scale, while large-scale experiments with SOEC are also underway. In addition, emerging technologies such as Anion Exchange Membrane and Direct Methanol Electrolysis show promise (Kumar & Lim, 2022), although they have not reached commercial viability yet. Therefore, they are not included in the immediate options for short-term hydrogen production solutions.

For the hydrogen to be genuinely called ‘green’ the power used in the electrolysis process must be sourced from non-carbon emitting energy sources. This integration of renewable energy sourcing and hydrogen production is part of an interesting research area, with many possibilities being considered.

Utilising wind energy for hydrogen production

Offshore wind energy has become a cornerstone of the European renewable energy strategy, boasting an installed capacity of 4.5 GW in The Netherlands alone by 2023 (Rijksoverheid, 2022). The European Commission’s ambitious targets aim for a surge in this capacity to 60 GW by 2030, escalating to 300 GW by 2050 (European Union, 2020). However, the expansion of offshore wind power is not without its challenges. The intermittency and seasonality of wind power necessitate reliable backup power and long-term energy storage solutions. Moreover, the increasing number of turbines compounds the complexity of integrating them into national power grids, which are already nearing capacity. This situation demands strategies to alleviate grid congestion and prevent power curtailment. For instance, forecasts for The Netherlands indicate a potential 13% power curtailment by 2030 due to grid congestion, barring significant steps towards electrification (TNO, 2022).

In this context, it is crucial to emphasise that the primary application of hydrogen in the upcoming future lies in its industrial use. The process of converting power to hydrogen and then back to power incurs substantial conversion losses, making it less efficient for direct energy supply purposes. Therefore, the focus is shifting towards utilising hydrogen primarily in industrial applications, where its role as a clean energy carrier and a raw material is indispensable. This approach not only maximises the efficiency of hydrogen usage but also aligns with the broader goal of decarbonizing industrial processes, thereby contributing significantly to the overall sustainability agenda. Nevertheless, offshore wind energy is a great source of energy for the production of green hydrogen. On further examination, several aspects create evident possibilities when producing green hydrogen from wind power offshore in The North Sea:

1. Hydrogen pipelines have been shown to possibly be economically superior to electricity cables, due to the advantage of reduced energy losses, this will be scrutinised in a later chapter (European Commission, 2020; North Sea Wind Power Hub, 2022). Moreover, on-site hydrogen conversion can further streamline the process by minimising the number of power conversions required (Taieb & Shaaban, 2019), thereby improving system efficiency again.
2. The geographical features of the European North Sea present opportunities for hydrogen storage. The region is abundant in salt caverns (Smith et al., 2005), which are ideal for large-scale and cost-effective hydrogen storage. Given that these caverns are predominantly offshore, on-site hydrogen production would significantly reduce the distance between production and storage facilities. This proximity offers the added benefit of repurposing existing gas networks (Tsiklios et al., 2022) for hydrogen transportation, thereby contributing to a circular economy. Furthermore, the North Sea is not a very deep sea, making it easier to built constructions compared to places which are deeper.
3. The scalability of offshore electrolysis surpasses that of its onshore counterparts. Unlike on land,

where space is often limited by residential and environmental constraints, the open sea provides ample room for expansion (European Commission, 2020). This makes offshore electrolysis a more viable solution for meeting the increasing demand for green hydrogen.

Collectively, these prospects between offshore wind energy and hydrogen production and storage offer an increased possibility to be a part of a sustainable energy future. While these prospects appear promising, it is important to conduct additional research into such integrated systems. Specifically, an analysis of the current state-of-the-art in W2H systems and the exploration of methods to expand knowledge about these systems, thereby facilitating their implementation.

1.2. Research question and scope

To clarify the viability of W2H systems, the overarching research question of this study is: *"What is the influence of including system reliability on a single offshore wind-to-hydrogen system's technical and economic performance, what effect do operational and maintenance strategies have on these results, and what is the effect when considering multiple systems?"*

To answer this question, the following sub-research questions are formulated:

1. What is the change in the systems' technical and economic performance if the reliability of the system has been simulated and integrated?
2. How do these parameters change if several operational and maintenance strategy variables are changed?
3. What are the changes when assessing a wind farm as an aggregate of multiple systems and how does this influence the technical and economic performance?

In delineating the research scope, this study is partly restricted to evaluating a single type of integrated wind-hydrogen system. This system can be adapted to include multiple identical but probabilistically variable units. Financial evaluation will be based on the full life cycle costs, specifically focusing on the Levelised Cost of Hydrogen (LCOH).

The study seeks to employ high-resolution data for variables such as component weight, performance, and costs. However, if such data are unavailable, lower resolution evaluations will be used. Constraints in computing power and their impact on simulation scope will be accounted for. Notably, the scope will not extend to different system types or external variables like policy and market conditions, but these could be accounted for in a specific case study.

1.3. Methodology

The research process begins with an exhaustive literature review to investigate offshore hydrogen production, maintenance strategies, and related fields. This foundational step aims not only to absorb the current state of knowledge but also to identify research gaps where this study can make a meaningful contribution.

Following the literature review, the focus shifts to data collection. Here, a specific system design for offshore hydrogen production is constructed through a rigorous comparative analysis of available technologies. This covers energy generation, hydrogen conversion systems, and other utilities. All relevant datasets, including efficiencies, reliability metrics, and financial parameters, are collated and organised into datasheets using Excel.

Upon the completion of data collection, the modelling stage commences. Three separate but interrelated models are developed. Firstly, the energy model is utilised in collaboration with Shell's Green Hydrogen team using MATLAB. This model, based on both academic and industry parameters, simulates the hourly hydrogen yield from a wind power dataset, the model will be updated to current and future standards and new features will be implemented to enhance its realism. Secondly, a Reliability, Availability, and Maintainability (RAM) model is created to simulate the system's overall reliability. Furthermore, a financial model is devised to calculate the LCOH, integrating data and outcomes from both the energy and reliability models. Lastly, once the models surrounding the single W2H system are addressed, the focus shifts to W2H farms, where multiple identical systems are modelled.

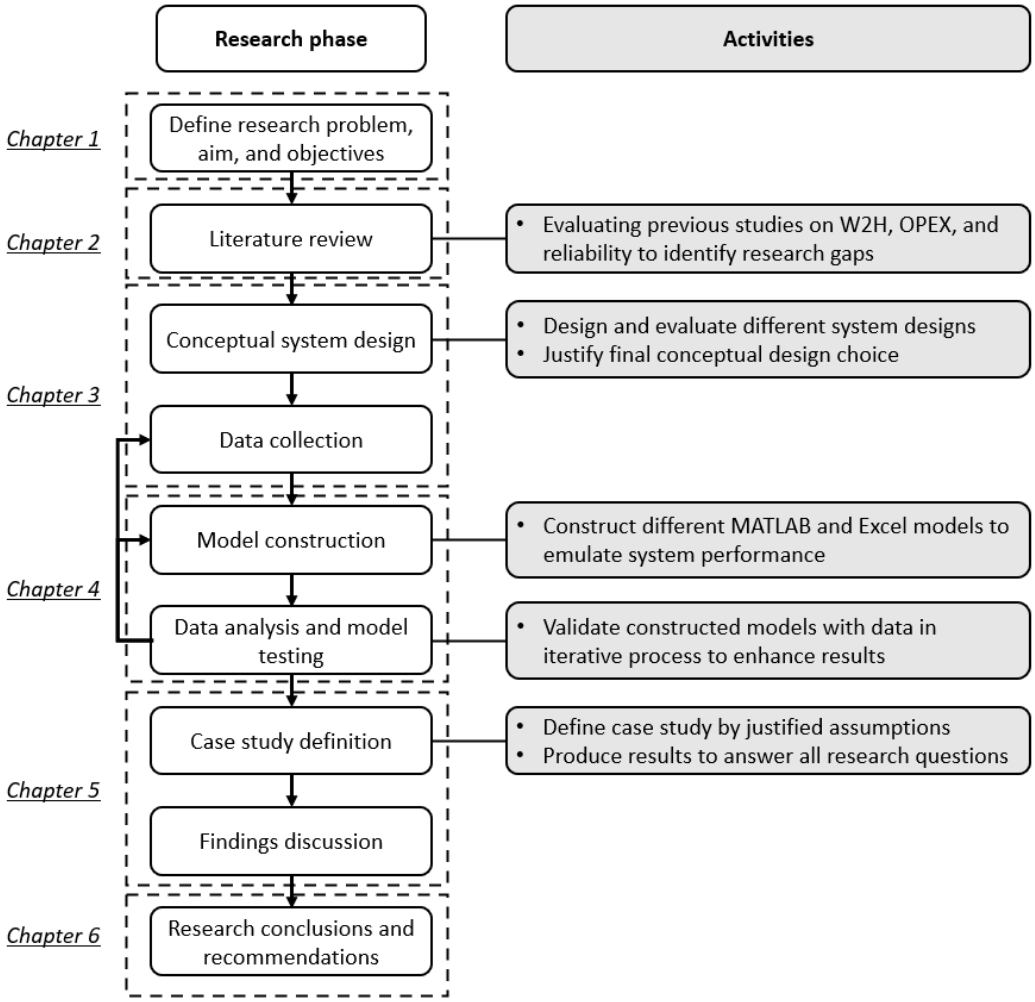

Figure 1.1: Research flow diagram describing methodology and report outline

Subsequently, the models are applied to a case study under certain assumptions that reflect a potential reality, generating results for both single and multiple systems. With these results, answers to the various sub-research questions will be provided, thereby addressing the overarching research question. These answers will be available in the conclusion. Finally, a list of recommendations will be presented, outlining and explaining advice for further research.

A schematic representation of the methodology can be found in the research flow diagram in Figure 1.1.

1.4. Report outline

The report is structured to systematically outline the stages of the research. Chapter 2 commences with a literature review, delving into the integration of the system and its individual components. This sets the foundational understanding for the research's focus. Chapter 3 then details the system components, elucidating their functional principles and the specific choices made for the system employed in this project. Chapter 4 progresses to discuss the various models and simulation methods used. It provides insights into their architectural design and how the system components are integrated within these models. In Chapter 5, the case study assumptions are presented with the corresponding results, assessing variability studies and both single and multiple system models. The report culminates in Chapter 6 with a section on Conclusion and Recommendation. This chapter synthesises the key findings and articulates recommendations derived from the study for further action or research.

2

Literature review

This chapter presents a review of the available literature on offshore wind-to-hydrogen (W2H) systems, with a specific focus on operational expenditures (OPEX) and reliability. Additionally, an overview of current and announced offshore W2H projects will be discussed.

2.1. Integration of offshore wind power generation and hydrogen production

The integration of offshore wind and hydrogen production has been a subject of academic research for years, aiming to facilitate the energy transition. Harrison et al. (2009), penned a comprehensive report on a Wind-To-Hydrogen project in the United States titled Wind2H2. This demonstration project was commissioned by the US government in collaboration with Xcel Energy. The objective of this research was to pinpoint the challenges associated with this configuration and to provide estimates of the expected Levelised Cost of Hydrogen (LCOH). Although in its preliminary stages, a LCOH of $6.25/kg appears promising. Furthermore, the criticality of the system integration on the project developers side is emphasised in this report. This is because components from different manufacturers might not necessarily be compatible. A significant takeaway that is directly applicable to the current research is that an analysis indicates a potential 7% cost reduction in hydrogen production if the wind turbine inverters are replaced with DC/DC converters that connect directly to the electrolyzer stacks.

Furthermore, subsequent studies, notably those by Groenemans et al. (2022) and Ibrahim et al. (2022), suggest that literature sees the advantages of offshore electrolysis. Particularly, this advantage is seen in a decentralised setup, meaning a standalone wind turbine and hydrogen production unit, as opposed to sharing a hydrogen production platform with multiple wind turbines. Groenemans et al.'s study revolved around hydrogen production which was deemed more economical offshore due to the offsetting of electricity losses. Ibrahim et al. explored a similar scenario but with floating wind turbines. His study corroborates the hypothesis about the decentralised setup, provided the wind farm is sufficiently large and located far out at sea. Furthermore, it is indicated that the Proton Exchange Membrane (PEM) electrolyser is likely to be superior in this decentralised arrangement due to its flexibility and footprint—characteristics which will be further elaborated upon in Chapter 3.

A considerable volume of research has delved into determining the ideal electrolyser type. Some findings highlight that PEM technology stands out as one of the front-runners in water electrolysis technologies (Serna et al., 2017), especially when directly coupled with renewable electric sources. In addition to this, the study presented an innovative control system, together with guidelines for effectively sizing electrolysers and the associated systems. In addition, Meier (2014) analysis contrasted PEM and solid oxide (SOEC) electrolyzers. One salient point that was made was that due to the reduced power consumption of auxiliary systems in PEM electrolysers, there's an enhanced hydrogen yield in all studied scenarios. Drawing from these systematic technical evaluations, it becomes evident that embedding the PEM cell within the wind turbine structure, and promoting independent offshore hydrogen production, holds a promising route for hydrogen generation via offshore wind power. Meier

(2014) further probed transmission methodologies, concluding their feasibility hinges predominantly on the proximity to the coast.

On the topic of the proportional capacity of the electrolyser versus the wind turbine, it is concluded by Mehta et al. (2022) that the typical design approach for turbines for such applications, characterised by augmented specific power, yields only a marginal influence on the LCOH. Additionally, it's concluded that oversizing the electrolyser bears possible advantages.

Integrating systems of this nature introduces a lot of challenges. Blasi et al. (2013) asserts that a strict selection of materials and components is paramount to counteract degradation stemming from exposure to an oxidising marine environment. However, implementing suitable protective casing for the electrochemical device could diminish these adverse effects. Furthermore, the study suggests that the PEM electrolyser reacts favourably to treated seawater, which paves the way for the deployment of PEM electrolysers in marine settings.

Furthermore, placing the electrolyser either within or onto a platform attached to the wind turbine is a point of contention. Gondal (2019) highlights that one of the primary challenges in offshore electrolysis pertains to the spatial demands of the hydrogen production unit. Contrasting this perspective, TNO (2022) offers a more optimistic outlook. They comment on the constraints posed by the dimensions of the current available electrolysers. Despite these spatial challenges, solutions seem plausible. The report posits that such spatial constraints can indeed be overcome with structural developments. Insights from professionals within the electrolyser manufacturing domain suggest that viable space can be identified not only within the turbine but also encompassing it. Field tests conducted off the coast of Nigeria have illuminated methods to accommodate power-to-gas installations around such a framework. It's important to acknowledge that PEM electrolysers might present specific advantages in this scenario, beyond the already acknowledged flexibility. The unique organisation of PEM electrolysers into discrete stacks allows for their distribution throughout the nacelle, the main turbine tower, and its surrounding gallery (Jepma et al., 2018).

Several synergistic relationships emerge when exploring the integration of offshore industries. A research conducted by Kumar et al. (2022) delves into the production of offshore green hydrogen in conjunction with aquaculture, shipping and port, and oil and gas sectors. The findings suggest that green hydrogen holds significant potential for the marine industry, given an anticipated long-term demand. Noteworthy synergies are identified in areas such as electrolysis-based hydrogen production, which potentially mitigates environmental concerns during decommissioning while prolonging the operational lifespan of offshore oil and gas platforms. Additionally, the upcycling of turbines and pipelines is highlighted, bolstering profitability and aiding in emission reduction.

2.2. Levelised Cost of Hydrogen

The Levelised Cost of Electricity (LCOE) and LCOH serve as key metrics for assessing the financial viability of energy projects by calculating the unit cost over the project's lifetime (Sens et al., 2022). These metrics incorporate Capital Expenditures (CAPEX), Operational Expenditures (OPEX), and Decommissioning Expenditures (DECEX) (Bernuy-Lopez, 2023; Ioannou et al., 2018).

The general formula, which can be applied to both LCOE and LCOH, is given by:

$$\text{LCOX} = \frac{\sum_{t=1}^{T} \frac{C_t^{\text{CAPEX}} + C_t^{\text{OPEX}} + C_t^{\text{DECEX}}}{(1+r)^t}}{\sum_{t=1}^{T} \frac{E_t}{(1+r)^t}} \tag{2.1}$$

In this equation, $C_t^{\text{CAPEX}}, C_t^{\text{OPEX}}, C_t^{\text{DECEX}}$ denote the annual capital, operational, and decommissioning costs, respectively. E_t represents the annual electricity or hydrogen production, r is the discount rate, and T is the total number of operational years for the project.

Numerous techno-economic analyses have been conducted on the LCOH associated with integrating offshore wind energy with hydrogen production. The derived values from these studies are listed in Appendix A, showcasing a non-exhaustive compilation of these results. The analyses align to varying degrees with the research of this thesis, as indicated by a check mark for confirmation, showing

the extent to which each study relates to this one. These analyses consistently exhibit one or multiple similarities to this thesis, particularly concerning key aspects of offshore wind turbines and a PEM electrolyser. However, variations exist in the scale of the installations and the inclusion of additional utilities across different studies. The LCOH values range from as low as €2.09/kg H_2 (Groenemans et al., 2022) to as high as €13.81/kg H_2 (Shin et al., 2023), highlighting the significant impact of various factors on the LCOH. Notably, the two studies that align on all four criteria, specifically those of (Groenemans et al., 2022) and (Egeland-Eriksen et al., 2023), report lower LCOH values, namely €2.09/kg H_2 and between €4.53 to €5.18/kg H_2 respectively. Upon further analysis, Groenemans et al. appears to economically assume very inexpensive components and low OPEX costs. Egeland-Eriksen et al. seems to base their assumptions on less optimistic scenarios, yet neither study appears to utilise the reliability or specific costs of maintenance in their evaluations. Aside from these specific offshore green hydrogen papers, a recent paper authored by Burchardt et al. (2023) discusses how various industrial sectors, primarily current grey hydrogen users, are willing to pay around or just above €6/kg H_2 by 2030. To make this a reality, significant investment in reducing hydrogen costs is necessary, through technological advancements and potentially subsidies. However, the publication rightly analyses that the costs of green hydrogen projects are currently higher than previously estimated and hoped for, consensus is that the prices in 2030 vary between €5/kg H_2 and €8/kg H_2 instead of the below €3/kg H_2, as was the hypothesis in just 2021. This increase is due to factors such as higher capital costs, supply chain constraints, system complexity, and a lack of infrastructure to connect producers with the industry. The paper advises the European Commission to implement laws and regulations to stimulate the green hydrogen market.

The LCOH serves as a critical metric for assessing the business case and, consequently, the feasibility of a project. It can be divided as CAPEX, OPEX and DECEX. CAPEX, which is relatively straightforward, includes costs associated with the project's initiation, procurement, and installation of the system, focusing mainly on purchasing and installation expenses. DECEX is also transparent, involving costs related to dismantling and recycling. In light of this, a more detailed examination of the OPEX is warranted to understand better the various elements contributing to these costs.

2.2.1. Operational expenditures

The operational expenditures refer to the ongoing costs for running a product, business, or system. In contrast to the CAPEX, which are one-time expenses for acquiring assets such as property, plant, or equipment, operational expenditures are recurring and are necessary for the daily maintenance and administration of a business (Sawyer, 2009). In the following sections, the literature on the OPEX terminology and its application to technical elements of the W2H systems is discussed.

Terminology

The precise categorisation of OPEX is often debated, although it is not the content of the categories that is disputed, but rather how they are organised. In this literature review, three categories are adopted: Operation, Maintenance & Repair, and Other Costs. The first two categories encompass the costs associated with operating a system and maintaining or restoring it to a functional state, respectively. The Other Costs category generally encompasses elements such as training and professional development, marketing and communication, research and development, and taxes and fees, and due to their smaller impact, influence by company strategy and local regulation will not be further exploited.

The decomposition of the first two categories is debated and can be accomplished in a variety of manners. Presently, a lack of standardised terminology implies that there is no definitive or universally accepted method. However, some breakdowns can offer more clarity than others, a point illustrated in Figure 2.1, where the confusing terminology from three different publications is presented. This discussion is primarily based on sources discussing an offshore wind turbine, but the principles are equally applicable to other technical systems.

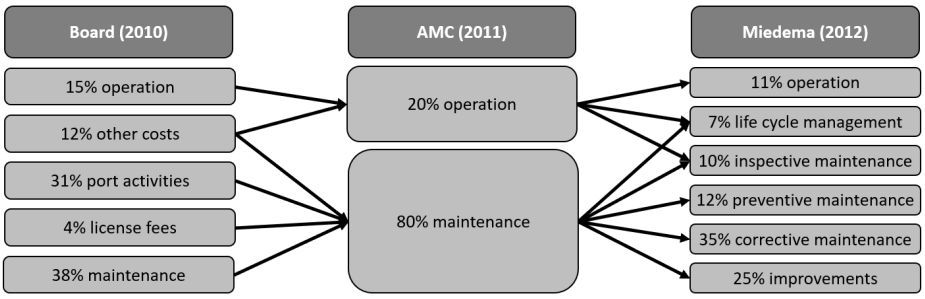

Figure 2.1: Conflicting terminologies in offshore wind turbine OPEX decomposition from various studies, adapted from Lagerveld et al. (2014)

Operations pertains to the primary processes associated with the operation of the wind turbine. It encompasses the routine activities necessary for the wind turbine to function optimally. Maintenance constitutes all technical, logistical, administrative, and managerial actions during the turbine's life cycle, designed to retain or restore the turbine to a state in which it can perform its required function. It also encapsulates activities such as 'Port Activities', licensing fees, and other variable or unspecified costs. Life Cycle Management involves activities that benefit both operating and maintenance. LCM covers aspects such as the planning and scheduling of maintenance activities. Inspective Maintenance is recognised as a distinct type of maintenance in this study, it is often seen as an operational activity or part of preventive maintenance. Preventive Maintenance refers to measures undertaken to forestall equipment failures before they occur. Corrective Maintenance is maintenance conducted after a malfunction or breakdown, aimed at restoring the turbine to a functional state. Improvement encompasses refits, major overhauls, and modification programs designed to maintain the optimal performance of the wind farm.

Main system components

Offshore Wind Turbine - The OPEX of offshore wind farms is dependent on various factors. In a parametric CAPEX, OPEX, and LCOE analysis by Ioannou et al. (2018), these financial indicators were developed as a function of wind turbine capacity, water depth, distance from the port, and wind farm capacity. The study revealed an inverse exponential reduction in OPEX with an increasing wind turbine rating, due to a decrease in the number of units required per wind farm. Furthermore, an increase in the distance from the shore resulted in an exponential rise in OPEX. The study found that the water depth had no significant effect on the OPEX, while an increase in wind farm capacity resulted in a proportional rise in OPEX. The outcome of this study was three distinct formulas per unit of energy that provide an estimation of the CAPEX, OPEX, and LCOE. These findings could be an intriguing objective for research project on integrated electrolyser in wind turbine configurations. Another report mentioned that increasing of the significant wave height has a direct relation to a higher OPEX (Röckmann et al., 2017), as this influences the accessibility of the site to perform maintenance on.

As per the same study, the cumulative CAPEX for a 504 MW wind farm situated in the North Sea was estimated to be around €1.6B, with the OPEX approximated at €50M annually. When the OPEX is projected over the typical lifespan of approximately 25 years, it constitutes nearly 80% of the CAPEX. It is vital to note that these computations do not account for inflation or the discount rate, implying a possible upward adjustment of the resultant percentage. A study by BVG (2018) presents a rough estimate of the CAPEX for an offshore wind turbine at €2.37M per MW, and the yearly OPEX at about €76K per MW. Upon extrapolating this over the analogous lifespan, the derived percentage is also approximately 80%. In a study conducted by Stehly et al. (2019), it was concluded that the OPEX costs for a 6.1 MW fixed-bottom offshore wind turbine amount to approximately $124/kW per year. Within this, the operating and maintenance costs range between $33/kW and $59/kW annually.

A recent paper asserts that the significance of Operating and Maintenance (O&M) modelling has been underestimated for years due to the absence of suitable models (Rinaldi et al., 2021). In this paper, a methodology is delineated for the construction of precise and specific O&M models, which consequently results in an accurate business case and clearly delineates areas for optimisation. Furthermore, the paper demonstrates that the consideration and estimation of additional key performance indicators, such

as contribution to downtime and costs of repair or replacement of individual components, can enhance the transparency of the calculations and capture uncertainties associated with the future operation of a wind farm. A research gap identified in this article is the application of the principles of these models to other configurations, which is the objective of the thesis. This article builds upon an earlier work by the same author (Rinaldi et al., 2017), which focuses on fixed-bottom offshore wind parks and also places more emphasis on explaining the model, whether or not in combination with specialised Reliability, Availability, and Maintainability (RAM) software. These two articles serve as a robust foundation for a potentially similar model for the intended electrolyser-wind turbine configuration, based on RAM modelling combined with Monte Carlo simulations.

PEM electrolyser - The OPEX and performance longevity of a PEM electrolyser are governed by several interconnected factors, primarily system size, operational parameters, and materials used for component construction (Ahmed et al., 2022; Bertuccioli et al., 2014; Frensch, 2018; Khatib et al., 2019).

Generally, OPEX accounts for routine maintenance, unexpected repairs, and necessary system overhauls to ensure efficient operation. The OPEX is often quantified as a fraction of the CAPEX, lying between 2 to 5%. However, this approximation excludes the end-of-life stack replacement costs, which can substantially escalate the total OPEX (Bertuccioli et al., 2014).

Bertuccioli et al. (2014) noted that the costs associated with system maintenance scale non-linearly with the system size, primarily because material costs scale linearly with the system size, whereas labour costs linked with operations and maintenance manifest in a lower cost per MW for larger installations. Consequently, smaller plants typically incur an annual material OPEX equating to 1.5% of the CAPEX, alongside an operational cost of 5% of the CAPEX. In contrast, larger installations are projected to accrue a significantly lower operational cost of approximately 2%.

2.2.2. Operations

Context

In the operational phase of an offshore wind-hydrogen project, various expenses and activities are crucial for the system's effective functioning. The operational expenses encompass rental or lease payments for the seabed, insurance costs to secure the infrastructure against various risks, and transmission charges paid to national electrical grid authorities (Shafiee et al., 2016). These costs are generally determined by factors such as the wind farm's revenue, its installed capacity, and the average price per unit of energy produced.

Operation involves a multi-faceted approach to manage different components of the integrated system, aiming for optimal performance based on specific objectives like maximising hydrogen production or ensuring component longevity (M. H. A. Khan et al., 2022). This includes the monitoring and control of wind turbines to generate electricity efficiently, the management of integrated PEM electrolysers for hydrogen production, and the oversight of the desalination process to supply purified water. Additionally, the operation phase involves managing the compression of hydrogen gas for pipeline transport, overseeing the pipeline network's integrity and safety, and ensuring seamless system integration and coordination. Each of these operational aspects is critical for the overall performance and efficiency of the offshore wind-hydrogen project.

Wind turbine

Navigating the operational complexities of offshore wind farms involves a balance between efficiency and risk minimisation. Traditional operational methods often employ a dedicated controller and power converter for each turbine, making the system vulnerable to severe weather conditions and complicating maintenance (Hur, 2021). To address these challenges, new strategies have emerged. One such proposal suggests that a group of turbines share a single controller and converter, thereby improving reliability and reducing downtime, albeit at the cost of increased installation complexity due to the need for additional components like substations and offshore cables (Hur, 2021).

Another strategy, previously proposed by González et al. (2015), involves selectively reducing the power output of upwind turbines to increase aerodynamic power for downwind turbines by affecting the induced wakes, thereby enhancing overall energy extraction. This is optimised through a genetic

algorithm that selects the ideal pitch angle and tip speed ratio for each turbine, increasing efficiency and reducing mechanical stress, which in turn extends turbine lifespan and overall farm availability. Optimisation of these strategies can be achieved through various means. Identifying factors that impact operational costs and availability is crucial (Martin et al., 2016). Decision support models and tools also play a vital role in this optimisation process (Hofmann, 2011). For instance, when implementing the shared power converter strategy, the careful placement of the substation is essential to ensure accessibility during adverse weather conditions (Hur, 2021).

Emerging trends in offshore wind farm operations, such as the use of advanced analytical methods like Fuzzy FMEA and the shift towards shared power converters and genetic algorithms for individualised turbine operation, indicate the field's rapid evolution. The operational focus is increasingly on factors like turbine reliability, accessibility, meteorological conditions, and condition monitoring, all aimed at reducing O&M costs (Hur, 2021).

The ultimate goal is to simplify the operation of offshore wind farms, reduce failure rates, and minimise non-scheduled maintenance. Decision support models that consider financial, health, and environmental variables over the project's lifetime are becoming increasingly important (Hofmann, 2011). This strategic focus on balancing the initial higher costs of innovative operational strategies with their long-term benefits is indicative of a move towards more efficient and sustainable offshore wind farm operations.

PEM electrolyser

The operational parameters of offshore PEM electrolysers, such as pressure, temperature, current density, and intermittency, significantly influence their economic viability (Buttler & Spliethoff, 2018). For example, excessive compression could risk membrane perforation (Frensch, 2018), and high operational pressures, temperatures, and current densities can induce thermal and mechanical stress, accelerating material degradation (Escobar-Yonoff et al., 2021). Moreover, the frequent start-stop cycles, often resulting from intermittent renewable energy sources, can cause strain on stack components, leading to faster wear and tear (Frensch, 2018).

Optimizing these operational conditions is crucial for maximising electrolyser efficiency (Ahmed et al., 2022). High temperatures may reduce overvoltage, thereby enhancing hydrogen production, but could also shorten the system's lifespan due to membrane degradation. The electrolyte's circulation speed, which is largely dependent on the flow channel design, also has a significant impact on both performance and longevity.

Material selection is another critical factor in the operation of PEM electrolysers. Catalysts, for example, degrade over time due to various processes such as dissolution, poisoning, sintering, and passivation (Bernt et al., 2020). Strategies like the addition of inert oxides and formation of solid solutions have been proposed to counteract this degradation (Khatib et al., 2019). The membrane itself is also subject to mechanical and chemical degradation, influenced by factors like membrane thinning, ion exchange site occupation by metals, and thermochemical effects. To mitigate these challenges, reinforcing materials like polymer fibres and cost-effective coatings on the bipolar plates have been suggested (Khatib et al., 2019).

2.2.3. Maintenance & Repair

Context

"Maintenance and Repair" denote activities to sustain or restore system functionality, minimizing downtime. In system configuration, this term includes various strategies and tasks that ensure system integrity and reliability. Maintenance involves both preventive and reactive actions, catering to the needs of each component.

In maintenance and repair modelling, specific terminologies are crucial for asset health analysis (Faulstich et al., 2011). "Failure rates" measure asset failures over time, often increasing due to "degradation," or gradual wear. "Mean Time To Failure" (MTTF) predicts the time from an asset's start to its first failure. "Mean Time to Detect" (MTTD) is the average time to identify failures. "Mean Time Between Failures" (MTBF) is the average interval between consecutive failures, including repairs. "Mean Time to Repair" (MTTR) shows the average time to fix a failure. Design metrics include reliability, availability, and maintainability (Cevasco et al., 2021).

Two primary types of O&M are corrective and preventive (Rinaldi, 2018). Corrective maintenance addresses issues after they occur and is cost-effective for small components. However, it may result in costly downtime, potential damage to associated equipment, and high costs for medium or high-priority equipment. On the other hand, preventive maintenance aims to avert issues before they arise and has three subcategories: periodic, predictive, and proactive.

Periodic maintenance is carried out at set intervals and effectively prevents system failures. However, it can be wasteful, may not prevent certain types of failures, can introduce new problems, and often requires a large inventory of parts. Predictive maintenance employs monitoring equipment to reduce inventory costs, downtime, and damage to associated equipment, while also avoiding unnecessary parts replacement. Despite these advantages, when implemented alone, it does not address the root causes of problems, and the condition-monitoring equipment can be costly. Proactive maintenance uses historical data and improvement cycles to schedule maintenance activities, addressing the root causes of problems and reducing maintenance costs beyond predictive levels, while also extending equipment life. The primary drawback of proactive maintenance is its high initial cost (Pillay & Wang, 2003). The differences between these maintenance strategies are visualised in Figure 2.2.

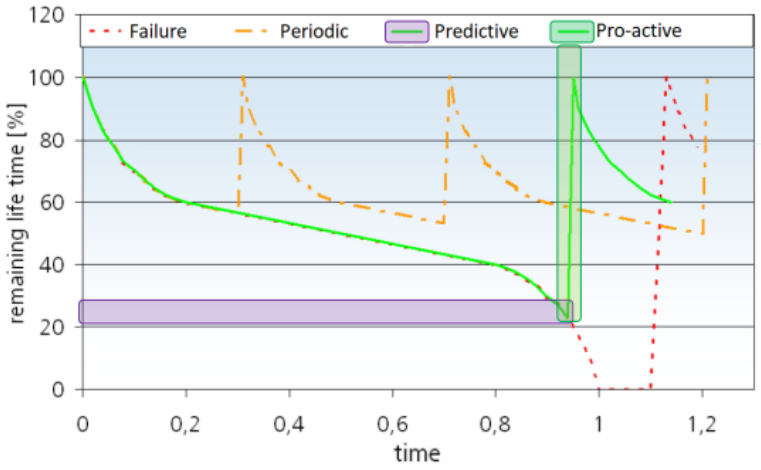

Figure 2.2: Different maintenance actions and their impact on system failure, adapted from Rinaldi (2018)

Repair classifications exist along a spectrum, as outlined by Pham and Wang (1996). Perfect Maintenance restores the system to a like-new state, resetting its failure distribution to time t=0 but often at higher costs. Minimal Maintenance returns the system to its pre-failure state. Imperfect Maintenance achieves an intermediate state, modelled through a virtual age equation with a rejuvenation parameter. Worse Maintenance leaves the system functional but deteriorated, with higher failure rates. Worst Maintenance leads to immediate system failure due to unintended consequences during maintenance. System availability is closely tied to the type of repair executed, a factor to consider in system design.

System reliability encompasses various failure mechanisms: degradation, random failure, and other forms (Shaw, 2009; Sheng & O'Connor, 2017). Degradation involves a gradual performance decline due to factors like wear, environmental conditions, and external influences. This is common in systems like offshore wind turbines and electrolysers, which degrade over time due to harsh conditions. Degradation can be quantified in units like power output loss, lifetime hours, or downtime percentage, varying across components. Random failure is unpredictable and can occur regardless of system age or condition. In offshore wind turbines and electrolysers, such failures could be due to severe weather or manufacturing defects. The bathtub graph in Figure 2.3 visualises system failure rates over time, comprising three phases: infant mortality, random failures, and wear-out failures (Klutke et al., 2003). Infant mortality has a high failure rate due to manufacturing or installation errors. The subsequent phase involves random failures with a relatively constant rate, representing the system's "useful life." The final phase sees an increase in failure rates due to ageing and degradation. In offshore wind turbines and

electrolysers, these phases are evident, each with its own set of contributing factors.

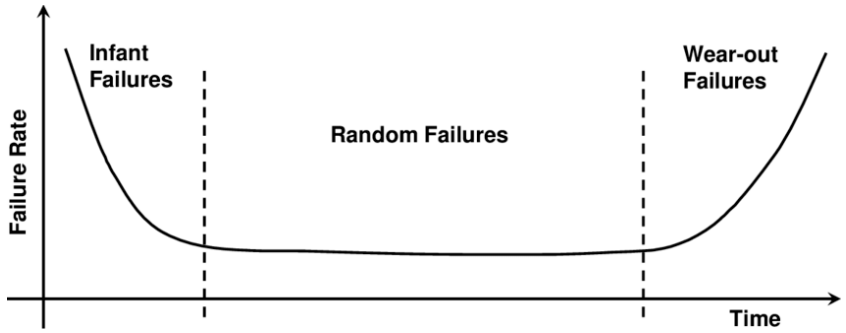

Figure 2.3: Bathtub curve indicating the evolution of failure rate over the life cycle (Katsavounis et al., 2014)

Wind turbine

O&M expenses significantly affect LCOE and LCOH, mainly due to equipment costs and revenue losses (Dinwoodie & McMillan, 2014). Efficient maintenance is thus essential for a robust business case. Failures can be gradual, due to long-term operation and ageing, or abrupt, caused by short-term overload (Luengo & Kolios, 2015). Offshore wind farms are increasingly adopting proactive over corrective maintenance strategies (Ren et al., 2021). These integrate preventive schedules and condition-based maintenance, using condition monitoring systems and optimisation techniques.

Critical tools include the Potential-Failure to Functional-Failure (P-F) curve model, which identifies optimal preventive intervention times (Clark, 2019). Asset-specific techniques like lubricant analysis and corrosion monitoring extend the P-F interval. The Failure Mode and Effects Analysis (FMEA) further aids in system-wide failure understanding and preventive planning (Pillay & Wang, 2003). Condition monitoring collects data on various turbine aspects, enabling anomaly detection and proactive maintenance, thereby reducing failures and enhancing uptime (Wiggelinkhuizen et al., 2008; Yang et al., 2014).

PEM electrolyser

Maintenance and repair costs, which form a substantial part of the OPEX, scale differently with the system size. Unlike material costs, labour costs do not scale linearly with the system size, which can be attributed to labour economies of scale and potential automation opportunities in larger installations (Bertuccioli et al., 2014). Regular maintenance can significantly prolong the operational life and overall efficiency of the PEM electrolyser. This includes routine checks of bipolar plates (BPs) and other critical components for signs of corrosion, especially when stainless steel BPs are used due to cost considerations. Strategies such as implementing effective passivation techniques using non-noble materials like Nb can improve the durability and performance of PEM electrolysers (Ahmed et al., 2022). Finally, voltage degradation rates, lying slightly below or between 4 μV/h, signify a minor increase in the energy required to produce a unit of hydrogen over the electrolysers operational lifespan. This degradation indirectly influences the economic feasibility of offshore hydrogen production (Felgenhauer & Hamacher, 2015; Lee et al., 2020).

2.3. Current and future offshore hydrogen projects

The current stage in the integration of offshore wind and hydrogen production, whether offshore or not, is still in its infancy. However, several projects employing this setup have already been announced, and these projects are at various stages, from conceptual designs to commissioning. This list of projects offers valuable insights, showcasing successful implementations of energy harvesting techniques, scalable operations, and innovative design integrations. A non-exhaustive list can be found in Appendix B. This appendix provides an overview of several projects, including their size and planned commissioning dates. Currently, hundreds of joint ventures are developing such projects, involving both public and private entities, ranging from product developers to investors. This non-exhaustive list comprises 40 distinct projects, and it is worthwhile to examine a few of these projects in more detail due to their unique characteristics. When one examines this table, it becomes apparent that there are many projects

planned, but on a very limited scale in the very short term, in megawatt range. However, looking further ahead, from 2030 onward, projects on a substantial gigawatt scale are planned. Although planning is the first step in a long process, it demonstrates the market's willingness based on the understanding that this technology will be of great importance. A few of these projects are worth highlighting in further detail.

The AquaVentus initiative, for example, has successfully combined offshore electrolysis plants with wind farms (Aquaventus, 2021). By scaling up to 10 GW by 2035 and utilising pipeline systems for hydrogen transport, the project serves as a model for economically viable, large-scale renewable energy systems.

The DOLPHYN project, with a target scale of 4GW by the mid-2030s, offers key learnings in the production of hydrogen from offshore floating wind in challenging deep-water locations (Caine, 2021). It provides a useful template for harnessing renewable energy in demanding environments.

The Bantry Bay green energy facility, a collaboration between Zenith Energy and EI-H_2, represents an innovative venture focused on the dual production of green hydrogen and green ammonia. Its ambition to develop a 3.2 GW energy offshore wind facility in Ireland by 2028 offers meaningful insight for developing comprehensive renewable energy strategies (Raine, 2022).

The Lhyfe and Centrale Nantes project, anticipated to scale between 10 to several 100s MW by 2024, is distinguished as the first offshore green hydrogen production facility powered by a nearby floating wind turbine. This represents an innovative approach to energy production, offering valuable lessons for future offshore operations as stated by RVO (2021), whom, in this publication exploit other hydrogen developments in France, and contains an extensive analysis of other opportunities .

Also, the OYSTER project (Biebuyck, 2022) is pioneering a unique, marine-adapted system that combines desalination, electrolysis, and hydrogen production. Its adaptability and resilience against harsh marine conditions provides an insightful model for other offshore electrolysis projects.

Lastly, he PosHYdon initiative, spearheaded by Nexstep and TNO, aims to generate green hydrogen offshore using wind-powered electrolysis on Neptune Energy's Q13a-A platform in the North Sea (Buijs et al., 2022). The project investigates the practicalities and effects of offshore conditions on hydrogen production, and is a collaboration involving partners such as Neptune Energy, Gasunie, Eneco, and others. The insights derived could pave the way for large-scale offshore green hydrogen systems.

2.4. Research gap conclusion

There is a notable interest in W2H systems in scientific literature, seemingly driven by the need for an energy transition where green hydrogen plays a key role in a sustainable future. These studies mainly focus on system configuration and the trade-offs between onshore and offshore hydrogen generation. Interestingly, the LCOH calculated in these studies appears favourable and aligns with European goals. There is extensive coverage of W2H projects currently being tested, constructed, or planned – reaching gigawatt scales by 2030. However, these studies seem to overlook the focus on OPEX

This OPEX, primarily composed of system operation and maintenance costs, is scrutinised in research on individual systems like electrolysers or wind turbines. These studies draw conclusions on yield optimisation and durable usage of installations, estimating OPEX based on CAPEX. Yet, there appears to be a lack of information regarding the reliability of these systems, which could potentially impact the LCOH – both on the numerator side, affecting OPEX, and in the denominator, influencing the systems' yield. Therefore, the research gap is identified as the effects of reliability, operation, and maintenance on W2H systems.

3

System components

This chapter examines the different components of offshore wind farms for hydrogen production, including energy transmission methods, electrolysis technologies, power conversion processes, and structural elements. Each section focuses on the functionality, benefits, and challenges of these components, providing an understanding of their roles in an efficient system. The insights gained here are required for appreciating the technical complexities and operational dynamics of coupling wind energy generation for hydrogen production and will form the basis on which the models for this research are created.

3.1. Energy transmission

Hydrogen and electricity stand as the primary contenders for energy transmission in offshore wind farms focusing on hydrogen production. This comparison seeks to elucidate the influences of farm distance from the shore and other variables on these two transmission methods, culminating in a conclusion about the most viable option for energy transportation.

Hydrogen Steel pipelines offer the most economical option for transporting large volumes of hydrogen gas. Using pressure differentials, the gas moves from a high-pressure inlet to a lower-pressure outlet. This, however, leads to a parabolic gradient of pressure drop, necessitating the periodic placement of compression stations at intervals of approximately 80-100 km (Witkowski et al., 2017). Importantly, these pipelines can be retrofitted from existing natural gas pipelines, potentially reducing the capital cost by up to 90% (Tsiklios et al., 2022). Technically, the pipelines for hydrogen and natural gas share many characteristics; however, due to hydrogen's corrosive nature, a layer of iron oxide will be applied to protect the pipelines. When it comes to efficiency, hydrogen pipelines are remarkable, experiencing only minuscule fugitive emissions and transmission losses, typically around 0.1% per 1000 km (Miao et al., 2021).

Electricity Electricity transmission has evolved from relying solely on High Voltage Alternating Current (HVAC) lines to increasingly incorporating High Voltage Direct Current (HVDC) lines for distant offshore installations (Rahman et al., 2021). HVAC cables suffer from resistive losses and the "skin effect," which contribute to power losses of approximately 6.7% per 1000 km (Miao et al., 2021). Conversely, HVDC cables demonstrate lower resistive losses (around 3.5% per 1000 km) and operational voltages between 400 kV to 1100 kV, making them more efficient and capable of transporting greater power (Calado & Castro, 2021). However, their system design is more complex due to the inclusion of converter stations, which introduce additional costs and conversion losses.

Conclusion For offshore wind farms beyond 100 km from the shore, the economical balance tips in favour of hydrogen pipelines, due to their lower transmission losses and potential cost reductions from pipeline retrofitting. Conversely, for installations closer to the shore and below the break-even distance of around 60 km for HVDC lines, electrical cables may still be economically viable. The decision, thus,

hinges on specific variables such as distance, capacity, and existing infrastructure. In this case, as has become clear from the introduction, the hydrogen-based transport is the preferable option. It must be emphasised that this pertains to a situation where hydrogen is the desired product. When hydrogen is used as an energy carrier to be subsequently converted back into electricity, this conclusion does not apply due to conversion losses.

3.2. Offshore electrolysis configurations

Centralised The centralised approach streamlines the energy transmission process by housing all key components on a single platform. This consolidation yields a simpler infrastructure within the farm, eliminating the need for small dimension pipelines from each wind turbine and thus potentially reducing maintenance and operational complexities (Groenemans et al., 2022; Singlitico et al., 2021).

However, this system is not without drawbacks. Centralised brine discharge could have more severe environmental impacts due to its concentrated nature. Further, the overall initial capital expenditure (CAPEX) for constructing the central platform can be significantly higher, which may deter investment (Ibrahim et al., 2022; Reuß et al., 2017).

Decentralised In contrast, the decentralised configuration places hydrogen conversion equipment on each wind turbine. This decentralisation enables various advantages, such as energy and cost savings by negating the need for converters or an extra platform (Ibrahim et al., 2022). Furthermore, it allows for continuous hydrogen production even in the event of individual electrolyser failure. The scale of technology is also well-developed, requiring no prerequisite modifications to commercially available electrolysers, and offers quicker and easier maintenance access to individual turbines (Groenemans et al., 2022).

Decentralised brine discharge could reduce environmental risks by facilitating better dispersion, and the system benefits from substantial cost savings and reduced developmental timelines (Reuß et al., 2017). However, the effects on the environment are still under consideration. Furthermore, this model requires a backup source for low wind output scenarios, and the system itself may be more complex than its centralised onshore counterparts.

Conclusion Both the centralised and decentralised configurations present unique advantages and challenges. The decentralised model in contrast to the centralised version, offers a range of benefits like cost savings, reliability, and reduced environmental impact, although it carries its own complexities and potential for operational disturbances. Nevertheless, based on the available literature, the decentralised configuration appears to offer a broader array of advantages, especially in terms of cost-effectiveness and short term viability. However, the choice between the two would depend on the specific use case. Whereas in this instance, the decentralised configuration will be chosen.

3.3. Wind turbine

The conceptual 15 MW offshore wind turbine under investigation serves as an academic benchmark, collaboratively designed by the National Renewable Energy Laboratory (NREL), the Technical University of Denmark (DTU), and the International Energy Agency (IEA) (IEA, 2021). This Class IB direct-drive machine incorporates several elements that make it an intriguing object of study for both academic and industrial applications.

The turbine's 15 MW capacity is strategically aligned with contemporary developments in wind turbine sizes, acting as a progressive yet commercially viable model. This capacity allows the turbine to serve as a suitable benchmark that captures the essence of emerging technologies without being exceedingly experimental. For this turbine, a 240-meter rotor diameter has been chosen. Adding to its architectural considerations, the turbine's supporting structure comprises an isotropic steel tube. This design contributes to both the turbine's structural stability and its longevity. A hub height of 150 meters has been optimised to meet operational and maritime prerequisites. The turbine is build upon a solid foundation, which will be elaborated on in Section 3.7.

In terms of drivetrain configuration, the turbine employs a direct-drive mechanism. This approach minimises the number of moving components, which might inherently result in lower maintenance re-

quirements. This aligns well with previous studies showing that direct-drive turbines are often less demanding in maintenance when compared to their gearbox-driven counterparts, especially in challenging offshore settings (Kaa et al., 2020; Zaaijer et al., 2017). Moreover, the permanent magnet generator, featuring an external rotor radial flux topology, has been favoured due to its fabrication simplicity and structural robustness. While direct-drive turbines generally have higher CAPEX costs, the simpler and more robust design will have a positive impact on the costs for the operation and maintenance of the turbine, making the costs of these turbines comparable, or even a bit lower (Carroll et al., 2015).

3.4. Electrolyser

In this section, the focus will initially be on contrasting prevalent electrolyser technologies, specifically Alkaline Electrolysis (AEL) and Proton Exchange Membrane (PEM) Electrolysis , to ascertain their suitability for the current research context. As promising as emerging technologies like Solid Oxide Electrolyser Cells (SOEC) and Anion Exchange Membrane Electrolysis (AEM) may be, they are not commercially viable for immediate implementation due to their current Technology Readiness Level (TRL) and Manufacturing Readiness Level (MRL) (Bianchi & Bosio, 2021; IEA, 2022b). Subsequently, the following section will delve into a detailed examination of the chosen electrolyser system, along with its Balance of System components, to offer a comprehensive overview of the system.

3.4.1. Electrolyser technology comparison

In the assessment of electrolyser technologies for integration into offshore wind turbine systems, this study will employ an analysis focusing on operational parameters, efficiency, available capacity, durability, and economic aspects. Operational parameters such as operating temperature, pressure, and load flexibility are important, especially given the fluctuating nature of wind energy and the need for adaptability (Lange et al., 2023). Efficiency, indicated by stack and system efficiencies, gains particular importance in an offshore context where energy is premium. Additionally, spatial optimisation metrics like power per stack and hydrogen production rate are vital due to offshore platform constraints. Durability measures, including lifetime and efficiency degradation rate, provide insights into long-term performance and maintenance needs. Lastly, economic parameters like Capital Expenditure (CAPEX) and Operational Expenditure (OPEX) offer a financial lens to assess the viability of electrolyser integration. A full comparison table with metrics can be found in Appendix D, the following figures have been adapted from the works of Buttler and Spliethoff; Ibrahim et al., unless quoted otherwise.

AEL The Alkaline Water Electrolyser (AEL) employs a liquid electrolyte comprising 20-40% sodium hydroxide (NaOH) or potassium hydroxide (KOH), which contributes to an alkaline environment with a high pH range of 13-14. The system utilises nickel-based electrodes immersed in this alkaline solution, separated by a diaphragm that allows only hydroxide ions to pass through (Grigoriev et al., 2020). In terms of operational parameters, AELs function between temperatures of 60-90°C and pressures of 10-30 bar. A plus for intermittent operation is their load flexibility, which ranges from 20-100% of nominal load, although cold start-up times can be as long as 60-120 minutes. When assessing efficiency, AEL exhibits a nominal stack efficiency (Lower Heating Value, LHV) between 63-71% and a system efficiency of 51-60%. The spatial optimisation metrics indicate that each stack can achieve a maximum nominal power of 6 MW. However, this requires a substantial footprint of 95 m^2/MW, which could pose a significant challenge in offshore environments. For durability measures, AEL systems show a lifetime ranging from 55,000-120,000 hours with an efficiency degradation rate of 0.25-1.5% per year. Economically, the technology has a CAPEX ranging from €800-1500/kW, and an OPEX that is about 2-3% of the CAPEX. AEL is widely regarded for its cost-effectiveness due to the absence of rare materials and has considerable potential for improvement, particularly in its efficiency metrics (Grigoriev et al., 2020).

PEM First introduced in the 1960s, the PEM Electrolyser consists of a solid polymer as an electrolyte and employs platinum group metals as electrocatalysts (Shiva Kumar & Himabindu, 2019). The operational temperature for PEM electrolysers ranges from 50-80°C, and they operate at higher pressures between 20-50 bar, which is higher than alkaline and therefore compression of hydrogen afterwards is less necessary. They stand out in their load flexibility, capable of operating from 0-100% of nominal load

and boasting rapid cold and warm start-up times of 5-10 and 0.2 minutes, respectively. Efficiency-wise, PEM systems have a stack efficiency of 60-68% (LHV) and a slightly lower system efficiency ranging from 46-60%. Spatially, PEM electrolysers are designed for compactness, requiring only half of the space compared to AEL, with a footprint of 48,000 m²/GW . In terms of durability, the lifetime for PEM ranges from 50,000 to more than 60,000 hours, with some sources projecting up to 78,000 hours by 2030 (M. A. Khan et al., 2021). However, they suffer from a higher annual efficiency degradation rate of 0.5-2.5%. Economically, PEM systems have a higher CAPEX, ranging from €1400-2100/kW, and an OPEX that constitutes 3-5% of the CAPEX, one of the main disadvantages is the need for rare metals like platina and iridium, which are used as electrodes. These materials are rare and expensive.

Conclusion Both technologies have their merits and shortcomings, primarily dictated by their intrinsic material and design attributes. AEL offers cost advantages and a robust, mature technology but may suffer from spatial constraints, particularly in offshore settings. On the other hand, PEM provides operational flexibility and spatial efficiency but at a higher cost and increased efficiency degradation rate. Therefore, the PEM system will be chosen to use in this system. Technological advancements and scaling are expected to gradually alleviate these issues for both technologies by 2030, which parameters shall be used will depend on the project definition of the use case (Clean Hydrogen JU - SRIA, 2022).

3.4.2. Electrolyser system

In delineating the operational mechanism of a pressurised PEM electrolyser, it's crucial to differentiate between balanced pressure and differential pressure systems. Under balanced pressure, both sides of the electrolyser are harmonised in pressure (Tsotridis & Pilenga, 2021), regulated by an anode and cathode control valve, akin to the mechanism of alkaline electrolysis. Conversely, the differential pressure system solely pressurises the hydrogen side, while maintaining near-atmospheric conditions on the oxygen side, necessitating a meticulously engineered stack capable of withstanding differential pressures reaching several mega pascals. A notable advantage is the economical component selection for the oxygen side.

According to Smolinka, the power supply to the system is managed by a rectifier that transitions alternating current (AC) to direct current (DC). The circulation of reactant water is facilitated mostly by a circulation pump on the anode side, accompanied by a heat exchanger in the loop to mitigate stack damages by dissipating excess heat. During operation, heavy metal ions dislodged from the stack and system components are entrapped by the ion exchanger filling, which albeit increasing water conductivity, compromises its quality accelerating stack degradation. The system is provisioned with reactant water from a fresh water supply, which is initially purified to meet requisite quality standards. A feed water pump elevates the water pressure to the anode side pressure, channelling it into the process, with external re-coolers often deployed for anode circuit cooling, transferring process heat to the external environment. The water circulation pump ensures seamless water flow through the anode channel.

The PEM electrolysis stack is a pivotal component, encompassing the Membrane Electrode Assembly (MEA) which is structured into five integral layers:

1. Anode gas diffusion layer
2. Cathode gas diffusion layer
3. Anode catalyst layer
4. Cathode catalyst layer
5. Membrane

A visual representation of the PEM stack is shown in Figure 3.1

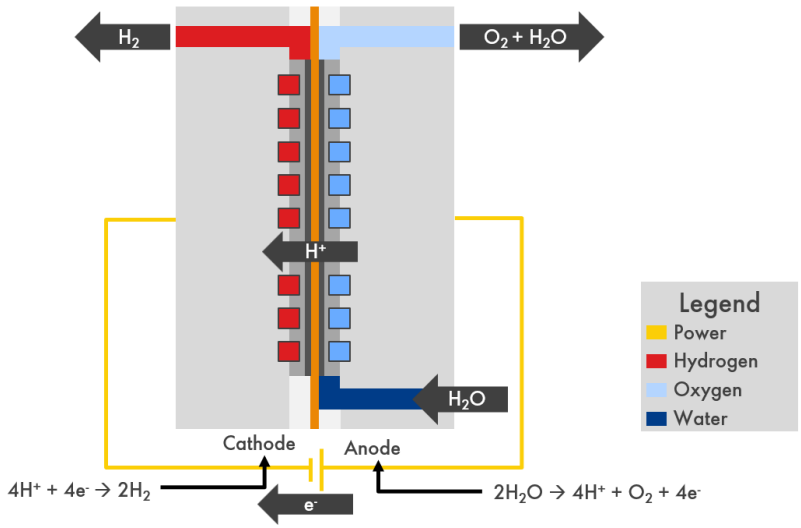

Figure 3.1: Schematic visualisation of a PEM stack including the membrane, catalysts, diffusion layer and bipolar plates, adapted from Shell internal document

The membrane, with a thickness range of 50 – 250 μm, is crafted from a polyethylene-based polymer, tailored with fluorine and sulphonic acid, often identified by its commercial name, Nafion™. The sulphonic acid group's hydrophilic properties are vital for membrane efficiency, as its conductivity is hydration-dependent. This acid group sustains a stable, desirable level of hydration, with the interplay of ionic bonding and water enabling proton traverse through the membrane. The membrane-induced acidic milieu dictates material selection within the electrolyser, precluding the use of Nickel and Cobalt due to their elevated corrosion rates, rendering platinum for the cathode and iridium oxide for the anode as preferred choices given their conducive and durable nature in the corrosive setting.

In the hydrogen section, the apparatus comprises a hydrogen/water phase separator, a demister for expelling fine water droplets from the hydrogen stream, and a condensate trap which, by reducing the temperature, extracts water vapour from the flow. Post deoxidation, the resultant water is condensed in a cooler, segregated and ejected from the process. The heat exchanger is responsible for evacuating the excess heat from the PEM electrolyser using water as a coolant. The de-oxo unit, following hydrogen cooling to eliminate extant water steam, ushers the hydrogen through an autocatalytic converter or deoxygenator, eradicating oxygen traces through cold combustion triggered by catalysts, with water output being purged by ion exchange resins and silica or other desiccants. The oxygen removal is orchestrated by a deoxidiser reactor, typically leveraging a palladium catalyst, while the regenerative bed dryer signifies a penultimate phase towards hydrogen purification, where the hydrogen is channelled through a gas drying unit known as a Dryer, employing either pressure swing or temperature swing adsorption for fine drying.

The oxygen section encapsulates an oxygen/water phase separator, functioning as a buffer to modulate water flow within the circuit, a sink for wastewater collection, and a mechanism for oxygen-water separation. Similar to the hydrogen section, a demister is employed to eliminate fine water droplets from the oxygen stream, ensuring a clean, separated output.

Additionally, the system incorporates several balance of plant components essential for optimal operation. Instrument air, crucial for actuating valves and other pneumatic devices, ensures precise control and operational functionality. Nitrogen, vital for purging and inerting purposes, aids in maintaining a safe operational environment. On the metering platform, two emergency shutdown valves are integrated, serving as critical safety components to halt operations in exigent scenarios. Other equipment on the platform, while functional, aren't crucial for immediate production. The HVAC system, responsible for regulating temperature and ensuring a conducive working environment, is categorised as non-critical and is attended to as required. Continuous liaison with vendors is emphasised to uphold the reliability and efficiency of these components, although this research will not delve deeper into these systems

due to their simplistic functionality or lesser significance to the core operations of the PEM electrolyser system.

For this specific PEM electrolyser, an interesting design feature is considered: an integrated electrolyser setup with a primary focus on the containerisation of key components. These components include the electrolysers, hydrogen and oxygen separators, along with the associated cooling systems and pumps. The layout hosts three electrolyser containers per platform, each designed for a 5 MW capacity and housing the essential inlet separation facilities and electrolysers. In this decentralised framework, each container is crafted to function as a standalone unit, enabling independent servicing of specific equipment without impacting the overall system. All additional ancillary equipment pertinent to utility services, such as water treatment and cooling systems, are placed outside the containers on the platform. Each stack is equipped with a 5 MW transformer and a rectifier for every pair of 2.5 MW electrolyser stacks. This configuration of 6x 2.5 MW electrolyzer power is an assumption, and the (economic) optimisation of this configuration could be an interesting subject for further research, also considering the role of oversizing compared to the potential breakdown of an electrolyser container. Although traditionally aligned in parallel, these stacks have been modelled in MATLAB in series per container to mitigate potential electrical disruptions. A distinctive aspect of this decentralised design is the ease of entire container replacement, instead of just faulty component repair, in the event of malfunctions, as any defective component within a container is critical to production output from that container. This possibility will be analysed in the results chapter.

3.5. Power conversion

Wind turbines predominantly produce alternating current (AC) power. To facilitate hydrogen production through electrolysis, a systematic transformation of this power is essential to align with the electrolyser's direct current (DC) requirements. The wind turbine's output is characterised by fluctuating strength, frequency, and a voltage of approximately 690 volts. To channel this power efficiently to the platform's integrated systems, a series of conversion stages is implemented. At the initial stage, the 'wild AC' output of the wind turbine is processed by a rectifier. This device converts the AC into DC, which is directly supplied to the electrolyser stacks. Following the rectification, an inverter is utilised to transform a portion of the DC back to AC. This AC, which operates at a steady frequency, is then directed to power other platform components, such as the water treatment facility and various supporting utilities. Notably, all these utilities, especially those with motors, operate on a three-phase system and typically use 400V AC with a frequency of 60 Hz, a standard for offshore applications. To safeguard the system and enhance its longevity, cables enabling the power distribution across the platform are ingeniously embedded within its structure. This design not only bolsters safety but also minimises potential wear and tear induced by environmental elements.

As a final note, there's a concept presented by AquaSector that posits a fully integrated electrolyser into an offshore wind turbine. This design envisions the turbine and the electrolyser operating as a single synchronised system to produce green hydrogen directly. This innovative approach warrants further exploration and could offer further refinements to the described system. This project, which includes plans for a large-scale offshore hydrogen park in the German North Sea, is a collaboration involving Shell, RWE, Gasunie, and Equinor. The aim is to have a 300 MW pilot operational by 2028 and to scale up to 10 GW by 2035.

3.6. Water treatment

The goal of treating water in PEM electrolyser systems is twofold: first, to make sure that clean, high-quality hydrogen and other gaseous products are produced; and second, to make sure that important system parts like membranes and catalysts last longer. Inadequate water treatment could compromise both the system's efficiency and the longevity of its integral components. On a commercial scale, the ASTM's Type II standard, representing deionised water, is seen as a benchmark. However, many manufacturers show a preference for even purer water with lower conductivity, referred to as Type I. Meeting these standards is crucial for ensuring that the produced hydrogen aligns with desired product specifications. Table 3.1 summarises the water quality requirements essential for efficient operation, as described in the Type II system requirements.

Table 3.1: Specifications for electrolyser water quality (ASTM International, 1999)

Component	Unit	Value
Conductivity	μS/cm	1
Resistivity	MΩ/cm	1
Total Organic Carbon	μg/L	50
Sodium	μg/L	5
Silica	μg/L	3
Chloride	μg/L	5

To ensure the attainment of the desired water quality, a comprehensive water treatment system is indispensable. This system is designed to transform North Sea water into water with the precise characteristics required for the intended use. The first component employed for this transformation is the seawater intake pump, which draws up the seawater. Integrated within this pump is a preliminary fine screening mechanism aimed at eliminating larger particulate matter. This initial filtration stage is critical as it protects the downstream equipment from potential damage caused by these particles.

Following this initial filtration, the system transitions to the so-called pre-treatment phase, which notably includes ultrafiltration. Ultrafiltration, serving as a pre-treatment measure, utilises membrane technology to effectively eradicate a broad spectrum of contaminants. The contaminants in question range from microbiological entities such as viruses and bacteria, to chemical substances like organic acids and enzymes. Performance metrics of this method are quite promising, showcasing a water recovery rate of 95% and a particulate removal efficiency exceeding 99%.

The subsequent stage in this water treatment journey is Reverse Osmosis (RO), a predominant technology for desalination. The primary objective of RO is to substantially reduce the concentration of dissolved solids. This is achieved by applying pressure to the seawater, propelling it through a semi-permeable membrane. This membrane is meticulously designed to allow the passage of water molecules while substantially restricting the passage of other particles, including the majority of salts. Globally, RO is responsible for over 60% of desalination capacity, targeting a conductivity of 20 µS/cm, which is equivalent to a Total Dissolved Solids (TDS) concentration of approximately 12.8 mg/L. The average recovery rate in this stage is 70%, with OPEX being a consideration, especially due to the periodic necessity for membrane maintenance or replacement. After this step, post-treatment ensures the final adjustments to the water quality, aimed at e.g., preventing corrosion in subsequent parts of the system.

To attain the correct conductivity, Electrodeionisation (EDI) is also essential. EDI is primarily geared towards further reducing water conductivity to meet the stipulated specifications. This method ingeniously melds ion exchange and electrodialysis, leveraging ion-exchange membranes and direct electrical current for high-efficiency ion removal. The key performance indicators for EDI are notable, with a water recovery rate of 99.99% and ion removal efficiency also exceeding 99%, showcasing the robustness and efficacy of this integrated water treatment system. After this step, the deionised water is ready for circulation through the electrolyser system.

3.7. Structural components

Located on the wind turbine tower at the specified location, the platform operates as a central hub for crucial equipment, principally encompassing the power conversion apparatus, electrolysers alongside their auxiliaries, and the water treatment facility. The construction sequence initiates with the monopile placement, a foundational structure delving to a maximum depth of 45 metres, succeeded by the positioning of the transition piece, a crucial element for connecting the wind turbine to the monopile foundation, besides hosting various functionalities such as cable connection provisions, a landing area for boats, and a corrosion protection mechanism for the foundation. Following these foundational steps, the assembly of caissons, the platform, and the remaining turbine components takes place. Equipment, depending on its designated function, is either situated within the nacelle or on the platform adjacent to the transition piece.

The foundation is notably characterised by the monopile substructure, encompassing both the foun-

dation itself and the transition piece, with the monopile fashioned with a 10-metre outer diameter, signifying a notable progression in prevailing manufacturing and installation technology, and featuring a thickness profile varying from 55 mm within the pile to 44 mm at the transition piece. Integrated within the system is a caisson for seawater piping and brine discharge, alongside the J-tube, a crucial conduit for pipeline tie-in, facilitating hydrogen transportation by providing a shielded path for cables or pipelines between the seabed and the platform, thereby minimising exposure to external environmental elements. Culminating with the platform's distinct functionalities, often dubbed as the H_2 add-on, it accommodates the H_2 solution control system, inclusive of the electrolyser electrical structure embodying a transformer, rectifier, and BESS. Furthermore, the platform houses the balance of plant for the electrolysers, encompassing the water intake and treatment systems, brine and heat discharge mechanisms, and the H_2 offtake. A distinct electrolyser control system is also incorporated within this platform. Given that the electrolyser is slated to embody 15 MW of power, with a footprint of 45 m2/MW, the platform necessitates at least 675 m2 of space solely for the electrolyser. Nonetheless, the design could potentially incorporate multiple levels or the stacking of certain components to optimise the spatial configuration.

3.8. System overview

The subject of this investigation is a decentralised framework for offshore hydrogen generation, underpinned by wind energy. Each aspect of the system, residing a considerable distance off the nearest coastline, represents an integrated ensemble of technologies, which collectively aim to facilitate a seamless operation.

The primary power source is a 15 MW direct-drive wind turbine, as formulated by the National Renewable Energy Laboratory (NREL). The turbine is positioned offshore to capitalise on the abundant wind resources available at sea. This technology plays an integral role in electricity generation, which is subsequently converted for utility and electrolysis applications.

Adjacent to the wind turbine is a platform that houses power conversion units. These units are responsible for converting the electrical output from the wind turbine into a form that is compatible with utility grids as well as the electrolyser. They serve as the bridge between raw electricity generation and its subsequent utilisation in the system. The power conversion units used in this system are a rectifier and inverters, also known as a B2B converter.

The electrolyser, based on PEM technology, is also located on the platform. It is split into six stacks, each with a 2.5 MW capacity, totalling 15 MW. This arrangement ensures maximum power efficiency, achieved through parallel construction of the stacks. To enhance modularity and withstand the harsh marine environment, the electrolyser stacks are enclosed in shipping containers, with two stacks per container. The Balance of Plant (BOP) is also located in the containers. They contain the components necessary to facilitate the hydrogen production for an electrolyser, or the exportation to the pipelines.

The platform also features a water treatment facility designed to purify seawater, rendering it suitable for the electrolysis process. This facility ensures a consistent supply of high-quality water for the electrolyser, thereby playing a crucial role in hydrogen production. To maintain water circulation in the electrolyser system, pumps are incorporated into the design. Notably, the present configuration omits a compressor, as a PEM electrolyser can operate under high pressure. Therefore, the necessity of a compressor will depend on the specific transport requirements for the hydrogen produced.

In terms of weight distribution, as described by a restricted Shell source, the electrolysers, water modules, BOP equipment, and pipelines collectively contribute approximately 250 t. The platform and extra foundational elements add around 100 t, culminating in a total topside weight of 350 t. This is in addition to the wind turbine and its foundation, which weigh 3390 t, this data has been produced by Shell.

A visual overview of the system is provided in Figure 3.2.

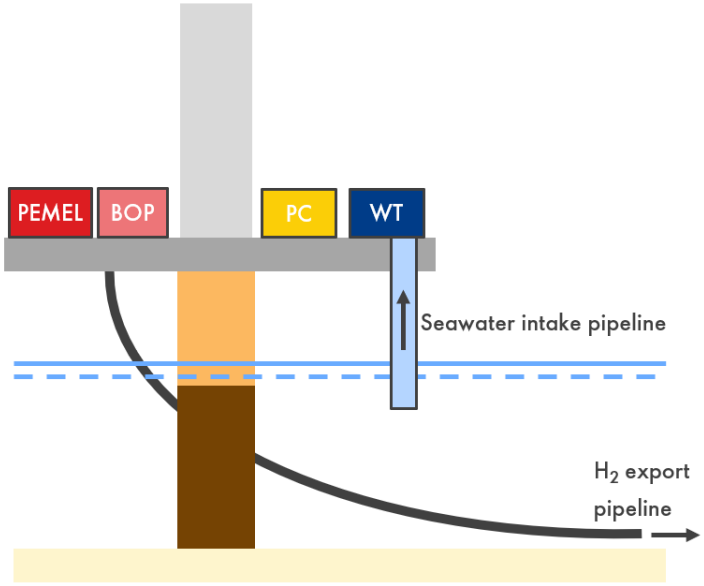

Figure 3.2: Visual representation of the different W2H system components placed on a platform attached to an offshore wind turbine

4

Model constructions and simulations

Within this research, various models are utilised, each targeting different aspects of the investigation. This study builds upon an existing energy model developed within the Shell team, aiming to analyse the production of the configuration. New models are also crafted, including a RAM model constructed specifically to probe the system's dependability. This chapter elucidates the modelled components within the system and sheds light on the underlying logic of these models. Conclusively, a validation will be conducted to discern the model's precision.

4.1. Energy model

The energy model comprises multiple components, each with its own set of parameters. The simulation operates given the wind data input, emulating the behaviour of this Wind-to-Hydrogen (W2H) configuration and producing hydrogen for the given situation. Consequently, the model provides insights into pivotal parameters such as the hydrogen yield, the number of start/stop events, and power fluctuations. The model's accuracy is enhanced by incorporating state-of-the-art efficiency parameters and by simulating real-world constraints, like the stack replacement of the electrolyser.

4.1.1. Model architecture

The original model was constructed in three phases. Firstly, it involved the identification of the system configuration: discerning which elements were present and understanding their interrelationships. Following this, system sizing is undertaken, where, using a wind speed analysis, the elements are scaled according to the anticipated energy yield. Subsequently, the final phase pertains to modelling this system and generating results that provide insights into the estimated hydrogen production. The model consists of separate components of the W2H unit, incorporating physical interrelations and coefficients to simulate an energy yield as realistically as possible. The relations between the different components are schematically displayed in Figure 4.1.

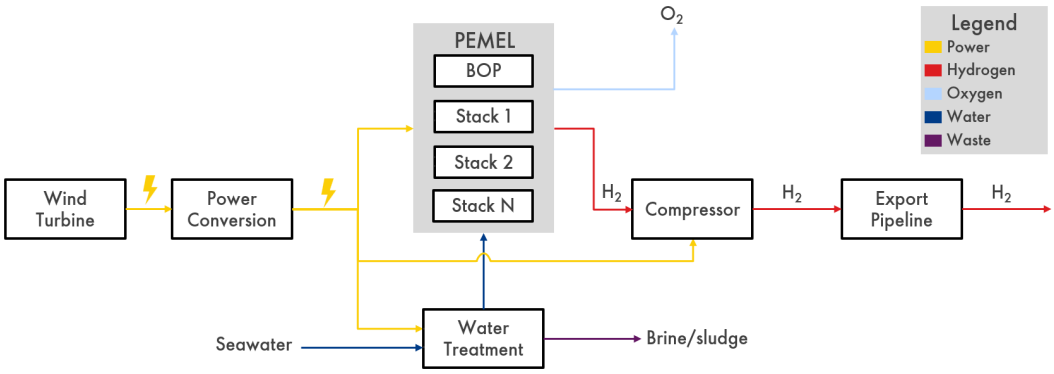

Figure 4.1: Block diagram of the energy yield model with the physical relations between these elements

In this figure, it is illustrated that the wind turbine generates energy in the form of electricity, which is then transported to the power conversion unit to be converted into the appropriate current. Subsequently, the electricity continues to the supporting elements of this system, such as the water treatment where seawater is transformed into water suitable for electrolysis, the balance of plant of the electrolyser, and the hydrogen compressor. Naturally, the electricity also powers the electrolyser stacks, which convert water into hydrogen that then proceeds on its journey. A detailed explanation of the different components functions are found in Section 4.1.2.

Maths and performance indicators

In assessing the performance of the energy model, several key indicators are utilised to scrutinise the system's efficacy concerning its energy production-related parameters. These indicators are:

- Hydrogen Yield: Simulated on an hourly basis and can be aggregated over various time spans to provide a comprehensive view of the system's productivity.
- Number of stack replacements: Indicates the maintenance requirements over the system's lifetime and, by extension, its overall durability.
- Module Switch Frequency: A factor influencing the degradation rate of the system.
- Power Fluctuation: Another factor that can affect the rate of stack degradation.

For this research, only the hydrogen yield and stack replacements are considered, but for further research, the other indicators could become a point of focus.

4.1.2. Components

In the subsequent paragraphs, the methodology of the modelling of the different components is detailed.

Wind turbine

The wind turbine discussed is a conceptual 15 MW turbine, based on the IEA design, the parameters of which have been published for scientific research purposes. Within the model, this wind turbine is characterised by its design parameters. In Equation 4.1.2, the power curve equations are outlined which govern the turbine operations according to an hourly wind speed.

$$P_w(t) = \begin{cases} 0, & \text{if } v_{\text{wind}} < v_{\text{cut-in}} \\ P_{\text{calc}}(v), & \text{if } v_{\text{cut-in}} \leq v_{\text{wind}} < v_{\text{rated}} \\ P_{\text{rated}}, & \text{if } v_{\text{rated}} \leq v_{\text{wind}} < v_{\text{cut-out}} \\ 0, & \text{if } v_{\text{cut-out}} \leq v_{\text{wind}} \end{cases} \tag{4.1}$$

Here, the wind speed is denoted by v. The operational logic encapsulated from these equations is straightforward: the turbine remains dormant below the cut-in wind speed. Post this threshold, power

generation initiates, intensifying progressively until the rated wind speed is attained. Beyond this point, the turbine consistently delivers its rated power, up until the cut-out wind speed, at which operation halts for safety considerations. Within the range of the cut-in and rated wind speeds, the power's relationship with the wind speed is cubic, represented by:

$$P_{\text{calc}}(v) = \frac{1}{2}\rho C_p A v^3 \tag{4.2}$$

Here, the air density, ρ, denotes the mass of a cubic meter of air, while C_p is the power coefficient, illustrating the turbine's efficiency in converting this into kinetic energy. A represents the rotor-swept area, indicating the volume of wind the turbine interacts with. The maximum power coefficient, $C_{p_{\text{max}}}$, is calculated using the following relation:

$$C_{p_{\text{max}}} = \frac{P_{\text{rated}}}{0.5\rho A v_{\text{rat}}^3} \tag{4.3}$$

Where for the velocity v and P, the rated wind speed and power are taken. However, the turbine's output power is not solely dictated by the wind speed. Several operational losses, arising from inefficiencies in the generator, mechanical components, and the electrical subsystem, play a pivotal role. Moreover, when considering a cluster of turbines, wake-induced losses emerge due to interference from surrounding turbines. Yaw misalignment is another form of loss, however, it is assumed that this is monitored and adjusted constantly and thus this loss is reduced to zero.

Table 4.1: Efficiencies affecting the performance of the wind turbine

Parameter	Unit	Value	Reference
Generator	%	3.5	EIA, 2020
Mechanical	%	1.0	Barthelmie et al., 2009
Electrical	%	1.0	Barter et al., 2023
Wake	%	10.0	Moriarty et al., 2020

The variables used to describe the system are presented in Table 4.2.

Table 4.2: Design parameters of the 15 MW IEA wind turbine

Parameter	Symbol	Unit	Value	Reference
Rotor diameter	D_r	m	240	EIA, 2020
Cut-in speed	$v_{\text{cut-in}}$	m/s	3	EIA, 2020
Rated speed	v_{rated}	m/s	10	EIA, 2020
Cut-out speed	$v_{\text{cut-out}}$	m/s	20	EIA, 2020
Rated power turbine	P_{rated}	MW	15	EIA, 2020
Air density	ρ	kg/m^3	1.225	EIA, 2020

Given these variables, the model produces the power curve as seen in Figure 4.2.

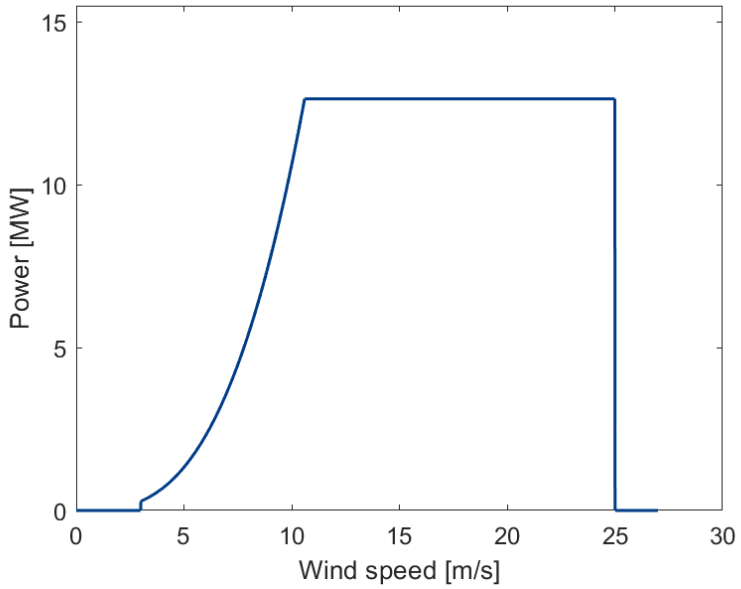

Figure 4.2: The wind turbine's resultant power curve after including all system inefficiencies

In this figure, it is evident that the wind turbine commences energy production at the cut-in wind speed, which is 3 m/s. Subsequently, the power output increases quadratically until the rated wind speed is attained at 10 m/s. Beyond this point, the power remains constant up to the cut-out wind speed. It is crucial to note that this describes the resultant power curve, taking into account the efficiency losses.

PEM electrolyser

The Proton Exchange Membrane (PEM) electrolyser system model is designed to simulate how electrical energy is transformed into chemical energy through water electrolysis. At its heart, the system relies on the electrolyser stack. When powered, this stack splits water, producing hydrogen and oxygen. The model focuses on efficiently managing power input, maintaining stack performance, and ensuring components are either maintained or replaced as needed. It's based on six stacks, each with a capacity of 2.5 MW, as described in Section 3.4.2. Key performance parameters, such as startup times, efficiency curves, degradation, and stack replacement, are integral to the model, allowing for various power management simulations.

Performance in a PEM electrolyser is comprehensively quantified through an efficiency curve as shown in Figure 4.3. This curve is a composite of two pivotal components. The first is the Direct Current (DC) efficiency curve, which illustrates the efficiency alterations corresponding with an incremental partial load (Lettenmeier, 2021). The secondary component amalgamates various elements accountable for ancillary system losses, including the Faraday efficiency. This efficiency factor encapsulates losses due to membrane diffusion, electrical current, and hydrogen purification stages (Lettenmeier, 2021). The combined effect of these two components gives rise to the system's overarching efficiency curve. This curve, based on the specific supplier, may integrate additional factors such as stack efficiency, AC/DC conversion losses, water treatment, cooling mechanisms, and hydrogen purification (Lettenmeier, 2021), the efficiency curve adapted for this study is from Lettenmeier. As seen in the figure, the maximum efficiency is set at 80% of the nominal efficiency. Furthermore, the minimum required load is set at 8% (Martinez Lopez et al., 2023).

An electrolyser efficiency of 50 kWh/kg H_2 (Yates et al., 2020) is employed in the model which is inclusive of the Balance of Plant (BOP) when considering the efficiency curve too, following projections for the year 2030. This efficiency value serves as a pivotal element in the model's power management algorithms and output predictions. In the results chapter, different technology development cases will be applied to evaluate the sensitivities.

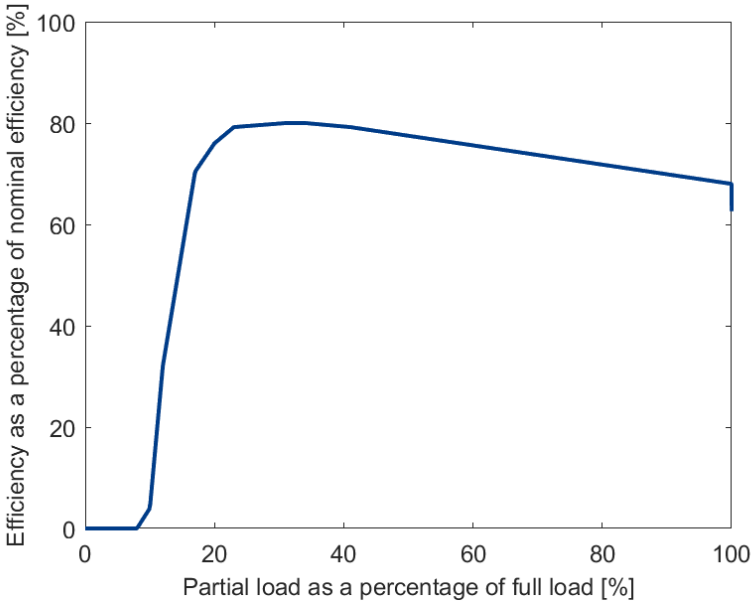

Figure 4.3: PEM relative efficiency curve as a function of the load

Degradation is an inherent characteristic of the electrolyser stacks, and the model accounts for this by continually recalibrating each stack's efficiency. This ensures that the model's hydrogen production predictions closely mirror real-world results. The lifetime of a stack is gauged at 80,000 operational hours (Yates et al., 2020), influenced by a degradation rate of 0.2% per 1,000 hours (Yates et al., 2020). However, as the degradation rate is modelled as a function of time, it will be interesting to see what influence the stack replacement frequency and timing has on the hydrogen yield and Levelised Cost of Hydrogen (LCOH). Timely stack replacement is a crucial aspect that the model meticulously manages. Replacement criteria are twofold: the stack's cumulative operational hours and the total elapsed time since its last replacement. Once one of these criteria is met, a replacement process is initiated for one or multiple stacks. Furthermore, startup times are included in this model, with cold startup taking one hour and warm startup requiring five minutes. The water consumption of the stacks equals 10 L/kg H_2 (M. Khan et al., 2021).

Strategies have been formulated by Philippo for the distribution of electrical power across its six stacks, each with a capacity of 2.5 MW, placed in parallel, resulting in a total capacity of 15 MW. Three key modes of operation are used. The *Fixed Mode* provisions power based on a pre-established setpoint. In contrast, the *First-On Strategy* adopts a sequential approach, initiating power allocation with the first stack and then redistributing any residual power among the remaining stacks. The *Equal Mode* strives to equally distribute power across all active stacks.

Table 4.3: Stack characteristics in the PEM electrolyser model

Parameter	Unit	Value	Source
Total stacks	–	6	Section 3.4.2
Individual stack capacity	MW	2.5	Section 3.4.2
System Total Capacity	MW	15	Section 3.4.2
Overall system efficiency	kWh/kg H_2	50	Yates et al., 2020
Degradation rate	% per 8760 hrs	2.0	Yates et al., 2020
Stack lifetime	hrs	80,000	Yates et al., 2020
Cold startup time	hr	1	Yates et al., 2020
Warm startup time	min	5	Yates et al., 2020
Water consumption	L/kg H_2	10	M. Khan et al., 2021

Water treatment

The model calculates the energy requirements for water treatment in several key stages. Initially, a consumption rate of 0.01 m^3/kg of hydrogen is used to determine the amount of deionised water needed (M. Khan et al., 2021). The conversion rates from deionised to desalinated and desalinated to salt sea water are known within Shell. The product of these conversion rates ζ amount to 1.35 and 1.67, respectively. Meaning that for 1 m^3 of desalinated water, 1.67 m^3 of sea water is needed. While 1.35 m^3 of desalinated water are needed for 1 m^3 of deionised water. This means that for every 2.25 m^3 of sea water taken in, 1 m^3 of deionised water is produced, obtaining a conversion rate of 44.4%.

Two principal equations are used for energy calculations. The first equation calculates the power required for pumping, P_{pump}, as:

$$P_{\text{pump}} = \frac{Q_{\text{pump}} \rho_{\text{sea}} g h_{\text{pf}}}{\eta_{\text{pump}}} \tag{4.4}$$

The second equation governs the volumetric flow rate Q_{pump} through the system:

$$Q_{\text{pump}} = Q_{\text{pem}} \frac{1}{\zeta_{\text{filter}} \zeta_{\text{ro}} \zeta_{\text{edi}}} \tag{4.5}$$

These are integrated to yield a consolidated equation for energy requirements:

$$P_{\text{pump}} = \frac{Q_{\text{pem}} \rho_{\text{sea}} g h_{\text{pf}}}{\eta_{\text{pump}} \zeta_{\text{filter}} \zeta_{\text{ro}} \zeta_{\text{edi}}} \tag{4.6}$$

The energy consumption rates for various water treatment steps are outlined in Table 4.4, with pre-treatment requiring 0.7 kWh/m^3 , Reverse Osmosis 3.0 kWh/m^3 , post-treatment 0.2 kWh/m^3, and Electrodeionisation 0.6 kWh/m^3.

Table 4.4: Energy consumption in various water treatment steps

Treatment step	Energy consumption [kWh/m^3]	Reference
Pre-treatment	0.7	Shell estimate
Reverse Osmosis	3.0	Kim et al., 2019
Post-treatment	0.2	Shell estimate
Electrodeionisation	0.6	Lopez et al., 2017

These figures are integrated combined with the energy consumption of the pump, which is calculated accordingly to the electrolyser's needs and pump parameters that include a pump head height of 16 m (comprising a 15 m platform height and 1 m for lower tide levels), a seawater density of 1025 kg/m^3, and a pump efficiency of 92% (Shell internal knowledge), concluding all variables necessary for the calculation.

Power conversion

The wind turbine produces an alternating current (AC) characterised by its fluctuating current strength and frequency, as well as a notably high voltage of approximately 690 volts or even higher. To make this current compatible for the electrolyser and the other utilities on the platform, it needs to undergo a transformation process.

The transformation is achieved in two main steps: initially, a back-to-back (B2B) converter, comprising both a rectifier and an inverter, is used. This converter modifies the AC with its varying frequency into another AC, but with a constant frequency. It also adjusts the voltage to levels suitable for the platform's utilities. Following this, a rectifier is employed to convert the adjusted AC into a direct current (DC). This DC is then appropriately conditioned to be directed towards the electrolyser stacks. It should be noted that these transformation components have efficiencies of 99% for the inverter (Hayashi, 2013) and 98% for the rectifier (Yin et al., 2016).

4.2. RAM model

The Reliability, Availability, and Maintainability (RAM) model is the tool that, based on various properties of the components, maps out the reliability performance of the W2H system. Similar to the energy model, the architecture of the RAM model will be elucidated, including the inputs from the different components and the outputs.

4.2.1. Model architecture

The proposed model is a complex chain of interconnected components, arranged in both series and parallel configurations. It incorporates multiple known parameters such as failure rates, number of backup components, and the impact of a component's failure on the overall system, and is programmed to incorporate weights and financial data when they become available in the future. The model employs Monte Carlo simulation for system reliability analysis, running the process multiple times to generate a distribution function of outcomes. This enables drawing conclusions with a quantifiable level of certainty. Various methods exist to estimate the optimal number of simulations, ensuring computational efficiency without sacrificing accuracy.

The model is designed based on a Reliability Block Diagram (RBD) as visible in Figure 4.4. In such a model, the W2H system can be viewed as a "pipeline", where the subsystems are linked based on dependency. If a component fails, it can be seen as a "leak in the pipeline", preventing the flow to the next subsystem. Once fixed, full output is possible again. Notably, after the Electrolyser BOP, the diagram branches into three different electrolyser containers. If one of these containers is defective, the other two can still deliver productivity. Within these subsystems, there are more detailed flow diagrams, which also work together in parallel or series configurations.

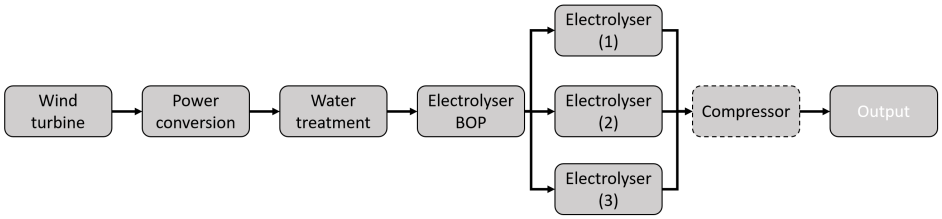

Figure 4.4: Reliability block diagram indicating the subsystems in a single W2H system

The model calculates what happens per time step in terms of failures, repairs, and other actions. An average performance will be calculated in this process. Thus, the model produces an RBD with filled values for factors like reliability, which is then incorporated into the complete system analysis. An illustration of this is visible in Figure 4.5, where it is evident that a certain level of reliability enters the 'electrolyser stack' block, an unreliability is subtracted, and then it progresses to the next block. This also illustrates that there are three parallel flows, pertaining to the three electrolyser containers that work in parallel with each other. If one is interested in a more detailed process flow chart for the RAM model, this is shown in Appendix E.

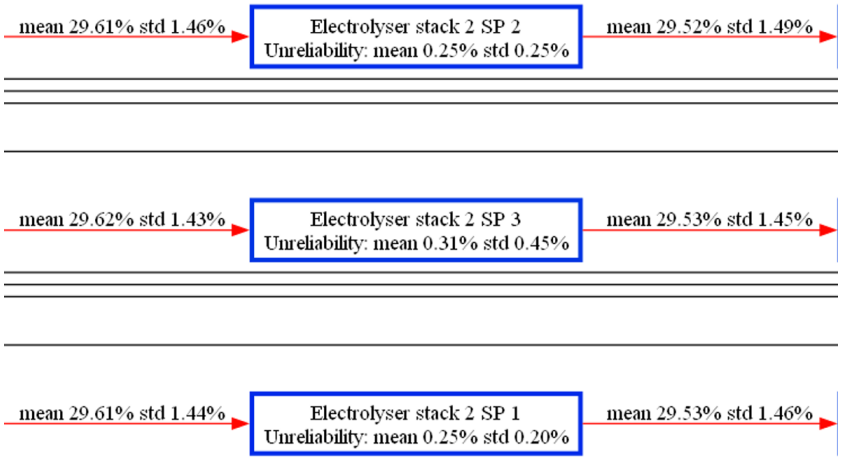

Figure 4.5: A screenshot from the RAM model creating RBD diagrams with component characteristics

The model operates on a time-resolved basis, allowing for an hourly or daily operational timeline over the entire lifetime of the project. It runs a Monte Carlo simulation for a specified number of runs and evaluates component failure every hour based on its failure rate. Two crucial parameters—component location and impact on production—are used to assess the repercussions of component failure. If a component fails, a repair crew is dispatched, incurring a certain mobilisation time. Once arrived, the component is repaired within a defined time frame, restoring the system to full functionality.

Backup components designed for extra redundancy are also part of the system. They are automatically triggered but require one time step to activate, due to system risks. In case of multiple component failures, the repair crew prioritises fixing vital components over backups.

A crew is typically comprised of two engineers, a standard corroborated by Shell. The model also allows for varying the number of crews per system. A decision must be made regarding the resolution of the data (hourly or daily), which affects the results accordingly. For instance, a repair requiring 25 hours will take two days in a daily simulation.

Plug-and-play features are integrated, allowing for full container replacement of a defective component rather than on-site repair. The efficacy of this maintenance strategy is also evaluated. Weather accessibility, based on wind data, is modelled to assess its impact on maintenance activities. Periods are randomly generated where maintenance operations cannot be conducted due to adverse weather conditions.

Scheduled maintenance is incorporated, assumed to be one week per year per system. The model allows for the inclusion of a degradation rate as a factor influencing failure rates but is set to zero in the base case. It focuses on critical component failures, omitting less severe errors like minor leaks. However, the failure of non-critical components such as the regeneration cycle, which results in approximately a 7% reduction in system output, is also considered. Also, when a (sub)system is down for 100%, it is modelled that no other components in that specific system can break down, as the system has become fully non-operational. Also, a constant failure rate is applied which simulates random failure.

The model can handle multiple systems but does not permit sharing of crews between them. Nevertheless, it does allow for the analysis of maintenance overlap between crews of different systems, providing insights similar to crew sharing.

Finally, the model's results provide a comprehensive RAM study, complete with plots showing system reliability, status, maintenance overlap, and the impact on system output.

Maths and performance indicators

In this section, one begins by establishing crucial terms that contribute to a nuanced understanding of failure and repair within the computational model.

- MTBF (Mean Time Between Failure) and FR (Failure Rate): MTBF is the average time interval before a failure occurs in an item or system, assuming proper maintenance, and is usually measured in calendar hours. MTBF is closely related to the Failure Rate (FR), which is the average number of failures per unit time, typically expressed as the number of failures per million calendar hours and symbolised by λ. Mathematically, FR is the reciprocal of MTBF. This relationship highlights how often failures occur and the expected time between these failures.
- MTTR (Mean Time To Repair) and Repair Rate: MTTR represents the average time required to repair an item or system, contributing to the total downtime. Correspondingly, the Repair Rate (RR) quantifies the average number of successful repairs within a given time frame. It is symbolised by μand is the reciprocal of MTTR. This metric emphasises the efficiency and speed of the maintenance process, linking the time taken for repairs with the frequency of successful repairs.

There are also metrics to evaluate the system's RAM performance:

- Unreliability (UR) and Reliability (R): Unreliability represents the proportion of time when a system fails unplanned, defined as:

$$UR = \frac{\Sigma\text{unplanned annual downtime} \times (\text{output reduction}/\text{nominal output})}{totaltime} \tag{4.7}$$

  Reliability, calculated as:

$$R = 100\% - UR \tag{4.8}$$

  indicates the likelihood of the system performing as expected, excluding planned shutdowns.
- Planned Shutdowns (PS): Denotes the time when the system is unavailable due to scheduled maintenance, including turnarounds and other deliberate outages.
- Availability (A) and Unavailability (UA): Availability suggests the probability that a system can perform its intended function, inclusive of planned shutdowns, and is calculated as:

$$A = 100 \tag{4.9}$$

  Unavailability, the inverse of Availability, signifies the likelihood of system non-performance and is defined as:

$$UA = 100\% - A \tag{4.10}$$

In the computational model, various inputs serve to define the attributes of the components within the system. Components are organised in both series and parallel configurations, each following distinct simulation principles.

In a series arrangement, the failure of a single component leads to the complete system failure. Essentially, the system's reliability is determined by its least reliable component. The reliability RS for such a series configuration can be represented as:

$$RS = R_1 \times R_2 \times \ldots \times R_n \tag{4.11}$$

When the reliability of each component differs. If all components possess the same reliability, the equation simplifies to:

$$R_{system} = R^n \tag{4.12}$$

Conversely, in a parallel layout, the system continues to function unless all components fail. This results in a total system reliability that surpasses that of any individual component. The reliability R for a parallel system is formulated as:

$$R = 1 - \prod(1 - R_i) = 1 - (1 - R_1) \times (1 - R_2) \times \ldots \times (1 - R_n) \tag{4.13}$$

In cases where components have varied reliabilities. For identical components, the equation becomes:

$$R = 1 - (1 - R)^n \tag{4.14}$$

For hybrid systems that involve a combination of both series and parallel configurations, the strategy is to disassemble the system into homogeneous subsystems. The reliability of these segregated subsystems is computed initially. Subsequently, these values are reintegrated, using either series or parallel methodologies, to deduce the comprehensive system reliability.

In the assessment of the precision of results stemming from Monte Carlo simulations, specific statistical measures and probability rules are applied. The calculation involves determining the sample size or the number of simulations, n, through the equation:

$$n = \left(\frac{Z\sigma}{E}\right)^2 \tag{4.15}$$

where Z is the Z-value corresponding to the desired confidence level, σ represents the standard deviation of the sample, and E is the allowable error.

It's crucial to note that the standard error, which is derived from the given Z-value, standard deviation, and mean, plays a pivotal role. The standard error can be of two types, the Reliability Standard Error (RSE) offers an estimate of the standard deviation for the calculated system reliability. The Availability Standard Error (ASE) functions analogously to the Reliability Standard Error but pertains to the system availability metric.

These standard errors form the foundation for computing confidence intervals for both reliability and availability. Specifically, the lower and upper bounds of the Reliability Confidence Interval can be calculated as follows:

$$\text{Reliability Confidence Interval} = \text{Mean Reliability} \pm (Z \times \text{RSE}) \tag{4.16}$$

For Availability, the confidence interval is determined in a similar manner. These calculated intervals provide a quantifiable range within which the actual system reliability and availability are likely to reside, thereby offering a measurable gauge of the precision of the simulation outcomes.

4.2.2. Components

The wind turbine, as outlined in this format, is described as a system with several components: the blades, the blade bearing, the main bearing, the yaw ring, a generator, and a transformer. After this, within the broader energy model, the energy produced by the wind turbine transitions to the other components of the entire system. This wind turbine, as an entity, hasn't been subjected to extensive analysis in this model for two primary reasons. Firstly, wind turbines, as individual technologies, are better established, and their optimal configuration is relatively well-understood. Secondly, the wind turbine itself and its individual components tend to have notably low failure rates. Therefore, they are less likely to be the culprits in system-wide malfunctions. However, it's important to emphasise that the wind turbine, as a unit within the overarching system, plays a pivotal role. It undeniably holds a significant place in this analysis. The data related to the wind turbine and its components has been sourced from Shell's internal datasets.

The failure data concerning the electrolyser, BOP, power conversion, and water treatment facility has been sourced from the Offshore Reliability Data (OREDA) project and by Safder et al. OREDA is spearheaded by the Norwegian Petroleum Directorate and involves collaboration with prominent oil and gas enterprises. The central aim of OREDA is to enhance both safety and cost efficiency by promoting the anonymous exchange of maintenance and operational records of offshore equipment. As a result, a comprehensive reliability database is established, facilitating its use in RAM studies within the consortium of participating organisations. Notably, Shell is an active participant in this collaboration, thereby permitting its use of the data for investigative purposes. While the direct data remains confidential and is bound by usage restrictions, efforts to disseminate the generalised findings are currently under exploration. The data is structured as follows:

1. Inventory Part: This section provides a detailed description of each equipment unit for which data has been collected. Accompanying these descriptions are technical specifications including size, capacity, and operating mode.
2. Failure Part: This section chronicles all failure incidents throughout the observed period. Within the context of the database, a failure is defined as an event that necessitates the issuance of a work order followed by a corresponding maintenance action. The database categorises failures into four types: critical, degrading, incipient, and unknown. For the purposes of this model, the primary focus is on critical failures, with the potential inclusion of degrading failures pending further verification. Additionally, failure rates are documented in terms of a mean value, a lower and upper bound indicating a 90% confidence interval, and a standard deviation.
3. Maintenance Part: This section delineates both corrective and scheduled maintenance actions for each equipment unit, incorporating the type of action, the frequency, and the man-hours involved. The data also captures the downtime duration, the time taken for a component to transition from offline to online status. The repair time is highlighted as the period actively devoted to the component's rectification. Preliminary analysis suggests that, on average, the ratio of man-hours to repair time is two, signifying that each maintenance task typically involves the expertise of two qualified engineers. It's noteworthy that a significant proportion of the repair time can be ascribed to accessing the failure site, and if engineers could readily access the site, this time could perhaps be considerably reduced.

To ensure confidentiality, the failure data is not mentioned for each component, but a summary is provided for each subsystem. In Table 4.5, the failure data is presented, showing that the electrolyser subsystem has many components and is likewise most susceptible to failure. This stems from the fact that electrolysers contain very fine and complex components compared to, for example, the wind turbine. Additionally, the average repair rate of a component is shown, indicating that a repair to a wind turbine takes longer - arising from the fact that these components are more difficult to ship and replace due to their size. It is important to note that this average repair rate is excluding time to diagnose and mobilise.

Table 4.5: Failure data originating from Shell and OREDA participants

Name of subsystem	Number of components in individual subsystem	Average failure rate [day-1]	Average repair rate [days]
Wind turbine	5	3.7E-4	5.0
Power conversion	2	2.9E-5	1.0
Water treatment system	10	1.3E-3	2.3
Electrolyser BOP	15	1.0E-3	1.7
Electrolyser container	14	1.2E-3	1.5
Compressor	1	3.0E-4	3.0

4.3. Techno-economic model

The techno-economic model is a less complex model compared to the other two. It encompasses conducting a financial analysis and integrating the technical inputs derived from the other two models. This section will also elucidate the architecture of the model, as well as the financial assumptions underpinning this analysis.

4.3.1. Model architecture

To assess the financial feasibility of the system, a third model, a techno-economic model, is constructed. The dynamics of this model are considerably simpler. Using the cost of technologies derived from the literature, an estimate is made of the total system costs over the system's lifetime. Financial viability is calculated by considering the energy returns over the system's lifetime, and these performance indicators will be described in the subsequent section.

Maths and performance indicators

For the techno-economic analysis, the LCOH is utilised, a metric previously discussed in the literature review chapter. It serves as a crucial indicator in evaluating different hydrogen production methods, assessing the economic feasibility of in-house hydrogen production versus external procurement, or the viability of a business case. The discount rate is derived from the Weighted Average Cost of Capital (WACC), which represents the expected return required by investors for investing in such projects. These values vary, commonly ranging between 3% and 10% (International Renewable Energy Agency (IRENA), 2020), depending on the risk associated with the project.

4.3.2. Components

Wind turbine

In the context of the entire installation, the most significant impact on costs is attributed to the wind turbine. Various methods for cost estimation are discussed in the literature, which vary in their input variables, complexity, and application. The method applied in this study for cost estimation is based on the approach described by BVG. This method clearly delineates cost distribution, with adjustments made to suit the specific system under study. This results in a Capital Expenditure (CAPEX) of €2.03 million per MW and an OPEX of €70,000 per MW per year.

Given that the costs being analysed are for the year 2020, a projection to 2030 is necessary. This projection employs a learning rate concept, which is grounded in the single-factor learning curve method. The SFLC approach presupposes a defined rate of cost reduction (learning rate) correlating with each doubling of the cumulative installed capacity. This process, often termed 'learning-by-doing,' posits that the estimated CAPEX for a technology in a given year can be expressed through Equation 4.17:

$$CAPEX_{t=t} = CAPEX_{t=0}(\frac{Capacity_{t=t}}{Capacity_{t=0}})^{1-2^{\varepsilon}} \tag{4.17}$$

In this equation, the power term represents the learning rate as a fraction. The learning rate for wind turbines is assumed to be 10% (Shields et al., 2022), making a comparative analysis based on the installed capacity in 2020 and the projected capacity for 2030 possible. These total cost projections are shown in Table 4.6, with variations therein being a focal point for comparison in the sensitivity analysis section.

The installed offshore wind capacity in 2020 stands at approximately 65 GW, with projections for 2030 ranging from 200 GW to 300 GW depending on the growth rate . Both these values will be considered in the sensitivity evaluation. However, an average figure of 250 GW will be adopted as the nominal case for 2030.

Table 4.6: Wind turbine financial estimates for 2030 for different cases based on the capacity development

Costs component	Unit	2020	2030 nominal	2030 pessimistic	2030 optimistic
CAPEX	M€/MW	2.03	1.64	1.59	1.69
OPEX	k€/MW/year	70	60	57.5	62.5

PEM electrolyser

Within the literature, there is a wide array of cost estimations for the PEM electrolyser. For instance, one source predicts that by 2030, the specific CAPEX for the stacks will be $1.2 million per MW, and the BOP CAPEX will be $500,000 per MW, with a specific CAPEX amounting to 1.5% of the CAPEX annually (Smolinka, 2023). Additionally, this source estimates that the stack replacement costs, due at the end of the stacks' lifespan, will be equivalent to 50% of the stacks' CAPEX. In contrast, another source suggests significantly lower figures, with the specific CAPEX for the stacks estimated at $300,000 per MW, BOP CAPEX at $470,000 per MW, and OPEX at $25,000 per MW (Holst et al., 2021). For a 15 MW setup, this equates to a total CAPEX of $11.4 million, markedly less than the $28.5 million indicated by the former source, representing more than a 50% reduction.

Internal sources at Shell lean towards the higher estimates, suggesting that the figures from the first source provide a more realistic depiction. However, there remains substantial uncertainty due to the unpredictable evolution of the technology. Given this uncertainty, the study will consider various scenarios, which will be elaborated upon in the results chapter. The nominal case for these calculations is presented in Table 4.7.

Table 4.7: Cost estimation for the electrolyser, adapted from Smolinka

Component	Unit	Value
CAPEX stack	M€/MW	1.2
CAPEX BOP	M€/MW	1.4
Stack replacement	%/CAPEX stack	50
OPEX	%/CAPEX	3

Lastly, the compressor, as a separate component in the energy and RAM model, is demonstrated and simulated, with the assumption that it is financially a part of the electrolyser plant.

Water treatment

The costs associated with water treatment are closely linked to the volume of water requiring treatment, which in turn depends on the size of the overall installation. An analysis by Shokri and Fard estimates that the CAPEX for water treatment ranges from $900 to $2,500/$m^3$/day. Given the offshore conditions, it is anticipated that these costs will be on the higher end of this spectrum. Another study, by Caldera and Breyer utilises a CAPEX estimate of $9,500/MW of electrolyser capacity. Comparing these values yields different cost implications in each scenario, the most conservative estimate is adopted in this research, and the values from study Shokri and Fard are assumed. The CAPEX is projected to be between 2.5% and 10% of the CAPEX annually, according to these studies. Here, too, the more conservative estimate is employed.

Additionally, the Electrodeionisation (EDI) unit, a component of the water treatment system, warrants separate consideration. Unlike the Reverse Osmosis (RO) pricing, which accounts for pre- and post-treatment processes, the EDI costs are not included in these figures. It is assumed for this analysis that the CAPEX for the EDI unit is equivalent to that of the RO installation, effectively doubling the total CAPEX for this component of the water treatment system.

Platform

The expenditure for the platform and reinforcements to the wind turbine are based on Shell internal estimates. These are calculated at €160,000 per installed megawatt (MW) of wind turbine capacity. The CAPEX is projected to be 2% of the CAPEX annually.

Costs overview

Table 4.8: Financial data overview for the W2H system's components

Input parameter	Unit	Value	Reference
Wind turbine capacity	MW	15	-
Wind turbine CAPEX	M€/MW	1.64	BVG Associates, 2022
Wind turbine OPEX	k€/MW/year	60	BVG Associates, 2022
Electrolyser capacity	MW	15	-
Electrolyser CAPEX	M€/MW	1.7	IEA, 2019
Electrolyser OPEX	k€/year	34	IEA, 2019
Electrolyser stack replacement cost	M€/MW	0.48	IEA, 2019
Water treatment capacity (salt water)	m^3/day	89.7	-
Water treatment CAPEX	k€/m^3/day	5.0	Shokri and Fard, 2023
Water treatment OPEX	k€/m^3/day	0.5	Shokri and Fard, 2023
Platform CAPEX	k€/MW wind turbine	160	Shell
Platform OPEX	k€/MW wind turbine	3.2	Shell

4.4. Combined model

Combining the three models described above yields the most insightful conclusions. This approach allows for an analysis of a system based on energy yield, reliability, and lifetime economics. Connections have been established between the models to facilitate this. For instance, when calculating a LCOH, the reliability of the installation can be taken into account, providing a reliability interval for the LCOH compared to a LCOH where the installation would be 100% operational. Consequently, a more reliable estimate of the hydrogen price can be determined, offering a better indication of business prospects.

4.5. Multiple system model

To address the final sub-research question, the scope is expanded from a single W2H system to a W2H farm. In the subsequent sections, the architecture of the model, assumptions and differences in comparison to the single W2H model will be discussed.

4.5.1. Model architecture

The single system model was developed to simulate an individual W2H system. Although it can run multiple systems in a simulation, it does not support the simulation of shared engineering crews across multiple W2H systems. This limitation arises from the model's structure, which processes each system's entire life cycle, then the number of Monte Carlo simulations, before proceeding to the next system. To analyse the dynamics and effects of sharing engineers among different systems, a method has been devised. This method, implemented in Matlab, operates on the following principles: from the single system model, simulations are run with varying system sizes, ranging from e.g., 10 to 70 identical W2H systems. The model can report, at each time step, whether a W2H system is operational or not, an example of which is shown in Figure 4.6. A non-operational status indicates either ongoing repairs or awaiting repairs.

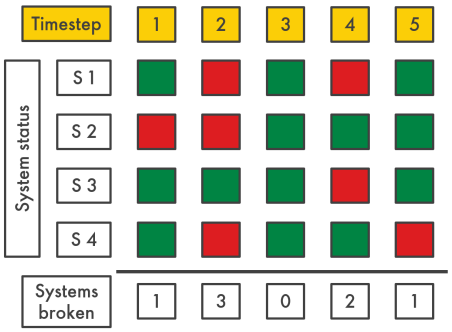

Figure 4.6: Example indicating the count in W2H system status for the delay calculation

At each time step, the number of W2H systems in maintenance is tallied to provide an overview. This metric measures the percentage of time a certain number of turbines are simultaneously under maintenance. For example, a 10-system W2H farm is more likely to have zero turbines under maintenance at the same time compared to a 70-system W2H farm. The term 'overlap in maintenance' has been coined for this metric.

Knowing the 'overlap in maintenance,' the new model calculates the delay in maintenance caused by this overlap. For instance, if there is one crew and two W2H systems needing maintenance, the second system experiences a delay equal to the repair duration of the other turbine, considering mobilisation and weather windows. This delay reduces the system's reliability due to increased downtime, impacting the LCOH through lower hydrogen yield. The model calculates the delay as a function of average repair duration, failure impact (since a failure in a subsystem does not always halt W2H production, and the number of available engineers. It then integrates these results to provide updated reliability, availability, and LCOH figures for each system size, compared to the original scenario without delay consideration.

A key consideration in comparing a W2H farm with a single W2H system is the role of the service operator. This group consists of engineers responsible for the maintenance of the farm. Depending on various factors such as the farm's size and distance to the Operations & Maintenance (O&M) port, the crew might either wait in the port or be on standby from a Service Operation Vessel (SOV). Such vessels accommodate the ship's crew, various engineers, and equipment and parts for repairs. In the W2H farm model, the number of SOVs is a variable, essentially representing how many engineers are ready to perform maintenance should the need arise. Additionally, the assumption remains that two engineers, on average, complete one job together. This is based on the understanding that not every engineer can perform every task, and there is a possibility of unforeseen circumstances such as illness occurring on board.

Repair duration and impact are averaged using data from datasheets and the following equations:

$$\text{Average MTTR} = \frac{\sum(\lambda_i \times R_i)}{\sum \lambda_i} \tag{4.18}$$

$$\text{Average Impact} = \frac{\sum(\lambda_i \times \text{Impact}_i)}{\sum \lambda_i} \tag{4.19}$$

By applying this model on the base case situation, the following analyses are performed:

W2H Farm Availability as a function of maintenance crew size As described above, the availability of the W2H farm can be calculated by scaling up from a single W2H system to a W2H farm and computing the maintenance delay. This allows for the determination of how the availability changes as the size of the W2H farm varies, as well as with different numbers of SOVs.

The literature LCOH considering calculated W2H farm availability With the aforementioned average availability of the W2H farm for various farm sizes and numbers of SOVs, the LCOH can also be calculated using data from the literature. This will provide insights into whether the assumptions made are a true reflection of reality.

An alternative LCOH considering calculated W2H farm availability Furthermore, an alternative calculation of LCOH can be applied to the average availability of the W2H farm. This calculation will alter the calculation of the LCOH on certain CAPEX and OPEX parts. The precise data will be discussed in the following paragraph. From this, a LCOH value will also emerge. A comparison between this and the previous calculation may potentially yield material for an intriguing conclusion.

A comparison between onshore and offshore OPEX expenses and LCOH Finally, this model is capable of conducting a global comparison between the scenarios of the farm being positioned offshore or onshore. There are many differences between these two situations, including energy output, CAPEX, and OPEX. To limit the scope of this study, the focus will be on the differences in OPEX. Additionally, the results of the LCOH calculations will be presented. However, it should be assumed that the lower CAPEX on land offsets the lower energy yield compared to the offshore variant. This is a basic assumption but primarily provides an analysis of the operational expenditures, which is the focus of this research. To make a fair comparison with an equal amount of personnel, this variable will not be varied. On land, one is not limited by the space on a ship, but the amount of personnel will nevertheless be equalised. The exact financial details will be provided in the following paragraph.

4.5.2. Alternative financial parameters

Compared to the single system model, there are modifications in the economic parameters available. This information, provided by Shell, is intended for internal use.

CAPEX

In terms of CAPEX, economies of scale are realised by distributing costs across multiple W2H systems. According to Shell's wind team, no additional benefits are observed beyond 50 turbines in a wind farm.

Therefore, a premium is applied for systems with fewer than 50 turbines. This premium is quadratic related, being 30% for a single turbine, 20% for 10 turbines, and 0% for 50 turbines. It is assumed that a similar principle applies to electrolysers. As stated, it is assumed that there are no differences in CAPEX between onshore and offshore. This is probably not realistic, however, it is assumed that the lower energy yield sets off the decrease in CAPEX in the LCOH calculation.

OPEX

Estimating the Operational Expenditures (OPEX) of such systems is challenging due to situational variances. Different departments within Shell have proposed varied estimates, as explained below:

In the first scenario, Shell estimates the daily rate for a SOV with a Walk-to-Work (W2W) bridge, staffed by six engineers and eight crew members, at approximately €15,000 per day.

The second scenario involves a SOV with W2W bridge, staffed by 24 engineers and eight crew members, costing €30,000 per day. The annual cost per engineer is about €50,000. However, due to offshore conditions and the nature of work, Shell's costs increase by 2.5 times, totalling €150,000 per engineer per year. This second scenario also addresses the possible integration of onshore maintenance costs. Here, the vessel costs are excluded, and employee salaries are multiplied by 1.5 instead of 3, mainly covering insurance and materials. Thus, an engineer costs €75,000 per year. This presents an interesting comparison between onshore and offshore W2H farms.

The Operational Expenditures (OPEX) within the model are distributed across operations, maintenance, and replacement costs. Maintenance costs are deduced from the previous calculations, while replacement costs are set at an annual rate equivalent to 1.0% of the CAPEX. These two components jointly form the comprehensive maintenance expenses included in the OPEX. For the estimation of operational costs, the model adopts the ratios based on the BVG study. This approach posits that operational costs amount to half of the total maintenance expenses.

For the model, the second OPEX scenario will be used due to its ability to separate vessel costs from engineer costs and the application of that possibility. The detailed distribution of these costs, offering insight into the financial aspects of operations, maintenance, and replacement, is systematically outlined in Table 4.9.

Table 4.9: OPEX costs dissected into operation, maintenance, and repair costs

Cost component	Unit	Offshore	Onshore
Operations	M€/year	6.1	1.1
Repair	M€/year	0.5	0.5
Maintenance	M€/year	11.6	1.8
Total	M€/year	18.2	3.4

The details behind the maintenance costs are shown in Table 4.10, where one should note that this considers merely one SOV, it is assumed that multiple SOVs will result in a multiplication of these costs.

Table 4.10: Components for the OPEX calculation for offshore and onshore situation

Metric	Unit	Offshore	Onshore
Engineers per SOV	-	24	24
Cost engineer	k€/year	150	75
Cost SOV	M€/year	7.95	0
Avg. mobilisation time	days	3.123	2.723

What becomes clear from establishing this alternative LCOH calculation is that the OPEX is predominantly independent of the size of the installations or the CAPEX. As seen in Table 4.9, for both onshore and offshore variants, maintenance constitutes the most significant portion of the OPEX and is independent of CAPEX. Thus will be further discussed in the multiple system results section.

5

Results and discussion

This chapter focuses on presenting the results of the research. It begins with a description of the case study, where the wind data will be analysed and the assumptions - encompassing aspects of hydrogen generation, maintenance, and economics - will be clarified. Following this, the results are presented, starting with a highlight on a single system. For this case, various sensitivity analyses are conducted, addressing both operational and maintenance aspects. The analysis then shifts to examining a wind farm size, evaluating the performance in terms of Reliability, Availability and Maintainability (RAM) and economic factors. The chapter concludes with the presentation of an improved Levelised Cost Of Hydrogen (LCOH) calculation, and an exploration of how this varies between offshore and onshore variant

5.1. Set-up of the case study

When developing models, it is ideal to test them on an existing site. This allows for verification of the model's outcomes against reality, and subsequently, exploration of potential optimisation methods. However, in cases where the specific construction does not yet exist, or its data is not available, another approach is needed. Therefore, this chapter will examine a hypothetical case study, situated somewhere in the North Sea. The following sections will detail the conditions at this location and outline the assumptions applied to the various models.

Context and scope

The geographical focus of this case study is a designated location in the North Sea. To maintain scientific rigour and uniformity across different aspects of this research, all assessments utilise the same hourly wind input. This is derived from 21 years of wind data, corresponding to the projected lifespan of the wind turbine field under study. While average wind speeds serve as a key metric, it's worth noting that they may not encapsulate the complete operational dynamics of the wind turbines. For instance, they might fail to capture extreme wind events that are not readily discernible from hourly datasets. The data set has been extrapolated to also be able to run projects with a lifetime of longer than 21 years (D'Ambrosio et al., 2020; Naimo, 2014). The wind speeds are measured at 150 m, which is convenient as the hub height is the same. When this is not the case, the power law shall be applied to adjust wind speeds to the hub height as described in Equation 5.1.

$$U(z) = U(z_{ref})(\frac{z}{z_{ref}})^{\alpha} \tag{5.1}$$

Where z_{ref} equals the reference height, 150 m in this situation, $U(z_{ref})$ the wind speed at 150 meters and z the desired height where the wind speeds need to be extrapolated to. $\alpha$is the wind shear exponent, which is a constant based on the type of terrain, for open water, this would be around 0.1.

Description of the W2H system location

The wind turbine field is located in the North Sea, specifically at least 150 km away from the nearest coast, an example of a suitable location is the Doggerbank. This seabank is potentially ideal for wind energy harvesting as it is relatively shallow, allowing for smaller foundations. Owing to this offshore location, the field does not rely on electrical cables for energy export. Instead, the energy will be exported as hydrogen. The field does not consist of a predetermined number of turbines, rather it will consist of anywhere between 10 and 70 Wind-to-Hydrogen (W2H) systems, totalling a combined power of anywhere between 150 MW and 1.05 GW. Different sizes of W2H will be scrutinised in this chapter.

For optimal performance and safety, the turbines are positioned three rotor diameters apart in the horizontal direction and also three diameters apart vertically. For hydrogen export, pipelines are laid in trenches following every two horizontal lines of turbines. These pipelines then converge towards the coast. Additional systems, such as compression stations or substations, may be deployed to regulate hydrogen flow, although the inclusion of these elements in this study remains undecided.

Wind data analysis

Shell has furnished wind data for the study location, not being the Doggerbank but something similar of which the location shall be kept restricted, encompassing parameters such as wind speed, direction, and temperature. The analysis of 192,863 hours of data yielded a Weibull scale factor of 11.59 and a shape factor of 2.22. In terms of operability, 5.07% of the observed wind speeds were below the cut-in speed of 3 m/s, and 0.45% exceeded the cut-out speed of 25 m/s. The mean wind speed was calculated to be 10.27 m/s, making it a favourable site for wind energy harvesting.

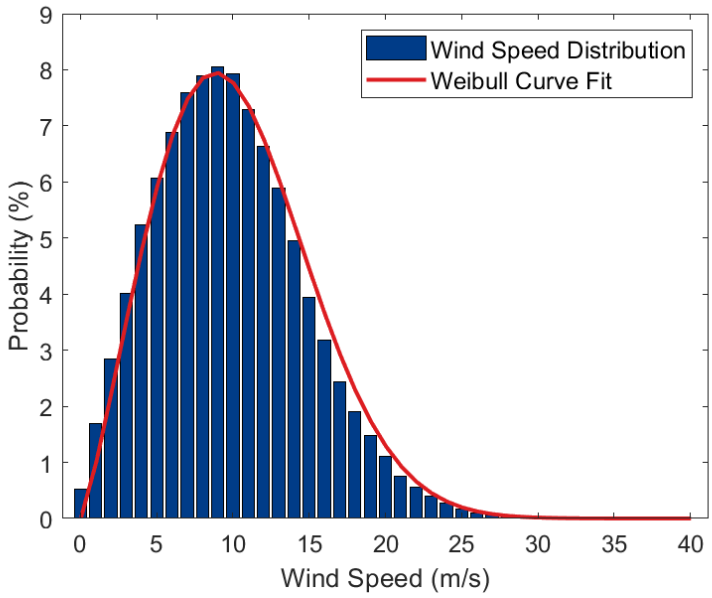

Figure 5.1: Weibull Distribution of the wind speeds at the study site

Geographical and economic parameters

The water depth at the location is 30 meters, which is a significant factor influencing the design and economics of offshore wind turbine installations (Sørensen et al., 2021). Economically, the discount rate is denoted as 7%. Furthermore, the commissioning time of the project is scheduled for 2030 and the project has a specified lifetime of 25 years.

5.1.1. Case study assumptions

In the summation below, an overview of the assumptions used for these models can be found with their explanation. Other assumptions, such as efficiencies and constants are described in Chapter 4.

Energy

- The lifetime of all system components, except the electrolyser stacks, are equal to 25 years.
- Degradation takes place in the electrolyser stacks, for now, other components are not under the influence of degradation.
- The chosen power management strategy is *Equal Power Division* since this strategy leads to a higher hydrogen yield according to Philippo (2023).
- The stack replacement strategy involves replacing all stacks after a certain operational time or total lifespan.
- The stack replacement has the same mobilisation time as other maintenance activities, and the replacement duration takes 1 day.

Maintenance

- Maintenance operations are contingent on wind conditions, specifically a maximum of wind power 5, equating to an accessibility rate of 56.5% based on the analysis in Equation 5.1. This reflects the unpredictable nature of weather, with maintenance windows being modelled as random events.
- The time allocated for mobilising maintenance activities is uniformly set at 24 hours, aligning with the timescale used in the study. The crew is assumed to be ready 24/7.
- A routine maintenance schedule is presupposed to occur semi-annually, with a duration of one day per session. The study will also explore the impact of varying this maintenance frequency. Small planned checks are assumed to be carried out opportunistically, whenever a crew is onsite for corrective maintenance. During scheduled maintenance, the system will be fully offline.
- A single maintenance crew is available for each system, consisting of two specialised engineers. This structure is informed by OREDA data and aligns with the practical skillsets required for diverse maintenance tasks.
- Initial assumptions include only random system failures. The influence of degradation on failure rates, following the typical 'bathtub curve' trajectory, will be examined in the sensitivity analysis to understand its impact over the system's lifespan.
- After maintenance has been done on a component, it will be restored to 100% operating efficiency
- Failure rate is constant, simulating random failure

Economic

- The economic evaluation utilises a consistent discount rate of 7%, providing a standard measure for the time value of money across the study.
- The simulation period spans 9131 timesteps, representing 25 years from 2030, inclusive of leap years, to provide a comprehensive long-term analysis.
- The system's operational lifespan is defined as a 25-year period, starting on January 1, 2030, and concluding on December 31, 2034, framing the temporal scope of the study.

5.2. Single system results

Initially, the models for the single W2H system are executed. This involves evaluating the energy, RAM, and techno-economic outcomes, running sensitivity cases, and drawing conclusions on the significance of these results.

5.2.1. Energy model

The simulation conducted through the energy model revealed that the total hydrogen production over a span of 25 years for a single W2H system is projected to be 21.45 kt H_2. This translates to an annual production rate of approximately 0.86 kt H_2. The detailed progression of this production over the system's lifetime is illustrated in Figure 5.2.

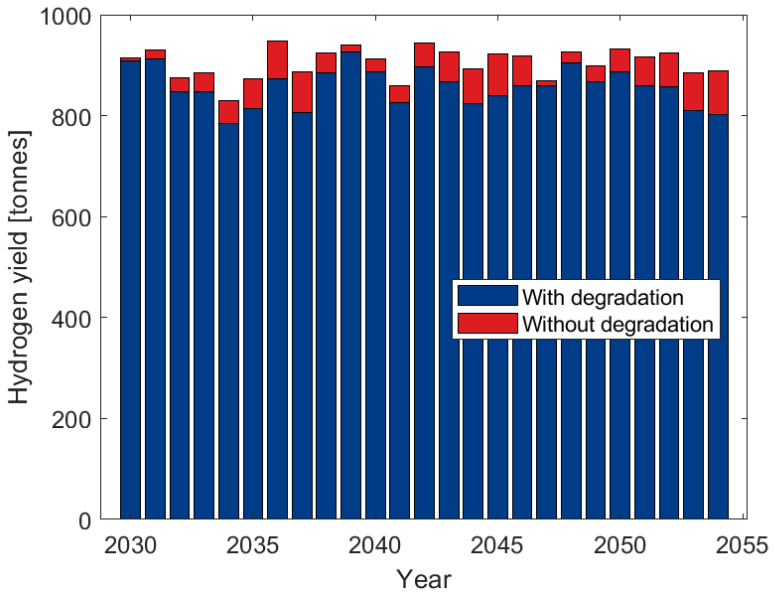

Figure 5.2: Annual hydrogen production in tonnes over the system's life time denoting the difference between inclusion and exclusion of stack degradation

This figure illustrates the annual hydrogen yield from 2030 to the project's conclusion at the end of 2054. The blue bars represent the actual hydrogen yield from the energy model. Additionally, the newly integrated aspect of stack degradation and replacement has been incorporated. The loss due to this degradation is evident in the red segments of the bars in Figure 5.2, which show the potential yield height if stack degradation were not a factor. Notable moments in the system's operation include stack replacements at two intervals: 2039 and 2047. The hydrogen yield, as shown in Figure 5.2, reveals a significant increase in hydrogen production following these replacement events. Furthermore, Figure 5.3 offers insights into the impact of stack degradation on hydrogen production efficiency. This degradation contributes to the observed decrease in hydrogen output over time.

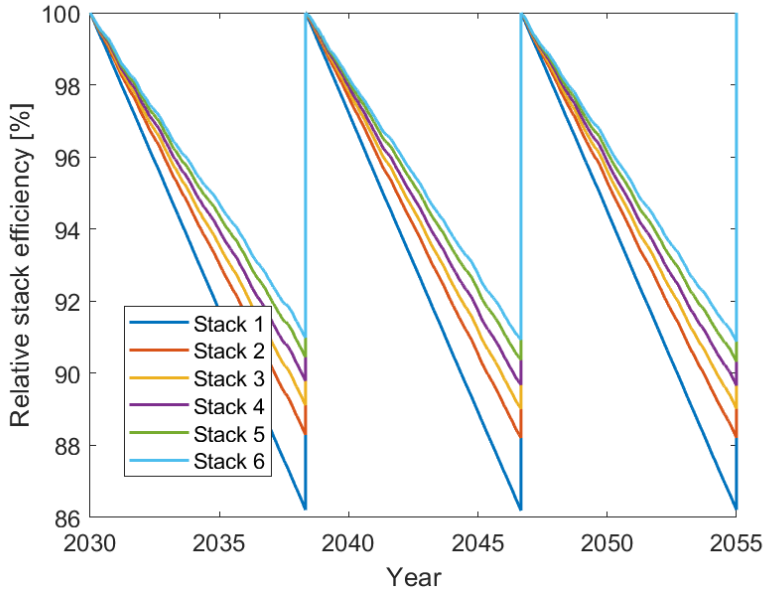

Figure 5.3: Stack degradation over the system's lifetime

Here, the term 'relative stack efficiency' denotes the performance of the stack without considering the efficiency curve. It focuses instead on the additional efficiency factor that must be accounted for due to degradation. This figure shows that the six different stacks each have a unique stack efficiency over time, but all start at 100% relative efficiency and after stack replacement start again at 100%. The variation in degradation among the stacks is attributed to the application of the chosen power management strategy, as previously described in Figure 4.1.2. It is evident that stack 1 degrades the most rapidly due to more frequent use, followed by stack 2, and so on, up to stack 6. At the moments of exchange, all stacks are replaced simultaneously, which is a stated assumption. Notably, there is a considerable difference in relative efficiency. For instance, when stack 1 reaches a relative efficiency of about 86%, stack 6 is at approximately 91.5%. For further research, it is recommended to explore the optimal replacement strategy, especially in a W2H farm scenario where multiple stacks are likely to experience similar degradation.

Following the calculation, the financial assessment of the project indicates a LCOH of €7.72/kg H_2. This metric can be dissected into either a technical or financial breakdown. In the financial breakdown, the LCOH is dissected into either Capital expenditures (CAPEX), Operational expenditures (OPEX) or Other Costs. Where 'Other costs' only entail stack replacement at this time. Furthermore, the technical breakdown encompasses the different component of the W2H system, where it is divided between the wind turbine, electrolyser, platform-related expenses, and water treatment. A comparative analysis of these cost components and their contribution to the overall LCOH is graphically represented in Figure 5.4. For this particular LCOH calculation, the RAM was not included.

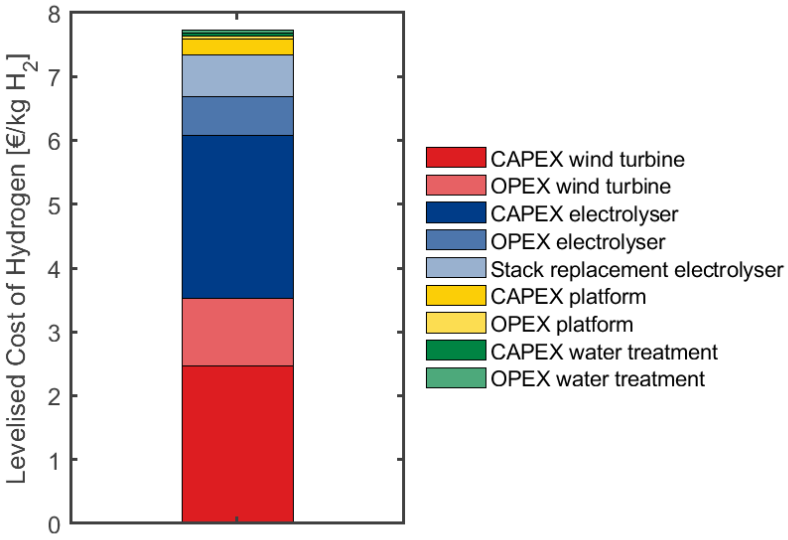

Figure 5.4: LCOH breakdown into financial and technical components - without RAM

In this figure, it is apparent that the total bar sums up to €7.72. The LCOH is predominantly influenced by the costs associated with the wind turbine and the electrolyser. Upon initially examining the financial breakdown, it is noticeable that the overall CAPEX accounts for a majority, contributing €5.29 (68.5%) of the total €7.72, whereas the total OPEX totals €1.78 (23.1%) and stack replacements are responsible for €0.65 (8.4%). The reason for this is not that the OPEX costs are significantly lower than the CAPEX. On the contrary, the model reveals that the total CAPEX costs amount to €52.9M, the total OPEX over the lifespan is €37.3M, and the cumulative cost for stack replacements is €14.2M. Hence, there is a distribution where the differences are proportionally smaller than when examining the LCOH. However, because the LCOH employs a discount rate, the annually amortised OPEX has a lower impact than the CAPEX, which is paid at the start of the project according to this calculation. On examining the technical breakdown, on the other hand, two aspects stand out: firstly, the dominance of the costs of the wind turbine at 46.5% of the total and the electrolyser with 48.3%, with the electrolyser unexpectedly

occupying a larger share within the LCOH. This can be attributed to the €14.2M in stack replacement costs that the electrolyser is subject to, a cost not incurred by the wind turbine. Secondly, it is notable that the components of the water treatment system and the platform have a very low share, totalling 5.2%. This suggests that investments in the platform or water treatment system, which improve the W2H system's functioning, likely have little impact on the overall LCOH. In other words, a doubling in the CAPEX of the platform does not significantly affect the LCOH, a principle not applicable to the electrolyser. It is also noted that not all components are included in this scope. However, it can be assumed that for the single W2H system, these are the major cost components, and the addition of other parts is unlikely to significantly impact the LCOH. For the bar charts showing the financial and the technical breakdown separately, this is shown in Figure F.1.

5.2.2. RAM model

The RAM simulations were conducted on the pilot case, which involves a scenario without backups for any single component. The Monte Carlo simulations were performed 250 times to ensure the accuracy of the results. An average reliability of 87.5% was observed, following an average availability of 87.0%. The 99% confidence interval is ±0.2%, indicating that one can be 99% certain that the true average result will differ by no more than 0.2%, either upwards or downwards. The result is visible in Figure 5.5.

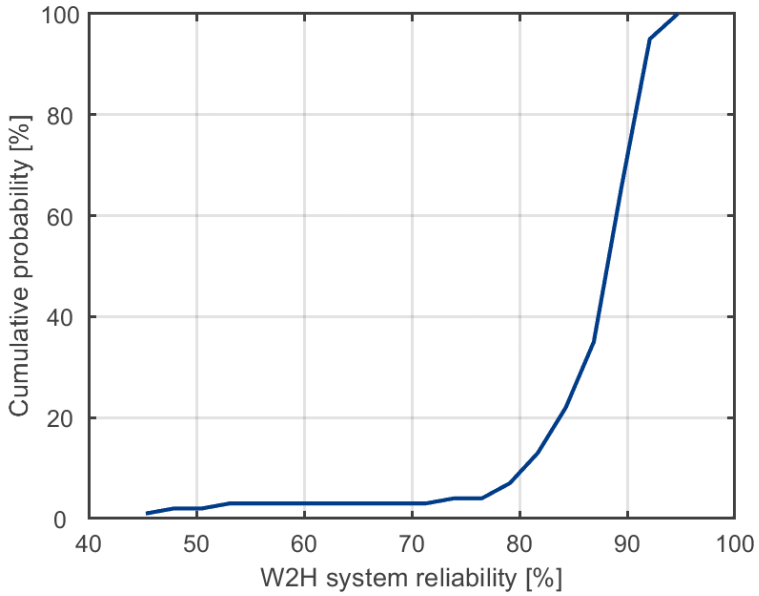

Figure 5.5: Cumulative probability distribution function for the reliability of the system without backups

Here, the cumulative probability of the average reliability of the W2H system is illustrated. It is evident that there is a small chance of an average reliability lower than 75%, after which the probability increases rapidly, crossing the average reliability at the imaginary line where the cumulative probability equals 50% at 87.5%.

The existence of a small yet present risk that the average reliability falls below 80% arises from a downward spiral of maintenance backlog, leading to reduced productivity of the W2H system. This situation typically begins with the failure of a component, resulting in partial productivity loss. During the time required for mobilisation and repair, other components may fail, creating a cascading effect of breakdowns. Such a scenario is detrimental to the system's performance, necessitating a solution to prevent these situations.

To enhance reliability, research was focused on system variations and the implementation of backups. Insights provided by Shell's green hydrogen team offered strategies for incorporating backups for several sensitive components of the W2H system. By integrating these backups into specific components,

an optimised version was simulated. The same number of simulations were applied to this version, yielding an average reliability of 88.6% and an average availability of 88.1%, with the 99% confidence interval also at ±0.2%. The incorporation of backups results in an increase of 1.1% in both reliability and availability. The effectiveness of this approach is illustrated in Figure 5.6.

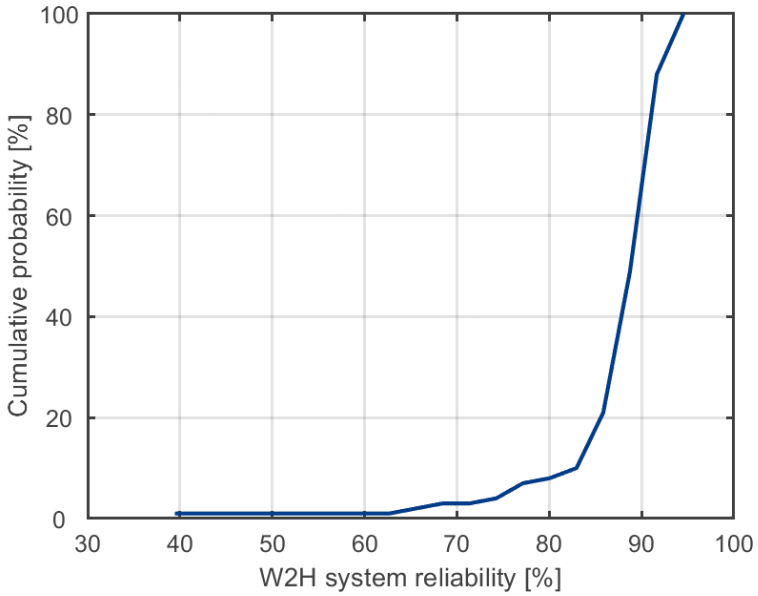

Figure 5.6: Cumulative Probability Distribution function for the reliability of the system with backups - the base case

When compared to the graph representing the W2H system without backup components, it is evident that the backups mitigate the risk of low system reliability, as the graph maintains closer proximity to the x-axis for lower reliability values. This system configuration is deemed realistic, and therefore, this variant with backups is henceforth considered as the *base case*.

The availability differs only marginally from the reliability, attributable to the relatively minor impact of planned maintenance in the base case, following from Section 4.2.1. The disparity between these averages is 0.5% in the base case, aligning with the extent of scheduled maintenance.

The average total number of failures for this simulation is 720.2 across 9075 timesteps where failure can occur, with the possibility of multiple failures occurring at different locations in the same timestep. A key conclusion from this data is that a maintenance crew would need to repair failures, on average, 28.8 times per year. It is noted that these failures include those of components with backups. These backups will be opportunistically repaired, meaning that the actual number of trips for corrective maintenance may be less than 28.8.

To analyse which subsystems are responsible for reducing reliability, one can refer to Figure 5.7, which displays the full load hours per subsystem.

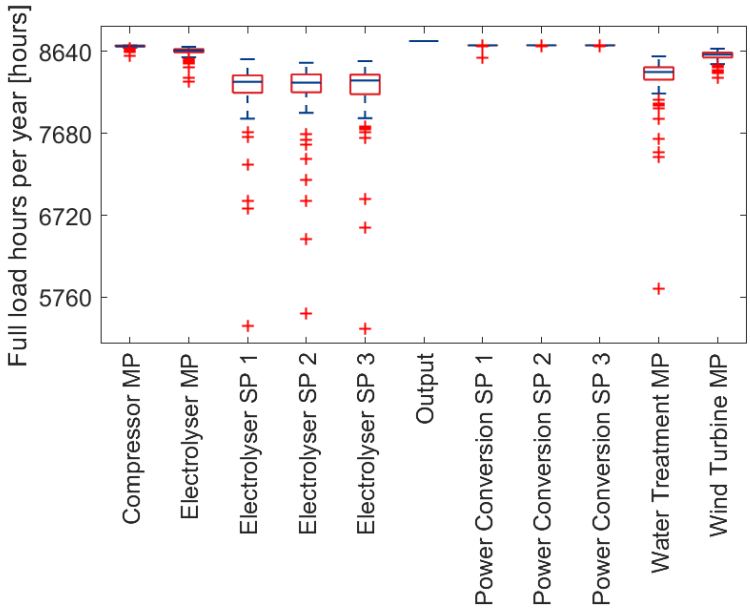

Figure 5.7: Full load hours per subsystem in the base case

This figure presents the full load hours for each subsystem in the form of a box plot. The y-axis displays the full load hours as the number of operational hours in a year, with the maximum being 8,712—deducting 48 hours from the total 8,760 for scheduled maintenance. The box plots illustrate the median with the blue line within the red square, which represents the quartiles. The crosses surrounding them denote the values that fall outside these intervals. The full load hours of the subsystems provide a good indication of which systems are prone to failure and, due to their longer repair times, are also detrimental to extended periods of downtime. In full load hours, this is weighted according to the impact a component has within the subsystem. Notably, there are two sensitive systems with both a lower average number of full load hours and more extreme negative outliers: firstly, the electrolyser containers, including the components within the individual containers, are prone to failure. The spread of the boxplot shows that in adverse situations, it can drop to as low as 5,760 hours annually, from a total 8,712 available operational hours considering planned maintenance per year, that would constitute an availability of around 60%. Furthermore, the electrolyser containers display similar average behaviour, logically since these containers are identical, this will be of advantage to the system as the probability that all these systems will perform that bad, is small. Secondly, the water treatment system is prone to failure. While in the case of the electrolyser containers, the impact is divided by three due to their parallel configuration, this is not the case for the water treatment system. From this, one concludes that improvements in the reliability of this system should focus on the water treatment system, this could be subject to further research. The other subsystems provide appropriate FLH figures, and should not be prioritised in reliability optimisation research.

5.2.3. Combined models

Integrating the system's availability, as derived from the RAM model, with the hydrogen production figures from the energy model, facilitates an evaluation of the average RAM adjusted hydrogen production. This equates to 18.9 kt H_2 over the system's lifespan, or an average of 755.0 t H_2 annually. Compared to a scenario where the reliability of the W2H system is not considered, there is a decrease in total hydrogen production by 2.6 kt H_2, or 102.0 t H_2 annually. This represents a reduction of 11.9%. Such a decrease in expected yield can be categorised as moderate, yet in terms of its overall effect, it could be described as having a significant impact. The 99% confidence interval, as calculated in the previous paragraph, amounts to ±0.2%. In this situation, this translates to an interval of 1.5 t H_2 per year.

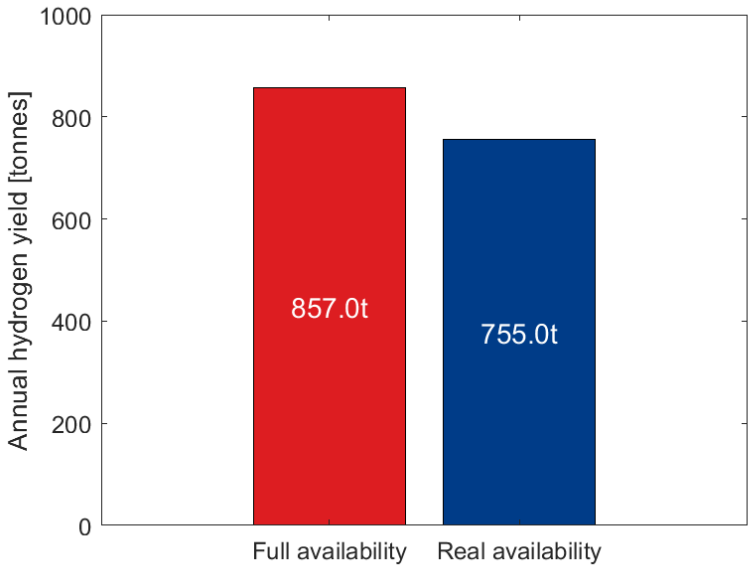

Figure 5.8: Average annual hydrogen yield adjusted for the W2H systems availability - with RAM

As the hydrogen yield is influenced by integration of RAM, the LCOH is likewise examined. The original LCOH, calculated without RAM modelling, stands at €7.72/kg H_2. Integrating the base case RAM model results in an adjusted LCOH of €8.76/kg H_2, as illustrated in Figure 5.9. This change represents an increase of €1.04/kg H_2, or a 13.5% rise. Here, the 99% confidence interval is described as an interval of €0.02/kg H_2.

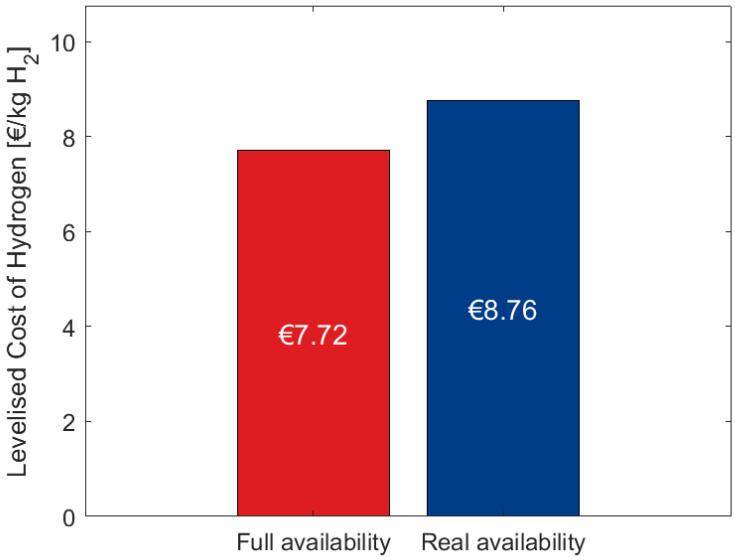

Figure 5.9: LCOH adjusted for system availability - with RAM

The integration of the RAM model into the technical and economic performance evaluations thus notably changes the outcomes. Specifically, the hydrogen production decreases by 11.9%. There is also a considerable effect on the LCOH, which increases by 13.5%. This increase corresponds to an additional €1.04/kg H_2, leading to an updated LCOH of €8.76/kg H_2.

5.2.4. Energy variable effects

To examine how the results change under the influence of high-impact parameters, in this case the technical development and costs of the electrolyser and the financial parameters of the wind turbine, a sensitivity analysis is conducted to evaluate how the LCOH changes when these are varied compared to the nominal base case. The decision to vary these components in groups is made because it falls within the scope of this research but does not constitute its primary focus. The central emphasis is attributed to the effects of the RAM model. This approach ensures a comprehensive examination of the system while maintaining a targeted focus on the most critical aspects of the study. The sensitivity study is conducted based on the case of an optimistic and a pessimistic scenario in comparison to the nominal situation. The input parameters are sourced from Chapter 4 and from the study by Yates et al., with the parameters being visible in Table 5.1.

Table 5.1: Technical variabilities electrolyser, based on the research by Yates et al.

Parameter	Unit	Nominal	Pessimistic	Optimistic
Technical parameters electrolyser				
Stack efficiency	kWh/kg H_2	50	55	45
Stack degradation rate	%/year	0.2	0.3	0.1
Water usage	L/kg H_2	10	11	9
Financial parameters electrolyser				
CAPEX stack	M€/MW	1.2	1.5	0.9
CAPEX BOP	M€/MW	0.5	0.6	0.4
OPEX stack	% of stack CAPEX	2.0	3.0	1.5
OPEX BOP	% of BOP CAPEX	2.0	3.0	1.5
Stack replacement	% of stack CAPEX	40	50	30
Financial parameters wind turbine				
CAPEX	M€/MW	1.64	1.69	1.59
OPEX	k€/MW/year	60	62.5	57.5

The results of the application of these various scenarios is presented in the Figure 5.10 below.

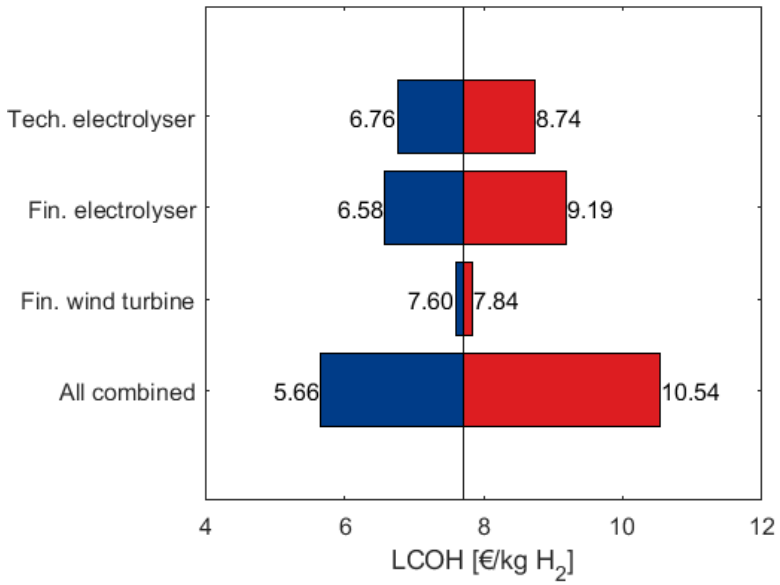

Figure 5.10: Energy and financial based sensitivity analysis - without RAM

In the first bar, only the technical parameters of the electrolyser are varied; in bar 2, the financial aspects of the electrolyser are varied; in bar 3, the financial parameters of the wind turbine are varied; and in

bar 4, all parameters are varied. The uncertainties surrounding electrolysers are visibly responsible for a spread in the results. On one hand, this is encouraging as enhanced development of the Proton Exchange Membrane (PEM) electrolyser could significantly reduce the LCOH; in an optimistic technical electrolyser performance scenario, it could reach €6.76/kg H_2, under the pessimistic scenario it could reach €8.74/kg H_2. The financial parameters of the electrolyser have an even bigger influence, where the optimistic scenario yields a LCOH of €6.58 and a pessimistic one results in €9.19. Less impactful are the financial parameters under both scenario's for the wind turbine, yielding a difference of just €0.12. This is due to the way of calculating the CAPEX and OPEX using the learning rate on capacity in 2030. Furthermore, it also proves that the wind turbine is a more developed technology, and the estimates of its future financials do not deviate as much as the electrolyser does. Most promisingly, the combination of optimistic variations yields a LCOH of €5.66, aligning with the results from similar studies. Conversely, the potential of pessimistic developments leading to a LCOH exceeding €10.54 presents a daunting prospect, offering little hope should this become a reality.

5.2.5. RAM variable effects

This section presents an analysis of the variation in different variables that impact the performance of the W2H system. Unlike the previous paragraph, which focused on the maximum achievable results, this section delves into the actual outcomes. In other words, while the previous paragraph assessed the potential hydrogen production under a scenario of 100% availability, this section examines how availability fluctuates when variables in the RAM model change.

The variables considered are categorised into three groups:

1. Service operator properties
2. Component selection and configuration
3. Maintenance strategies

Each category will be elaborated upon, and conclusions will be drawn regarding the significance of each aspect. The figures depicting these relationships can be found in Appendix F

Service operator properties

In this section, one explores the properties of the service operator, referring to the ability of engineers to perform their capabilities as engineers. This aspect is twofold: firstly, it involves the time it takes for the service operator to be ready to execute a task, which includes the state of the warehouse in terms of having the right parts organised and the speed at which they can arrive at the location. This aspect is referred to in the analysis as 'mobilisation time' - the duration from fault diagnosis to the commencement of repairs. Additionally, the effect of weather resilience is examined, which describes how well the Service Operation Vessel (SOV) withstands extreme weather conditions. These variations have been analysed for the base case and implemented into the model.

Mobilisation time The mobilisation time in the base case is taken as 1 day or 24 hours. Which could be the case following from the type of contract, average circumstances and crew capacities and the location of the system. Figure F.3 shows that this relation is of significant importance. When the average mobilisation time rises with one day, the availability of the system decreases by approximately 1.7%, this equals an increase in the LCOH of €0.20/kg H_2 when compared to the base case. It is concluded that mobilisation time affects the technical performance of a W2H system. With the impact on availability established, the question remains as to the economic implications of varying qualities among service operators with different mobilisation times. It is crucial to recognise that this involves a trade-off aimed at minimising LCOH, even at the expense of availability. Further research is needed to investigate the cost differentials associated with varying mobilisation times. Therefore, the conclusion is that there is an effect, and this trade-off is important.

Weather window capabilities Shell's internal sources indicate that the maintenance crew can operate up to a Beaufort scale wind force of 5, corresponding to a maximum wind speed of 10.7 m/s. This scenario offers a maintenance window of 56.5%. However, changes in the contractor's ability to work in higher or lower wind speeds significantly affect their repair window, as illustrated in Figure F.4. It is evident that a decrease in the maximum acceptable wind speeds leads to a marked decline; a

maximum of Beaufort scale 4 results in a 3.6 percentage point drop in availability and an increase in the LCOH by €1.42/kg H_2. Conversely, increasing the capacity to withstand wind force 6, described as a strong breeze compared to the fresh breeze at force 5, the availability increases to 91.9%, and the LCOH decreases by €0.68/kg H_2.

This analysis leads to the conclusion that weather resilience is an opportunity to increase availability, thereby making the capabilities of the service operator vital for the availability of the W2H system. Once again, this does not mean that one should always aim for the contractor with the highest maximum wind speed working conditions, as the goal is to minimise the LCOH, and the trade-off between increased availability and cost should be considered.

Component selection and configuration

In the domain of component selection and configuration within the W2H system, a multitude of variables exert influence on the system's availability. This analysis focuses on the reliability of components, particularly that of the PEM electrolyser, which currently remains an area of uncertainty. Additionally, the repairability of components is scrutinised, a factor that varies depending on aspects such as component accessibility and the ease with which manufacturers have facilitated the replacement or repair of parts. The study also examines the impact of adding or removing backup systems, further exploring how these decisions affect the overall functionality and dependability of the W2H system.

Component reliability Altering the reliability of components involves modifying their failure rate by a specific factor, directly impacting overall system reliability. The sensitivity analysis evaluated scenarios where component reliability was adjusted, either increased or decreased by predefined factors, resulting in notable changes in system reliability. In offshore autonomous systems, component reliability is bolstered by integrating advanced monitoring and predictive maintenance, alongside sophisticated manufacturing processes featuring comprehensive quality control. This approach, coupled with the design of components to endure extreme marine conditions such as corrosion and temperature fluctuations, significantly enhances their overall reliability and performance. When the failure rate is multiplied by 0.5 - effectively making it twice as reliable - the availability will increase to 93.1% and the LCOH will decrease to €8.29/kg H_2. On the other hand, with a multiplication factor of 1.5, which is a reduction in reliability by 50%, the availability decreases to 83.7% with an associated increase in the LCOH to €9.22/kg H_2. In Figure F.5, the full results are visible, from which it can be seen that the relationship between this factor and the availability appears to be reasonably linear in nature. The effect on availability is evident, and its consequences for the LCOH are clear if there are no further changes to the cost side. However, in the optimal design, this trade-off will also need to be considered as increased component reliability will likely come at higher CAPEX.

PEM reliability A crucial component in the W2H system is the PEM electrolyser. As previously discussed, this technology is likely to be widely used to achieve hydrogen production goals. Currently, PEM electrolysers are in use, but there is a paucity of public data regarding the reliability of their stacks. In the base case scenario, as described earlier, a Mean Time Between Failures (MTBF) of four years was assumed. However, this may not accurately reflect reality. Consequently, this assumption is varied in a separate sensitivity case, where the MTBF ranges from half a year to 16 years. The results are illustrated in Figure F.6. It is evident that the impact is not overly significant; an MTBF of half a year results in an availability of 87.4% and an increase of €0.08/kg H_2. On the other hand, extending the MTBF to 16 years raises the availability to 88.7%. This effect can be characterised as insignificant. The reason behind this is that the electrolysers are arranged in such a way that their failure does not result in zero production; rather, only one of the three containers will be out of operation. /kg H_2

Component repairability The repairability of components within the system is another variable that can be adjusted. Modifying this rate will change the speed at which a component can be repaired. In practical terms, repairability could be influenced by various factors, such as the engineers' skill level, the accessibility of the component in need of repair, and the component's inherent complexity. Since the model does not support the same type of analysis as used for failure rates, the approach here involves adding or subtracting days from the repair time, with a minimum repair time of one day. The relationship is depicted in Figure F.7. It is observable that shortening the repair rate follows the previously described

proportions of repair rates in terms of rising availability. When the repair rate is increased, this leads to a linear relationship. As illustrated, increasing the repair rate by five days for all components results in an availability of 80.3%. It appears that improving repairability does not significantly enhance availability, suggesting that it need not be a primary focus for further research. However, if increased or decreased CAPEX results in a reduction of the LCOH, it remains a viable option.

Backup configuration The configuration of the W2H system can also undergo modifications. As described in the RAM results, after internal research, an iteration in the configuration has been made, adding backups for selected components. To draw a comparison, a scenario was created where all components, where physically possible, have a backup. This increases the availability to 90.6%. This illustrates that the increase in availability is not as significant as one might expect, while the number of components, and thereby the CAPEX, increases substantially. Further research should determine the optimal configuration for this, where the capacities of the platform play a crucial role. Scenarios in which it might be more advantageous to integrate more redundancy include those with higher mobilisation times, lower maximum acceptable wind speeds, or increased repair times.

Maintenance strategies

The final category of variables encompasses maintenance strategies, specifically focusing on the methods chosen for executing maintenance activities. Within this scope, two key aspects are examined. Firstly, the impact of increasing planned maintenance is assessed. Secondly, the study delves into the implementation of plug-and-play electrolyser containers, evaluating their potential influence on system efficiency and reliability.

Planned maintenance The planned maintenance has been estimated to be 1 day, twice a year. In this time, the planned maintenance on the system will be carried out, doing checks and tests. During this time, the system will be offline, resulting in a decrease in system availability compared to the reliability. It is interesting to see what the effect on the availability is. The planned maintenance is the product of the frequency and duration, both of course having the same influence on the availability. As can be seen from the graph in Figure F.9, the current number of timesteps per year, being two, has a minor impact to the components availability, with only 0.49%. However, if one were to do planned maintenance for two weeks, twice a year, one would see a decrease of 6.9%. While having the system offline for two months per year, or sixty days, the availability would become 74.9%, which corresponds to a LCOH of €10.27/kg H_2.

Plug & Play electrolyser containers To decrease the time in which an electrolyser will not produce hydrogen due to faulty components, an innovative concept could be applied where plug&play of the electrolyser is utilised. In such a situation, a crane will lift off the broken electrolyser container and directly replaces it with a working substitute, thereafter, the faulty electrolyser will be repaired to be replaced once again with the next faulty container. This means an extra costs of approximately €8.5M, as follows from the LCOH calculation, as there will need to be a substitute electrolyser available. In Figure F.10, this effect is seen as an availability increase of 0.52%.

It can also be seen that the extra costs have an effect of plus €0.85/kg H_2 on the LCOH. From the data, it is found that this level of reliability increase would be worth the CAPEX investment if it was below €0.5M, that means that the system should be shared with 17 electrolyser containers, or approximately 6.66 systems. From the RAM model it is found that the number of swaps per electrolyser container would be on average 3 per year in the base case. That would mean 51 swaps per year, the probability that two electrolyser containers will have an overlap in swapping necessity is 99.87% following from the Birthday paradox theorem (Suzuki et al., 2006). Which has a negative influence on the availability. Therefore, it can be concluded that this isn't a maintenance strategy with positive influence under these conditions.

As with the backup plus strategy, this feature will be able to yield value if the repair time of components within the electrolyser container are higher than they are now, then the application will decrease that replacement time and could have a positive effect on the LCOH.

In addressing the logistical challenges associated with hydrogen production, it is pertinent to highlight the issue regarding the weight of an electrolyser container. Insights from Shell professionals indicate

that the mass of these containers surpasses the lifting capacity of a SOV crane. While this obstacle can be overcome with alternative strategies, it remains a significant operational consideration.

5.2.6. Discussion

These findings lead to the conclusion that the integration of the RAM model significantly alters the results of technical and economic performance calculations. In this context, the hydrogen yield shows a reduction of 11.9%. The impact on the LCOH is equally substantial, exhibiting an increase of 13.5%. This increment translates to a rise of €1.04/kg H_2, resulting in a revised LCOH of €8.76/kg H_2.

Within a contextual comparison, these LCOH compared to other offshore hydrogen projects reveals that only two projects report a higher LCOH (Schnuelle et al., 2020; Shin et al., 2023), and two studies indicate similar values under certain conditions (Giampieri et al., 2023; Lucas et al., 2022). The majority of studies present a lower LCOH. The definitive conclusion is that the inclusion of RAM models substantially impacts the calculations, and models excluding them may present a distorted view of the economic feasibility. Furthermore, the difference compared to studies with the most similar configurations, specifically those by Groenemans et al. and Egeland-Eriksen et al., was already significant but has become even more pronounced.

Additionally, it should be noted that the magnitude of the hydrogen yield or LCOH is not heavily dependent on the RAM models, but rather on the initial yield and LCOH. This is also evident from the operational sensitivity study, which indicates that further development of PEM technology could result in a significantly lower LCOH, potentially falling below €6. Continued investments and research will determine the actual prices by 2030.

The variables in the RAM model indicate that under the current *base case* conditions, the failure rate of the components is not the cause of a rapidly declining reliability. Instead, it is the time between failure and returning online, where rapid response is crucial. Employing a high-quality contractor with the appropriate capabilities is therefore of great importance. The key conclusion drawn from varying maintenance variables is not about achieving certain availabilities in a given situation, but rather that varying these variables leads to different availabilities, with some having a more pronounced effect than others. This does not mean that variables with a lesser effect are uninteresting. When the objective is to obtain the lowest possible LCOH, this is achieved by finding the costs to each variable and optimising for that particular scenario. For further research, it would be interesting to use specific prices whenever available for this purpose, thereby enabling more precise determinations. Unfortunately, this has not been possible during this study.

Lastly, these results are determined without subsequent validation, which constitutes a limitation to the certainty with which these results can be asserted. It is important that these models be tested as soon as data becomes available for comparison, in order to reinforce these conclusions.

5.3. Multiple systems results

Evaluating a single W2H system offers insights into the functioning of the system itself. However, in reality, not just a single system will be deployed, especially when the system is set up in a decentralised arrangement. Therefore, this analysis is extended to a W2H farm. In this section, the performance in terms of availability will first be calculated, followed by computing the LCOH using figures from the literature. An alternative calculation of LCOH will then be presented using assumptions on both CAPEX and OPEX which are not available from literature but are drawn for interviews and the outcomes of the single W2H system models. Finally, the analysis will include a comparison of the differences in onshore and offshore LCOH.

5.3.1. Maintenance delay

To determine the delay in maintenance activities due to multiple W2H systems requiring simultaneous maintenance, simulations were conducted to gauge this overlap for various wind farm sizes. These simulations ranged from 10 to 70 W2H systems, representing a W2H farm capacity variation from 150 MW to 1.05 GW. The results are illustrated in Figure 5.11.

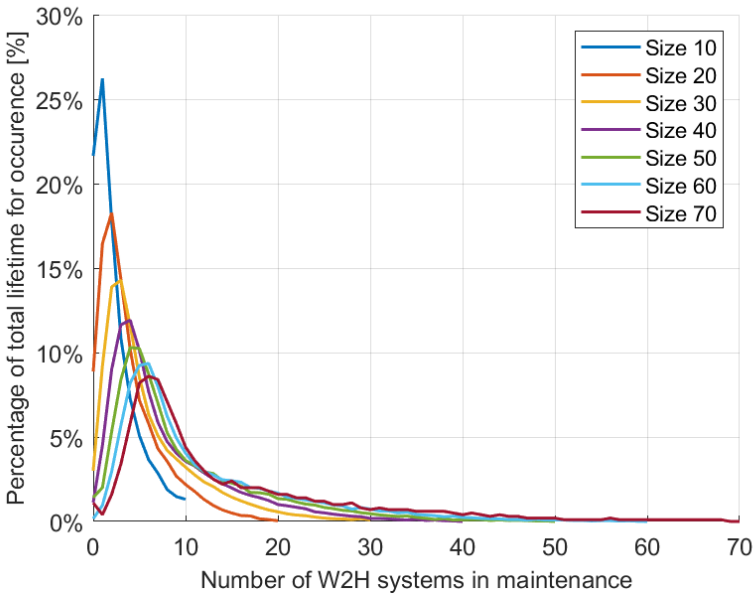

Figure 5.11: Overlap in maintenance between multiple W2H systems

A distinct pattern emerges in this figure. The peak number of systems requiring simultaneous maintenance decreases and shifts rightward for larger farms, aligning with expectations. It is clearly visible that the probability of having zero systems in maintenance simultaneously (meaning all systems are fully functioning) decreases as the farm size increases. For instance, this probability is 21.6% for a farm with 10 systems, 8.9% for 20 systems, and approximately 1% or less for farms with 40 or more systems. Consequently, the risk of being unable to meet maintenance demands increases rapidly. This data is utilised in the calculation to determine the average availability of W2H farms, taking these outcomes into account.

5.3.2. Availability and literature LCOH

Subsequently, the new average wind farm availability is evaluated while accounting for both the single system RAM adjustment and the delay in maintenance from the multiple systems. This new availability depends on the number of W2H systems in the farm and the availability of engineers, for this calculation, averages from the RAM model have been used, so it must be stressed that this provides an indication and not a precise result. Furthermore, the calculations are done for a varying number of SOVs, as previously described, these are the vessels with engineers, equipment and materials to perform the maintenance. The results are shown in Figure 5.12.

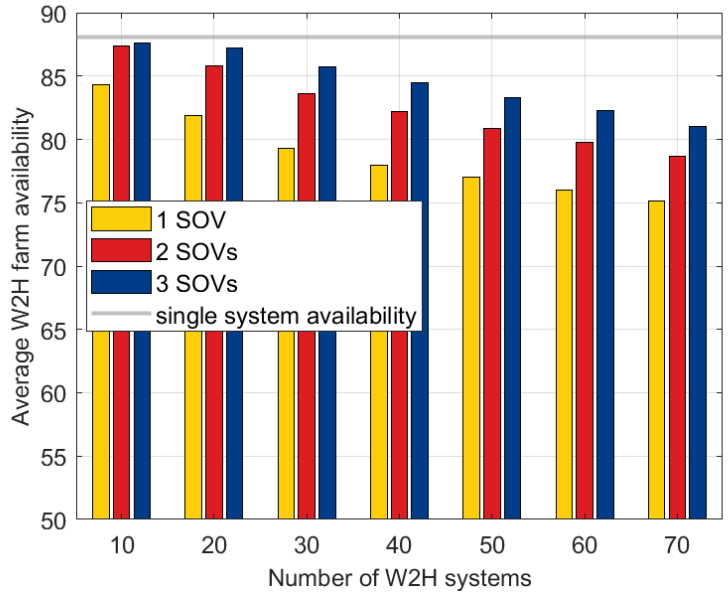

Figure 5.12: Average W2H farm availability for several farm sizes and number of SOVs

In this figure, one can observe that for the various farm sizes indicated on the x-axis, there are three different bars per farm, representing the calculated availability. Also visible is a grey line at availability equals 88.1%, as calculated for the average availability of the single system base case. As observed, the overlap in maintenance requirements decreases the average availability of the W2H farm, where this effect is stronger in larger farm sizes. Additionally, it is apparent that the number of SOVs enhances availability, a logical conclusion; the greater the capacity to perform maintenance, the smaller delay is incurred in its execution. It is now possible to assess how this impacts the LCOH of the W2H farm, as depicted in Figure 5.13, where one uses the standard literature method of calculating CAPEX and OPEX.

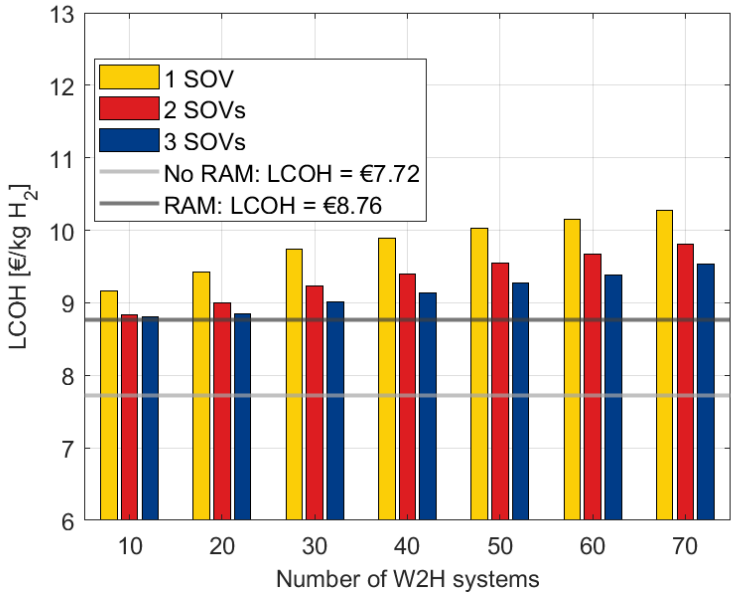

Figure 5.13: Average W2H farm LCOH for several farm sizes and number of SOVs

In this figure, the LCOH for different sizes is displayed using the same format as the above figures.

Additionally, there are two grey lines present. The light grey line at €7.72 represents the LCOH as calculated from literature for a single system, while the dark grey line indicates a LCOH of €8.76, as calculated for the single system with consideration of RAM adjustment. One observes that the optimal LCOH with RAM of €8.76 is approached in the scenario of 10 systems and 3 SOVs. This figure highlights the limitations of the current approach to calculating the LCOH. The LCOH increases with the increasing size of the W2H farm and decrease as more SOVs are available within a farm. Upon consideration, this seems counter-intuitive; larger farms should benefit from economies of scale, and the costs associated with higher maintenance capabilities through the higher number of SOVs should also influence the LCOH. However, the expenses related to this maintenance are not included in the standard method of OPEX calculation and OPEX is merely calculated as a percentage of the system's CAPEX. Therefore, an alteration should be made to the standard LCOH estimation method.

5.3.3. Alternative LCOH

The LCOH calculation is modified in two specific ways. Firstly, on the CAPEX side, economies of scale are applied, as detailed in Section 4.5.2. In terms of OPEX, it is largely decoupled from the CAPEX as described in Section 4.5.2, and as a result, specific maintenance costs are incorporated. Consequently, having a larger available crew for repairs also leads to an increase in financial expenditure. The outcomes of this approach are illustrated in Figure 5.14.

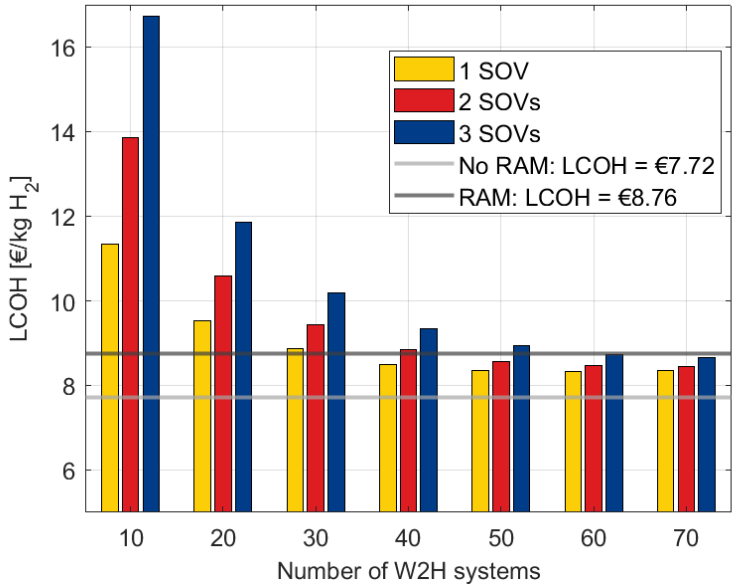

Figure 5.14: Average W2H farm alternative LCOH calculated for several farm sizes and number of SOVs

Here, the LCOH for the offshore W2H farm is visible for different farm sizes, with variations in the number of SOVs. Additionally, two grey lines are again present in the figure. The light grey line at €7.72 indicates the LCOH as calculated from literature for a single system. Meanwhile, the dark grey line shows a LCOH of €8.76, as determined for the single system when considering RAM adjustment. In this figure, it is apparent that the results differ significantly from the previous calculation. A phenomenon is observed where, as the W2H farms increase in size, the LCOH decreases. This aligns with the expected outcomes due to economies of scale and the distribution of costs. Notably, under current conditions, it is not advantageous to deploy more SOVs. The increased availability gained from additional SOVs does not justify the associated extra costs. Therefore, it is more economical to accept some delay in maintenance to save on the expenses of hiring extra personnel. Moreover, the data suggests that scaling up is beneficial. The LCOHs for wind farms with one SOV seem to follow an asymptotic curve, approaching a horizontal line around 70 W2H systems. The following figure compares the old LCOH calculation with this improved method, focusing on the single SOV scenario. Another notable finding is that the LCOH for W2H farms of size 40 and larger achieves LCOHs that

are lower than the RAM-adjusted LCOH for a single system. This phenomenon occurs despite the significantly lower average availability of the W2H farms, where costs are efficiently distributed across systems. From this, it is concluded that the LCOH for a single system, including RAM considerations, is not the minimum achievable. Lower LCOHs can be reached by efficiently defining maintenance strategies for W2H farms. To clarify the difference between the literature approach and the adjusted LCOH calculation, reference can be made to Figure 5.15 where this distinction is visible.

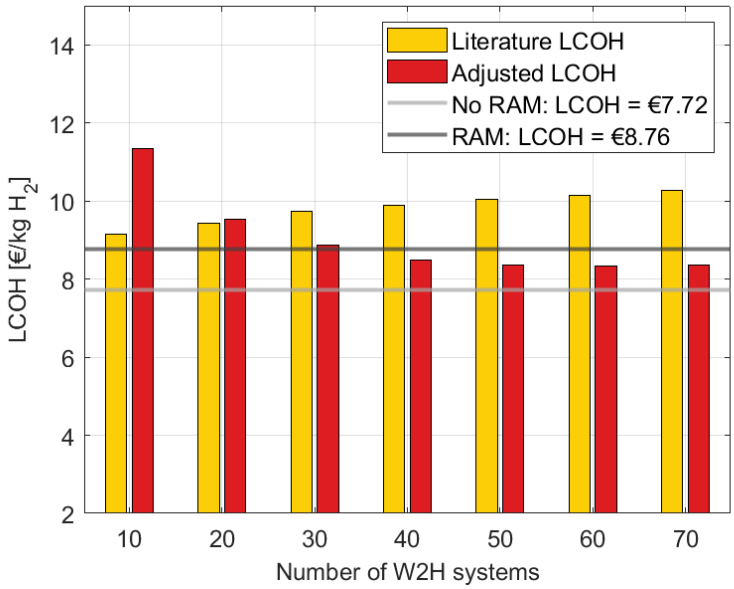

Figure 5.15: Comparison between lowest LCOH per farm size for literature and alternative calculation including RAM effect

In this figure, the literature LCOH and the adjusted LCOH are compared. The light grey line represents the LCOH from literature for a single system at €7.72, and the dark grey line represents the LCOH at €8.76 for the counterpart where RAM is included in the calculation. The difference is evident; when applying the conventional approach to LCOH calculation for single systems while still considering the system's availability, it significantly diverges from the alternative method. Adjusting this calculation to account for more realistic CAPEX and OPEX conditions could markedly refine the result. The divergence thus arises from decoupling the OPEX. In the literature-based LCOH, the amount comprising the OPEX slightly varies with the systems' availability, but ultimately, the percentage remains constant at 23.1%, just like in the single system. However, in the adjusted LCOH, the percentage does vary. For instance, in the case of one SOV for 10 systems, the OPEX percentage is 38%, and with 3 SOVs, it even reaches 59%, which is logical considering that this would mean an average of approximately one engineer per system permanently. In larger farm sizes, such as 60 systems, the OPEX percentage ranges from 6% with a single SOV, 12% with two SOVs, to 17% with three SOVs. This indicates that the increase in availability does not compensate for the rise in financials. The primary conclusion does not stem from the numerical values of the results, but rather from the calculation itself. The correlation between the size of the installation and the OPEX is an oversimplification of reality, leading to misconceptions when seriously considering the profitability of W2H farms. OPEX primarily depends on the maintenance capacities that can be offered, which in turn impacts the performance of a W2H system. However, the maintenance requirements between a 10 MW and a 15 MW system are not as significant as suggested in the literature. This is because they consist of exactly the same components with the same failure rate; only their size varies, which does not have as substantial an effect as might be assumed.

5.3.4. Onshore versus offshore

To compare onshore and offshore situations, one first examines the reliability of a single system when situated on land. Based on the assumptions of increased weather resistance and a reduced average

total repair time, due to the enhanced accessibility of the W2H system, the reliability is increased to 93.5%. Consequently, the availability is 93.0%. The next objective is to calculate the average W2H farm availability under the influence of 'delay in maintenance'. This is illustrated in Figure 5.16.

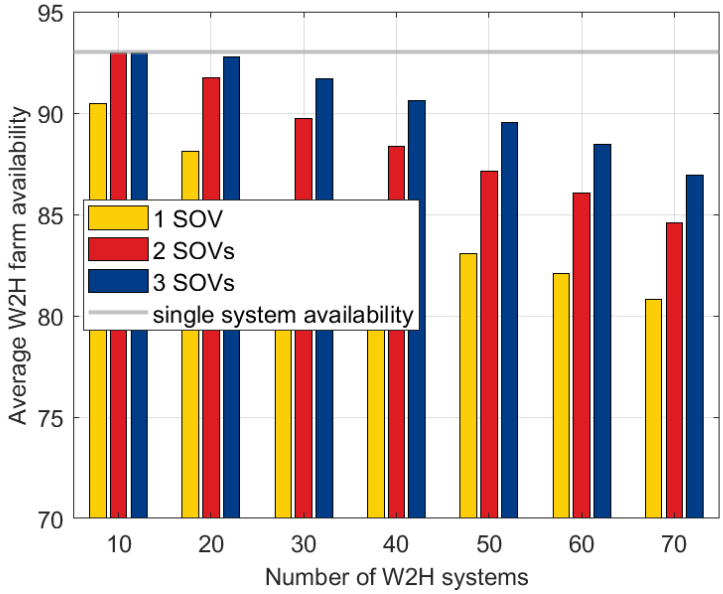

Figure 5.16: Average onshore W2H farm availability for several farm sizes and SOVs

Wherein the availability is depicted in the figure for the different farm sizes and numbers of SOVs. In this case, the grey line represents the availability of a single system, as shown at 93.0%. The difference with the offshore variant is apparent: the availability remains higher due to improved accessibility and optimal working conditions. Likewise, the addition of more SOVs continues to enhance availability. When one then applies this to the onshore economic assumptions, one calculates the onshore LCOH, which is shown in Figure 5.17. Since an onshore single system LCOH has not been calculated as in the offshore variant, and because the comparison is with the offshore counterpart rather than with literature, there is now no reference line with LCOH.

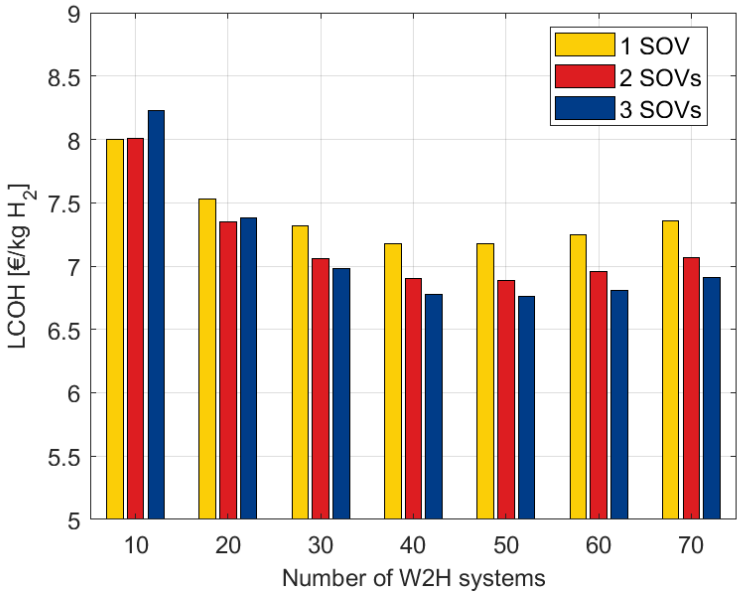

Figure 5.17: Average onshore W2H farm LCOH for several farm sizes and SOVs

In this figure, the average LCOH per farm size is plotted for various numbers of SOVs. Here, an interesting phenomenon arises that was not observed in the offshore variant; a shift occurs in the number of SOVs that lead to the lowest LCOH, where larger farms benefit from more engineers. Additionally, the lowest LCOH is found at 50 W2H systems, after which the LCOH will increase with further enlargement. This is due to the cessation of CAPEX scaling benefits beyond this size. Furthermore, it can be concluded that the optimal LCOH is likely not included here because the calculations incorrectly use SOVs, thus the exact sizes of maintenance crews. Onshore, one is much less bound to these constraints, allowing for an optimisation to find the minimal LCOH for an exact crew size, given the W2H farm size. Therefore, this thesis advises further investigation in this area. For this study, the objective is to compare with the offshore variant. The lowest LCOHs have been chosen for comparison for each W2H farm size, where the Figure 5.18 in the bar indicates with (1), (2), or (3) how many SOVs are maintaining that specific farm, resulting in that LCOH.

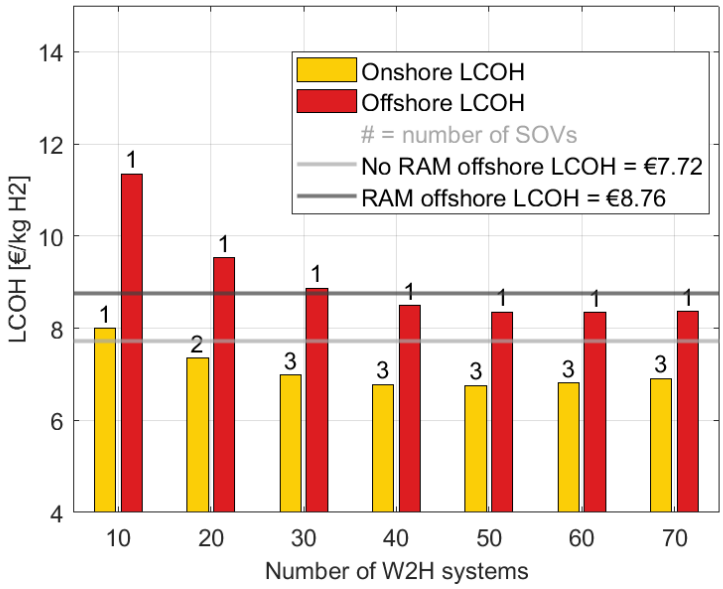

Figure 5.18: Comparison between lowest LCOH per farm size for onshore and offshore situation including RAM effect

Concluding, this figure illustrates the comparison between onshore and offshore scenarios for a W2H farm of varying sizes. For each size, the lowest LCOH is indicated, and above the bar, the number of SOVs in those situations is displayed. Additionally, the grey lines are included: The light grey line at €7.72 represents the LCOH as calculated from literature for a single system, while the dark grey line indicates a LCOH of €8.76, as determined for the single system with consideration of RAM adjustment. A marked difference in the LCOH between the onshore and offshore variants is observed. In the 10 Wind-to-Hydrogen (W2H) systems farm, the disparity is most pronounced, amounting to €3.35, with the LCOH of the onshore variant being 30% lower compared to its offshore counterpart. As the number of systems increases, this gap lessens; the difference stands at 23% (€2.18) for the 20-system variant and 17% (€1.45) for the 70-system variant. Given that the CAPEX and maximum theoretical energy yield are constants in this assumption, this discrepancy is solely due to improved availability and reduced CAPEX costs. This is evident from the OPEX percentage of the total LCOH, averaging around 6.2% for the onshore LCOH. Conclusively, another observation is that the LCOH for onshore dips even below the line of offshore LCOH without RAM integration. From this, it is concluded that onshore W2H systems should also be explored further in the quest for lower LCOHs.

5.3.5. Discussion

When simulating a W2H farm by multiplying a single W2H system, the likelihood of overlapping maintenance requirements causes a decrease in availability, calculated as the average availability of the W2H farm. This clearly depends on the contractor's capacity to repair these failures. Compared to a single system availability of 88.1%, this can decrease to 84.3% for a farm of 10 systems and even 75.1% for a farm comprising 70 systems, in the scenario of one SOV for the farm. Increasing the number of SOVs improves availability due to expanded repair capacities. Within current academic sources, OPEX is estimated as a percentage of the CAPEX, leading to an unrealistic LCOH as the additional costs for improved service are not included. In the alternative LCOH calculation, these costs are considered, resulting in a more realistic portrayal of reality. It suggests that for an offshore W2H farm, it is beneficial to upscale to at least 50 W2H systems, and that the increase in availability does not offset the costs incurred for the service, since the single SOV scenario results in the lowest LCOH of €8.35/kg H_2. Compared to the LCOH in the 100% availability situation from literature, this is an increase of only 8.1%. Limitations to these findings arise from the uncertain basis of the costs of these systems.

In the comparison between onshore and offshore LCOHs, it is found that the onshore variant is between 30% and 17% cheaper, depending on the size of the farm. Under these conditions, this difference is attributed to increased availability due to improved accessibility for maintenance and cheaper OPEX as

'offshore premiums' are eliminated. Nonetheless, this is a very general calculation as changes within CAPEX and capacity factor have been offset against each other. It serves as an interesting subject for further research.

According to Burchardt et al., the willingness to pay for green hydrogen above €6/kg H_2 is 430 kt per year, compared to the 15 Mt per year when the costs would be around €1.50/kg H_2. This research suggests that the EU's expectation for green hydrogen to reach €3 by 2030 is unattainable, and even the revised target of €5 - €8 may be on the low side. It appears that in the offshore scenario, the cost is likely to be slightly more than €8/kg H_2. However, in these times of high-tech innovation, progress can be rapid, and the collective societal effort towards achieving goals has often been underestimated.

6

Conclusions and Recommendations

This Masters thesis commenced with the objective of investigating the effects of system robustness of Wind-to-Hydrogen (W2H) systems on their techno-economic performance. In this chapter, we delineate the conclusions pertaining to this research. Section 6.1 presents the conclusions drawn from the results, addressing the various sub-research questions. Section 6.2 outlines the recommendations for future research.

6.1. Conclusion

In the conclusion, this thesis addresses the research question: *What is the influence of including system reliability on a single offshore wind-to-hydrogen systems' technical and economic performance, what effect do operational and maintenance strategies have on these results, and what is the effect when considering multiple systems?* This main research question has been divided among three sub-research questions, each of which has been comprehensively explored in the previous chapters. The conclusions to these sub-research questions are drawn and detailed below:

What is the change in the systems' technical and economic performance if the reliability of the system has been simulated and integrated?

When the reliability of the system is not accounted for, the single W2H system will have a lifetime yield of 18.9 kt H_2, or an average of 857 t H_2 per year. Based on the economic assumptions, this results in a Levelized Cost Of Hydrogen (LCOH) of €7.72/kg H_2, with the major financial contributions coming from the wind turbine and electrolyser.

Utilising sources within Shell, a realistic and improved design of the W2H system was created called *base case*. This design has been modelled in a computational Reliability, Availability, and Maintainability (RAM) model, wherein the robustness of the system is calculated. This reveals that the average reliability of the designed system is 88.6% following an average system availability of 88.1%, with a 99% confidence interval on these averages of 0.2%. The electrolysers and Balance of Plant (BOP) in the three parallel containers, along with the water treatment system, are marked as the most vulnerable components yielding the least Full Load Hours (FLH). When these results are combined with the techno-economic outcomes without RAM consideration, it implies that the hydrogen yield decreases by 11.9% to an average of 755 t H_2 per year and the LCOH increases by 13.5%, or a rise of €1.04/kg H_2, resulting in €8.76/kg H_2. From this, one concludes that the inclusion of system reliability plays a non-negligible role when calculating the technical and economic performance of W2H systems under these conditions.

How do these parameters change if the Energy Model and RAM Model variables are changed?

The techno-economic energy model and RAM model variables are independently altered. The energy model variables impacted the amount of hydrogen produced assuming 100% system availability, whereas the RAM variables influenced the proportion of the maximum yield represented by the actual hydrogen yield. The investigation into the operational variables revealed that the technical and

economic performances of the electrolyser are most significant, while the economic performance of the wind turbine has a minimal impact. Where an overall optimistic scenario could potentially achieve a RAM-excluded LCOH of €5.66/kg H_2, while an overall pessimistic scenario might lead to a RAM-excluded LCOH of €10.54/kg H_2. The variance between these scenarios, as well as comparisons with similar academic research papers and among those papers themselves, underscores the conclusion that continued research and investment are essential to bring clarity to this LCOH.

From the perspective of RAM model variables, several variabilities have been tested. Spanning across eight potential adjustments, their effects were measured. It is first evident that the failure rate of electrolyser stacks, which remains unestablished in the scientific community, has a very limited impact on the increase or decrease of system availability within certain margins. This is attributed to the setup where multiple electrolyser containers are connected in parallel, meaning that the failure of one electrolyser does not have disastrous effects on production. Regarding other categories of RAM variable effects, different impacts have been observed in service operator properties and component selection and configuration. It is concluded that a less significant effect is not necessarily less interesting. Ultimately, with a minimal LCOH as the goal, each choice must be weighed, considering whether the increase in system availability justifies the increase in financial resources needed to achieve those effects. Furthermore, it is concluded that the implementation of plug-and-play in the containers is not advantageous under these assumptions, as the benefits of increased availability do not outweigh the economic and operational challenges.

What are the changes when assessing a W2H farm as an aggregate of multiple single systems and how does this influence the technical and economic performance?

The study of a W2H farm as an aggregate of multiple single systems revealed insights into the technical and economic performance of a field of systems. The ”overlap in maintenance requirements” across multiple W2H farms was calculated to determine the average availability of the wind farm, considering the number of Service Operation Vessels (SOVs) and available engineers. It was found that as the farm size increases, the average availability decreases due to greater maintenance overlap. However, with more SOVs, the availability nears the maximum of a single system.

The conventional LCOH method, flawed in terms of CAPEX due to neglecting of economies of scale and OPEX as a percentage of CAPEX while OPEX is largely independent of CAPEX, showed the smallest field (10 W2H systems) with the highest level of maintenance capabilities having the lowest LCOH. In contrast, the alternative LCOH method, accounting for these factors, indicated a decrease in LCOH with increasing farm size, stabilising from a farm size of 50 onwards. Adding more SOVs for a W2H farm under these conditions does not provide net value; the rise in availability does not offset the increase in OPEX, resulting in a net LCOH increase.

Furthermore, a comparison in the LCOH between onshore and offshore settings was made, assuming variations in energy yield and Capital Expenditures (CAPEX) between the two settings offset each other. This simulation resulted in a LCOH that is 30% to 17% lower in an onshore scenario compared to offshore due to increased ability of performing maintenance, achieving a LCOH of €6.76/kg H_2, which is lower than the offshore single W2H system where RAM is not accounted for, concluding that this comparison of offshore, near-shore and onshore W2H farms should be subject to further research.

It is essential to conclude that the OPEX is largely independent of the installation’s size or CAPEX, except for the costs of replacement components. Maintenance crew costs, the largest portion of OPEX, do not scale with CAPEX. Instead, they depend on the system’s configuration and component specific reliability figures. The LCOH can possibly be estimated more precise when industry figures for maintenance costs and requirements based on the failure rate of such systems are used for a more accurate estimation. Consequently, the primary conclusion is that when research includes a calculation with the LCOH, there should be an awareness of whether these effects are incorporated or not, and that their inclusion could potentially lead to a clearer result. These LCOHs are used globally in academic, public, and private sectors to enable a sustainable world, and clarifying the future through improved estimates will potentially ease the complexity of this transition.

In conclusion, the answer to the main research question remains: ***”What is the influence of including system reliability on a single offshore wind-to-hydrogen system’s technical and economic***

performance, what effect do operational and maintenance strategies have on these results, and what is the effect when considering multiple systems?"

The application of RAM modelling significantly influences the techno-economic performance of W2H systems. While the exact numerical outcomes are sensitive to variations in the assumptions used, a non-negligible effect is nonetheless evident. When undertaking such a project, it's crucial to assess whether the positive or negative impact of the changing variables concerning potential yield or RAM, combined with the required investments, have a net positive effect on the goal, which typically involves producing the most cost-effective hydrogen possible. On a W2H farm scale, traditional estimates of LCOH are not applicable, especially when RAM is also considered. An alternative LCOH calculation is presented to increase the LCOH estimation accuracy. The key takeaway is not a numeric figure, but a qualitative message: increasing awareness within governments, scientific communities, and organisations about these RAM effects on W2H systems can make the path to affordable green hydrogen more transparent.

6.2. Recommendation

In conclusion, it is evident that both broadening and deepening the study of offshore W2H systems is necessary, with a particular focus on system reliability. Combining the results with the theoretical context yields the following four recommendations:

Including more data into the RAM model: The resolution of the RAM model can be significantly enhanced by acquiring more data. While the model already has built-in functions for incorporating various data points, the lack of suitable data has so far hindered its full utilisation. This includes key inputs like degradation rates, weight, and component specific purchase and replacement costs. Therefore, it's recommended that the green hydrogen team at Shell continues to use and update this model as more data becomes available. The availability of this data will not only improve insights into the physical aspects of the system but also allow for financial optimisation, considering the maximum available budget. For instance, an optimal system configuration could be devised with constraints like the platform's carrying capacity, the total budget, and an objective to minimise the LCOH, to make the optimal system configuration and maintenance strategy. Such advancements in the model will significantly contribute to the technical and economic efficiency of green hydrogen systems. An interesting goal could be to define a new formula that will yield a more accurate estimation of the OPEX based on certain, easy to estimate, figures. This research could serve as a basis to construct those new methods.

Including more types of Repair & Maintenance: To obtain a more realistic understanding of system operations, it is recommended to broaden the scope of failure types and maintenance strategies in the model. This should include the implementation of predictive maintenance and condition monitoring, an innovative and vital method for early failure detection, which significantly enhances system reliability. Additionally, incorporating non-critical failures and less-than-optimal maintenance scenarios, where components do not return to full operational capacity, is important. Moreover the inclusion of spare parts strategy would be of interest to this field of study. This involves identifying parts that should always be available and those that need to be stocked in the Operations and Maintenance (O&M) warehouse at the harbour.

Broadening of techno-economic scope: In the study of the techno-economic aspects of such systems, it is recommended to incorporation the effects of CO_2 abatement. Accounting for these externalities could shift the cost of green hydrogen relative to fossil fuel alternatives, potentially enhancing the financial viability of W2H systems. Furthermore, the technical scope of the study can be expanded to include elements such as hydrogen pipelines, batteries, external grids, and other components. This expansion would clarify the comparison and search for the optimal configuration of W2H systems, allowing for the quantification of the impacts of different configurations

Collaboration for data and validation purposes: The primary challenge encountered in this thesis was the scarcity of usable data, a situation understandable given the proprietary nature of such information for the companies involved. The use of OREDA data was instrumental in facilitating the current findings. However, the journey towards a sustainable, green future is complex and likely to incur significant costs, particularly if entities continue to operate in isolation. Therefore, it is advisable for a more collaborative approach in this transition. Developing methods for data sharing among com-

mercial companies, whether anonymised or not, is recommended. While data sharing might initially reduce competitive advantages, it has the potential to be mutually beneficial in the long term. Furthermore, such shared data could be pivotal in creating and validating predictive models for these systems, benefiting all stakeholders involved. Additionally, validating these results with contractors, especially in the context of Operational Expenditures (OPEX) using actual figures, should provide insights into the accuracy of the models. Such validation is essential to identify necessary adjustments, thereby enhancing the models' effectiveness and reliability.

References

Ahmed, K. W., Jang, M. J., Park, M. G., Chen, Z., & Fowler, M. (2022). Effect of components and operating conditions on the performance of pem electrolyzers: A review. *Electrochem 2022, Vol. 3, Pages 581-612*, *3*, 581–612. https://doi.org/10.3390/ELECTROCHEM3040040

Aquaventus. (2021). *Aquaventus green hydrogen from the north sea*.

ASTM International. (1999). *Standard specification for reagent water*. https://www.astm.org/d1193-99e01.html

Babarit, A., Gilloteaux, J.-C., Clodic, G., Duchet, M., Simoneau, A., & Platzer, M. F. (2018). Techno-economic feasibility of fleets of far offshore hydrogen-producing wind energy converters. *International Journal of Hydrogen Energy*, *43*(15), 7266–7289. https://doi.org/10.1016/j.ijhydene.2018.02.144

Barter, G. E., Sethuraman, L., Bortolotti, P., Keller, J., & Torrey, D. A. (2023). Beyond 15 mw: A cost of energy perspective on the next generation of drivetrain technologies for offshore wind turbines. *Applied Energy*, *344*. https://doi.org/10.1016/j.apenergy.2023.121272

Barthelmie, R. J., Hansen, K., Frandsen, S. T., Rathmann, O., Schepers, J. G., Schlez, W., Phillips, J., Rados, K., Zervos, A., Politis, E. S., & Chaviaropoulos, P. K. (2009). Modelling and measuring flow and wind turbine wakes in large wind farms offshore. *Wind Energy*, *12*, 431–444. https://doi.org/10.1002/we.348

Bernt, M., Hartig-Weiß, A., Tovini, M. F., El-Sayed, H. A., Schramm, C., Schröter, J., Gebauer, C., & Gasteiger, H. A. (2020). Current challenges in catalyst development for pem water electrolyzers. *Chemie-Ingenieur-Technik*, *92*, 31–39. https://doi.org/10.1002/cite.201900101

Bernuy-Lopez, C. (2023). Electrolysis technologies and Icoh: Current state and prospects for 2030.

Bertuccioli, L., Chan, A., Hart, D., Lehner, F., Madden, B., & Eleanor, S. (2014). *Study on development of water electrolysis in the eu final report e4tech sàrl with element energy ltd for the fuel cells and hydrogen joint undertaking*. www.e4tech.com

Bianchi, F. R., & Bosio, B. (2021). Operating principles, performance and technology readiness level of reversible solid oxide cells. *Sustainability (Switzerland)*, *13*. https://doi.org/10.3390/su13094777

Biebuyck, B. (2022). *State of play of off-shore green hydrogen projects*.

Blasi, A. D., Andaloro, L., Siracusano, S., Briguglio, N., Brunaccini, G., Stassi, A., Aricò, A. S., & Antonucci, V. (2013). Evaluation of materials and components degradation of a pem electrolyzer for marine applications. *International Journal of Hydrogen Energy*, *38*, 7612–7615. https://doi.org/10.1016/J.IJHYDENE.2012.10.062

Buijs, L., Bulder, B., Koornneef, J., Peters, R., & Sponsor, M. W. (2022). *Offshore hydrogen for unlocking the full energy potential of the north sea*. https://energy.ec.europa.eu/system/files/2022-09/220912_NSEC_Joint_Statement_Dublin_Ministerial.pdf

Burchardt, J., Hegnsholt, E., Holm, M., Klose, F., Ritter, D., & Schönberger, S. (2023). *Turning the european green hydrogen dream into reality: A call to action* (White Paper). Boston Consulting Group.

Buttler, A., & Spliethoff, H. (2018). Current status of water electrolysis for energy storage, grid balancing and sector coupling via power-to-gas and power-to-liquids: A review. *Renewable and Sustainable Energy Reviews*, *82*, 2440–2454. https://doi.org/10.1016/J.RSER.2017.09.003

BVG. (2018). *Wind farm costs – guide to an offshore wind farm*. https://guidetoanoffshorewindfarm.com/wind-farm-costs

BVG Associates. (2022). *Wind farm costs – guide to an offshore wind farm* [Accessed: yyyy-mm-dd]. https://guidetoanoffshorewindfarm.com/wind-farm-costs

Caine, D. (2021). *Erm dolphyn hydrogen*. www.erm.com

Calado, G., & Castro, R. (2021). Hydrogen production from offshore wind parks: Current situation and future perspectives. *Applied Sciences 2021, Vol. 11, Page 5561*, *11*, 5561. https://doi.org/10.3390/APP11125561

Caldera, U., & Breyer, C. (2017). Learning curve for seawater reverse osmosis desalination plants: Capital cost trend of the past, present, and future. *Water Resources Research*. https://doi.org/10.1002/2017WR021402

Carroll, J., McDonald, A., McMillan, D., Maples, B., & Mone, C. (2015). *Cost of energy for offshore wind turbines with different drive train types* [Uploaded by James Carroll on 22 January 2019]. University of Strathclyde. https://www.researchgate.net/publication/330546517

Cevasco, D., Koukoura, S., & Kolios, A. J. (2021). Reliability, availability, maintainability data review for the identification of trends in offshore wind energy applications. *Renewable and Sustainable Energy Reviews*, *136*. https://doi.org/10.1016/j.rser.2020.110414

Clark, K. (2019). *Improving maintenance by adopting a p-f curve methodology*. https://www.isa.org/intech-home/2019/march-april/features/improving-maintenance-by-adopting-a-p-f-curve-meth

Clean Hydrogen JU - SRIA. (2022). *Technology kpis: State-of-the-art and future targets* [Accessed: 28 February 2022]. https://www.clean-hydrogen.europa.eu/knowledge-management/strategy-map-and-key-performance-indicators/clean-hydrogen-ju-sria-key-performance-indicators-kpis_en

D'Ambrosio, D., Schoukens, J., Troyer, T. D., Zivanovic, M., & Runacres, M. C. (2020). Synthetic wind speed generation for the simulation of realistic diurnal cycles. *1618*.

Dinh, Q. V., Dinh, V. N., Mosadeghi, H., Pereira, P. H. T., & Leahy, P. G. (2023). A geospatial method for estimating the levelised cost of hydrogen production from offshore wind [Under a Creative Commons license]. *International Journal of Hydrogen Energy*, *48*(40), 15000–15013. https://doi.org/10.1016/j.ijhydene.2023.01.016

Dinwoodie, I. A., & McMillan, D. (2014). Operational strategies for offshore wind turbines to mitigate failure rate uncertainty on operational costs and revenue. *IET Renewable Power Generation*, *8*, 359–366. https://doi.org/10.1049/iet-rpg.2013.0232

Egeland-Eriksen, T., Jensen, J. F., Ulleberg, Ø., & Sartori, S. (2023). Simulating offshore hydrogen production via pem electrolysis using real power production data from a 2.3 mw floating offshore wind turbine. *International Journal of Hydrogen Energy*. https://doi.org/10.1016/J.IJHYDENE.2023.03.471

EIA. (2020). *Definition of the iea wind 15-megawatt offshore reference wind turbine technical report*. www.nrel.gov/publications.

Erbach, G., & Roniger, J. (2023). Towards climate neutrality [PE 757.574]. *European Parliamentary Research Service*. http://www.europarl.europa.eu/thinktank

Escobar-Yonoff, R., Maestre-Cambronel, D., Charry, S., Rincón-Montenegro, A., & Portnoy, I. (2021). Performance assessment and economic perspectives of integrated pem fuel cell and pem electrolyzer for electric power generation. *Heliyon*, *7*. https://doi.org/10.1016/j.heliyon.2021.e06506

European Commission. (2020). *A strategy to harness the potential of offshore renewable energy for a climate neutral future* (Technical Report SWD(2020) 273) [Accessed: 2023-10-13]. EU Commission. https://eur-lex.europa.eu/legal-content/EN/TXT/PDF/?uri=CELEX:52020SC0273

European Union. (2020). *Eu strategy on offshore renewable energy* [Accessed: 2023-10-13]. https://energy.ec.europa.eu/topics/renewable-energy/offshore-renewable-energy_en

Faulstich, S., Hahn, B., & Tavner, P. J. (2011). Wind turbine downtime and its importance for offshore deployment. *Wind Energy*, *14*, 327–337. https://doi.org/10.1002/we.421

Felgenhauer, M., & Hamacher, T. (2015). State-of-the-art of commercial electrolyzers and on-site hydrogen generation for logistic vehicles in south carolina. *International Journal of Hydrogen Energy*, *40*, 2084–2090. https://doi.org/10.1016/J.IJHYDENE.2014.12.043

Franco, B. A., Baptista, P., Neto, R. C., & Ganilha, S. (2021). Assessment of offloading pathways for wind-powered offshore hydrogen production: Energy and economic analysis. *Applied Energy*, *286*, 116553. https://doi.org/10.1016/J.APENERGY.2021.116553

Frensch, S. H. (2018). *Lifetime investigation of pem electrolyzers under realistic load profiles*. Aalborg University. https://doi.org/10.54337/aau300037423

Giampieri, A., Ling-Chin, J., & Roskilly, A. P. (2023). Techno-economic assessment of offshore wind-to-hydrogen scenarios: A uk case study [Under a Creative Commons license]. *International Journal of Hydrogen Energy*, *52*(Part B), 589–617. https://doi.org/10.1016/j.ijhydene.2023.01.346

Glenk, G., & Reichelstein, S. (2019). Economics of converting renewable power to hydrogen [A Publisher Correction to this article was published on 07 March 2019]. *Nature Energy*, *4*, 216–222.

Gondal, I. A. (2019). Offshore renewable energy resources and their potential in a green hydrogen supply chain through power-to-gas. *Sustainable Energy Fuels*, *3*, 1468–1489. https://doi.org/10.1039/C8SE00544C

González, J. S., Payán, M. B., Santos, J. R., & Rodríguez, Á. G. G. (2015). Maximizing the overall production of wind farms by setting the individual operating point of wind turbines. *Renewable Energy*, *80*, 219–229. https://doi.org/10.1016/j.renene.2015.02.009

Grigoriev, S., Fateev, V., Bessarabov, D., & Millet, P. (2020). Current status, research trends, and challenges in water electrolysis science and technology. *International Journal of Hydrogen Energy*, *45*(49), 26036–26058. https://doi.org/https://doi.org/10.1016/j.ijhydene.2020.03.109

Groenemans, H., Saur, G., Mittelsteadt, C., Lattimer, J., & Xu, H. (2022). Techno-economic analysis of offshore wind pem water electrolysis for h2 production. *Current Opinion in Chemical Engineering*, *37*, 100828. https://doi.org/10.1016/J.COCHE.2022.100828

Harrison, K. W., Martin, G. D., Ramsden, T. G., Kramer, W. E., & Novachek, F. J. (2009). *The wind-to-hydrogen project: Operational experience, performance testing, and systems integration*. http://www.osti.gov/bridge

Hayashi, Y. (2013). High power density rectifier for highly efficient future dc distribution system. *Electrical Engineering Publishing Company*, *1*, 49.

Hofmann, M. (2011). *A review of decision support models for offshore wind farms with an emphasis on operation and maintenance strategies* (1). www.nowitech.no

Holst, M., Aschbrenner, S., Smolinka, T., Voglstätter, C., & Grimm, G. (2021). *Cost forecast for low-temperature electrolysis – technology driven bottom-up prognosis for pem and alkaline water electrolysis systems* (Study) [Commissioned by Clean Air Task Force]. Fraunhofer Institute for Solar Energy Systems ISE. Freiburg, Germany.

Hu, K., Fang, J., Ai, X., Huang, D., Zhong, Z., Yang, X., & Wang, L. (2022). Comparative study of alkaline water electrolysis, proton exchange membrane water electrolysis and solid oxide electrolysis through multiphysics modeling. *Applied Energy*, *312*, 118788. https://doi.org/10.1016/j.apenergy.2022.118788

Hur, S. H. (2021). Reliable and cost-effective wind farm control strategy for offshore wind turbines. *Renewable Energy*, *163*, 1265–1276. https://doi.org/10.1016/j.renene.2020.09.049

Ibrahim, O. S., Singlitico, A., Proskovics, R., McDonagh, S., Desmond, C., & Murphy, J. D. (2022). Dedicated large-scale floating offshore wind to hydrogen: Assessing design variables in proposed typologies. *Renewable and Sustainable Energy Reviews*, *160*. https://doi.org/10.1016/J.RSER.2022.112310

IEA. (2019). *The future of hydrogen: Seizing today's opportunities* [Report prepared for the G20, Japan]. International Energy Agency. Paris, France. https://www.iea.org/reports/the-future-of-hydrogen

IEA. (2021). Iea wind annual report 2021. https://iea-wind.org/wp-content/uploads/2022/12/IEA_Wind_TCP_Annual_Report_2021.pdf

IEA. (2022a). Co2 emissions in 2022 - report. https://iea.blob.core.windows.net/assets/3c8fa115-35c4-4474-b237-1b00424c8844/CO2Emissionsin2022.pdf

IEA. (2022b). *Global hydrogen review 2022*. www.iea.org/t&c/

IEA. (2022c). *Renewables 2022*. https://www.iea.org/reports/renewables-2022

International Renewable Energy Agency (IRENA). (2020). *Green hydrogen cost reduction: Scaling up electrolysers to meet the 1.5°c climate goal* [Supervised by Dolf Gielen and Roland Roesch. Authors: Emanuele Taibi, Herib Blanco, Raul Miranda, Marcelo Carmo. Edited by Jonathan Gorvett. Supported by the German Federal Ministry for Economic Affairs and Energy (BMWI) and the Ministry of Economy, Trade and Industry (METI) of Japan.]. International Renewable Energy Agency. https://www.irena.org/publications

Ioannou, A., Angus, A., & Brennan, F. (2018). Parametric capex, opex, and lcoe expressions for offshore wind farms based on global deployment parameters. *Energy Sources, Part B: Economics, Planning and Policy*, *13*, 281–290. https://doi.org/10.1080/15567249.2018.1461150

IPCC. (2022). *Climate change 2022: Mitigation of climate change. contribution of working group iii to the sixth assessment report of the intergovernmental panel on climate change* (P. Shukla, J. Skea, R. Slade, A. A. Khourdajie, R. van Diemen, D. McCollum, M. Pathak, S. Some, P. Vyas, R.

Fradera, M. Belkacemi, A. Hasija, G. Lisboa, S. Luz, & J. Malley, Eds.). Cambridge University Press. https://doi.org/10.1017/9781009157926

IRENA, I. R. E. A. (2023). Hydrogen [Accessed: October 13, 2023]. https://www.irena.org/Energy-Transition/Technology/Hydrogen

Jepma, C., Kok, G.-J., Renz, M., Schot, M. V., & Wouters, K. (2018). *Towards sustainable energy production on the north sea-green hydrogen production and co2 storage: Onshore or offshore?*

Kaa, G. V. D., Ek, M. V., Kamp, L. M., & Rezaei, J. (2020). Wind turbine technology battles: Gearbox versus direct drive-opening up the black box of technology characteristics. https://doi.org/10.1016/j.techfore.2020.119933

Katsavounis, S., Konstantinidis, E. I., Botsaris, P., Katsavounis, S., Patsianis, ; N., Konstantinidis, ; E. I., & Botsaris, ; P. N. (2014). Reliability analysis on crucial subsystems of a wind turbine through fta approach. https://doi.org/10.13140/2.1.2524.3849

Khan, M. A., Al-Attas, T., Roy, S., Rahman, M. M., Ghaffour, N., Thangadurai, V., Larter, S., Hu, J., Ajayan, P. M., & Kibria, M. G. (2021). Seawater electrolysis for hydrogen production: A solution looking for a problem? *Energy and Environmental Science*, *14*, 4831–4839. https://doi.org/10.1039/d1ee00870f

Khan, M., Daiyan, R., Han, Z., Hablutzel, M., Haque, N., Amal, R., & MacGill, I. (2021). Designing optimal integrated electricity supply configurations for renewable hydrogen generation in australia. *iScience*, *24*, 102539. https://doi.org/10.1016/j.isci.2021.102539

Khan, M. H. A., Heywood, P., Kuswara, A., Daiyan, R., MacGill, I., & Amal, R. (2022). An integrated framework of open-source tools for designing and evaluating green hydrogen production opportunities. *Communications Earth & Environment 2022 3:1*, *3*, 1–18. https://doi.org/10.1038/s43247-022-00640-1

Khatib, F. N., Wilberforce, T., Ijaodola, O., Ogungbemi, E., El-Hassan, Z., Durrant, A., Thompson, J., & Olabi, A. G. (2019). Material degradation of components in polymer electrolyte membrane (pem)electrolytic cell and mitigation mechanisms: A review. *Renewable and Sustainable Energy Reviews*, *111*, 1–14. https://doi.org/10.1016/J.RSER.2019.05.007

Kim, J., Park, K., Yang, D. R., & Hong, S. (2019). A comprehensive review of energy consumption of seawater reverse osmosis desalination plants. *Applied Energy*, *254*, 113652. https://doi.org/10.1016/j.apenergy.2019.113652

Klutke, G. A., Kiessler, P. C., & Wortman, M. A. (2003). A critical look at the bathtub curve. *IEEE Transactions on Reliability*, *52*, 125–129. https://doi.org/10.1109/TR.2002.804492

Kumar, S., & Lim, H. (2022). An overview of water electrolysis technologies for green hydrogen production [Open Access under a Creative Commons license]. *Energy Reports*, *8*, 13793–13813. https://doi.org/10.1016/j.egyr.2022.10.127

Kumar, S., Baalisampang, T., Arzaghi, E., Garaniya, V., Abbassi, R., & Salehi, F. (2022). Synergy of green hydrogen sector with offshore industries: Opportunities and challenges for a safe and sustainable hydrogen economy. *Journal of Cleaner Production*. https://doi.org/https://doi.org/10.1016/j.jclepro.2022.135545

Lagerveld, S., Röckmann, C., Scholl, M., Bartelings, H., Burg, S. V. D., Jak, R., Jansen, H., Klijnstra, J., Leopold, M., Poelman, M., Smith, S., Stavenuiter, J., Veenstra, F., Veltman, C., & Westra, C. (2014). Combining offshore wind energy and large-scale mussel farming: Background & technical, ecological and economic considerations. www.imares.wur.nl

Lange, H., Klose, A., Lippmann, W., & Urbas, L. (2023). Technical evaluation of the flexibility of water electrolysis systems to increase energy flexibility: A review. *International Journal of Hydrogen Energy*. https://doi.org/10.1016/j.ijhydene.2023.01.044

Lee, H., Lee, B., Byun, M., & Lim, H. (2020). Economic and environmental analysis for pem water electrolysis based on replacement moment and renewable electricity resources. *Energy Conversion and Management*, *224*. https://doi.org/10.1016/J.ENCONMAN.2020.113477

Lettenmeier, P. (2021). *Efficiency – electrolysis* [White paper]. Siemens Energy. https://siemens-energy.com/electrolyzer

Lopez, A. M., Williams, M., Paiva, M., Demydov, D., Do, T. D., Fairey, J. L., Lin, Y. J., & Hestekin, J. A. (2017). Potential of electrodialytic techniques in brackish desalination and recovery of industrial process water for reuse. *Elsevier*. https://www.sciencedirect.com/science/article/pii/S0011916416310463

Lucas, T. R., Ferreira, A. F., Pereira, R. B. S., & Alves, M. (2022). Hydrogen production from the windfloat atlantic offshore wind farm: A techno-economic analysis. *Applied Energy*, *310*. https://doi.org/10.1016/J.APENERGY.2021.118481

Luengo, M. M., & Kolios, A. (2015). Failure mode identification and end of life scenarios of offshore wind turbines: A review. https://doi.org/10.3390/en8088339

Martin, R., Lazakis, I., Barbouchi, S., & Johanning, L. (2016). Sensitivity analysis of offshore wind farm operation and maintenance cost and availability. *Renewable Energy*, *85*, 1226–1236. https://doi.org/10.1016/j.renene.2015.07.078

Martinez Lopez, V. A., Ziar, H., Haverkort, J. W., Zeman, M., & Isabella, O. (2023). Dynamic operation of water electrolyzers: A review for applications in photovoltaic systems integration [Open Access]. *Renewable and Sustainable Energy Reviews*, *182*, 113407. https://doi.org/10.1016/j.rser.2023.113407

McDonagh, S., Ahmed, S., Desmond, C., & Murphy, J. D. (2020). Hydrogen from offshore wind: Investor perspective on the profitability of a hybrid system including for curtailment [Under a Creative Commons license, open access]. *Applied Energy*. https://doi.org/10.1016/j.apenergy.2020.114732

Mehta, M., Zaaijer, M., & Terzi, D. V. (2022). Optimum turbine design for hydrogen production from offshore wind. *Journal of Physics: Conference Series*. https://doi.org/10.1088/1742-6596/2265/4/042061

Meier, K. (2014). Hydrogen production with sea water electrolysis using norwegian offshore wind energy potentials: Techno-economic assessment for an offshore-based hydrogen production approach with state-of-the-art technology. *International Journal of Energy and Environmental Engineering*, *5*, 1–12. https://doi.org/10.1007/S40095-014-0104-6

Miao, B., Giordano, L., & Chan, S. H. (2021). Long-distance renewable hydrogen transmission via cables and pipelines. *International Journal of Hydrogen Energy*, *46*, 18699–18718. https://doi.org/10.1016/J.IJHYDENE.2021.03.067

Moriarty, P., Hamilton, N., Debnath, M., Herges, T., Isom, B., Lundquist, J. K., Maniaci, D., Naughton, B., Pauly, R., Roadman, J., Shaw, W., van Dam, J., & Wharton, S. (2020). *American wake experiment (awaken)* [Available at no cost from the National Renewable Energy Laboratory (NREL) at www.nrel.gov/publications.]. National Renewable Energy Laboratory. Golden, CO.

Naimo, A. (2014). A novel approach to generate synthetic wind data [Selection and peer-review under responsibility of AIRO]. *Procedia - Social and Behavioral Sciences*, *108*, 187–196. https://doi.org/10.1016/j.sbspro.2013.12.830

North Sea Wind Power Hub. (2022). *Grid-integrated offshore power-to-gas: A feasibility review and discussion of power grid-integrated offshore power-to-gas*.

OREDA participants. (2015). *OREDA Handbook* (6th). Offshore Reliability Data (OREDA).

Papadias, D. D., Peng, J.-K., & Ahluwalia, R. K. (2021). Hydrogen carriers: Production, transmission, decomposition, and storage. *International Journal of Hydrogen Energy*, *46*(47), 24169–24189.

Pham, H., & Wang, H. (1996). Imperfect maintenance. *European Journal of Operational Research*, *94*, 425–438. https://doi.org/10.1016/S0377-2217(96)00099-9

Philippo, T. (2023). The impact of power management strategies and module sizing for offshore wind turbine integrated electrolysis.

Pillay, A., & Wang, J. (2003). Modified failure mode and effects analysis using approximate reasoning. *Reliability Engineering & System Safety*, *79*, 69–85. https://doi.org/10.1016/S0951-8320(02)00179-5

Rahman, S., Khan, I., Alkhammash, H. I., & Nadeem, M. F. (2021). A comparison review transmission mode for onshore integration of offshore wind farms: Hvdc or hvac—a comparison review. *Electronics (Switzerland)*, *10*. https://doi.org/10.3390/electronics10121489

Raine, D. (2022). *Reducing hydrogen project costs through standardization*.

Ren, Z., Verma, A. S., Li, Y., Teuwen, J. J., & Jiang, Z. (2021). Offshore wind turbine operations and maintenance: A state-of-the-art review. *Renewable and Sustainable Energy Reviews*, *144*. https://doi.org/10.1016/J.RSER.2021.110886

Reuß, M., Grube, T., Robinius, M., Preuster, P., Wasserscheid, P., & Stolten, D. (2017). Seasonal storage and alternative carriers: A flexible hydrogen supply chain model. *Applied Energy*, *200*, 290–302. https://doi.org/10.1016/J.APENERGY.2017.05.050

Rijksoverheid. (2022). *Offshore wind energy* [Accessed: 2023-10-13]. https://www.government.nl/topics/renewable-energy/offshore-wind-energy

Rinaldi, G., Thies, P. R., Walker, R., & Johanning, L. (2017). A decision support model to optimise the operation and maintenance strategies of an offshore renewable energy farm. *Ocean Engineering*, *145*, 250–262. https://doi.org/10.1016/j.oceaneng.2017.08.019

Rinaldi, G. (2018). *An integrated operation and maintenance framework for offshore renewable energy*.

Rinaldi, G., Garcia-Teruel, A., Jeffrey, H., Thies, P. R., & Johanning, L. (2021). Incorporating stochastic operation and maintenance models into the techno-economic analysis of floating offshore wind farms. *Applied Energy*, *301*. https://doi.org/10.1016/j.apenergy.2021.117420

Röckmann, C., Lagerveld, S., & Stavenuiter, J. (2017). Operation and maintenance costs of offshore wind farms and potential multi-use platforms in the dutch north sea. *Aquaculture Perspective of Multi-Use Sites in the Open Ocean: The Untapped Potential for Marine Resources in the Anthropocene*, 97–113. https://doi.org/10.1007/978-3-319-51159-7_4

Rogelj, J., den Elzen, M., Höhne, N., et al. (2016). Paris agreement climate proposals need a boost to keep warming well below 2°c. *Nature*, *534*, 631–639. https://doi.org/https://doi.org/10.1038/nature18307

RVO. (2021). *Hydrogen sector study france hydrogen in france, developments and opportunities for the netherlands*.

Safder, U., Ifaei, P., Nam, K., Rashidi, J., & Yoo, C. (2018). Availability and reliability analysis of integrated reverse osmosis – forward osmosis desalination network [Received 19 December 2017; Accepted 20 January 2018]. *Desalination and Water Treatment*, *109*, 1–7. https://doi.org/10.5004/dwt.2018.22147

Sawyer, T. Y. (2009). *Operating and capital expenditures models*. Apress. https://doi.org/10.1007/978-1-4302-1899-9_9

Schnuelle, C., Wassermann, T., Fuhrlaender, D., & Zondervan, E. (2020). Dynamic hydrogen production from pv & wind direct electricity supply – modeling and techno-economic assessment. *International Journal of Hydrogen Energy*, *45*(55), 29938–29952. https://doi.org/10.1016/j.ijhydene.2020.08.044

Scolaro, M., & Kittner, N. (2022). Optimizing hybrid offshore wind farms for cost-competitive hydrogen production in germany. *International Journal of Hydrogen Energy*, *47*(10), 6478–6493. https://doi.org/10.1016/j.ijhydene.2021.12.062

Sens, L., Neuling, U., & Kaltschmitt, M. (2022). Capital expenditure and levelized cost of electricity of photovoltaic plants and wind turbines – development by 2050. *Renewable Energy*, *185*, 525–537. https://doi.org/10.1016/j.renene.2021.12.042

Serna, Á., Yahyaoui, I., Normey-Rico, J. E., de Prada, C., & Tadeo, F. (2017). Predictive control for hydrogen production by electrolysis in an offshore platform using renewable energies. *International Journal of Hydrogen Energy*, *42*(17), 12865–12876. https://doi.org/https://doi.org/10.1016/j.ijhydene.2016.11.077

Shafiee, M., Brennan, F., & Espinosa, I. A. (2016). A parametric whole life cost model for offshore wind farms. *International Journal of Life Cycle Assessment*, *21*, 961–975. https://doi.org/10.1007/s11367-016-1075-z

Shaw, R. (2009). *Reliability overview*.

Sheng, S., & O'Connor, R. (2017). Reliability of wind turbines. *Wind Energy Engineering: A Handbook for Onshore and Offshore Wind Turbines*, 299–327. https://doi.org/10.1016/B978-0-12-809451-8.00015-1

Shields, M., Beiter, P., & Nunemaker, J. (2022). *A systematic framework for projecting the future cost of offshore wind energy* (Technical Report NREL/TP-5000-81819). National Renewable Energy Laboratory. www.nrel.gov/publications

Shin, H., Jang, D., Lee, S., Cho, H.-S., Kim, K.-H., & Kang, S. (2023). Techno-economic evaluation of green hydrogen production with low-temperature water electrolysis technologies directly coupled with renewable power sources. *Energy Conversion and Management*, *286*, 117083. https://doi.org/10.1016/j.enconman.2023.117083

Shiva Kumar, S., & Himabindu, V. (2019). Hydrogen production by pem water electrolysis – a review [Under a Creative Commons license, open access]. *Materials Science for Energy Technologies*, *2*(3), 442–454. https://doi.org/https://doi.org/10.1016/j.mset.2019.03.002

Shokri, A., & Fard, M. S. (2023). Techno-economic assessment of water desalination: Future outlooks and challenges. *Process Safety and Environmental Protection*, *169*, 564–578. https://doi.org/10.1016/j.psep.2022.11.007

Singlitico, A., Østergaard, J., & Chatzivasileiadis, S. (2021). Onshore, offshore or in-turbine electrolysis? techno-economic overview of alternative integration designs for green hydrogen production into offshore wind power hubs. *Renewable and Sustainable Energy Transition*, *1*, 100005. https://doi.org/10.1016/J.RSET.2021.100005

Smith, N. J. P., Evans, D. J., & Andrews, I. J. (2005). *The geology of gas storage in offshore salt caverns* (tech. rep. GC05/11) [Report to the Department of Trade and Industry, October 2005]. Marine, Coastal and Hydrocarbons Programme, British Geological Survey.

Smolinka, T. (2023). *Cost forecast for low temperature electrolysis technology driven bottom-up prognosis for pem and alkaline water electrolysis systems*. Fraunhofer Institute for Solar Energy Systems ISE.

Sørensen, J. N., Larsen, G. C., & Cazin-Bourguignon, A. (2021). Production and cost assessment of offshore wind power in the north sea. *Journal of Physics: Conference Series*, *1934*, 012019. https://doi.org/10.1088/1742-6596/1934/1/012019

Stehly, T., Beiter, P., & Duffy, P. (2019). *2019 cost of wind energy review*. www.nrel.gov/publications.

Suzuki, K., Tonien, D., Kurosawa, K., & Toyota, K. (2006). Birthday paradox for multi-collisions. In M. S. Rhee & B. Lee (Eds.), *Information security and cryptology - icisc 2006*. Springer, Berlin, Heidelberg. https://doi.org/10.1007/11927587_5

Taieb, A., & Shaaban, M. (2019). Cost analysis of electricity transmission from offshore wind farm by hvdc and hydrogen pipeline systems. *2019 IEEE PES GTD Grand International Conference and Exposition Asia (GTD Asia)*, 632–636. https://doi.org/10.1109/GTDASIA.2019.8715900

TNO. (2022). *Profitability offshore wind in 2030 not self-evident* [Accessed: 2023-10-13]. https://www.tno.nl/en/newsroom/2022/11/profitability-offshore-wind-2030-self/

Tsiklios, C., Hermesmann, M., & Müller, T. E. (2022). Hydrogen transport in large-scale transmission pipeline networks: Thermodynamic and environmental assessment of repurposed and new pipeline configurations. *Applied Energy*, *327*. https://doi.org/10.1016/j.apenergy.2022.120097

Tsotridis, G., & Pilenga, A. (2021). *Eu harmonised protocols for testing of low temperature water electrolysers* (Technical Report EUR 30752 EN). Joint Research Centre (JRC), European Commission. Westerduinweg, 3 1755 LE Petten, The Netherlands. https://doi.org/10.2760/58880

UN. (2015). *The paris agreement*.

van Cappellen, L., Croezen, H., & Rooijers, F. (2018). Feasibility study into blue hydrogen: Technical, economic & sustainability analysis.

Wang, R., Ge, T., Ma, Q., Liu, X., Xia, J., Zhang, Y., & Zhou, G. (2017). Recent progress and perspectives of space air conditioning: Technologies and applications. *Applied Energy*, *188*, 770–789. https://www.sciencedirect.com/science/article/pii/S1364032116305366

Wiggelinkhuizen, E., Verbruggen, T., Braam, H., Rademakers, L., Xiang, J., & Watson, S. (2008). Assessment of condition monitoring techniques for offshore wind farms. *Journal of Solar Energy Engineering, Transactions of the ASME*, *130*, 0310041–0310049. https://doi.org/10.1115/1.2931512

Witkowski, A., Rusin, A., Majkut, M., & Stolecka, K. (2017). Comprehensive analysis of hydrogen compression and pipeline transportation from thermodynamics and safety aspects. *Energy*, *141*, 2508–2518. https://doi.org/10.1016/j.energy.2017.05.141

Woznicki, M., Le Solliec, G., & Loisel, R. (2020). Far off-shore wind energy-based hydrogen production: Technological assessment and market valuation designs [EERA DeepWind'2020, 15-17 January 2020, Radisson Blu Royal Garden Hotel, Trondheim, Norway]. *Journal of Physics: Conference Series*, *1669*, 012004. https://doi.org/10.1088/1742-6596/1669/1/012004

Yang, W., Tavner, P. J., Crabtree, C. J., Feng, Y., & Qiu, Y. (2014). Wind turbine condition monitoring: Technical and commercial challenges. *Wind Energy*, *17*, 673–693. https://doi.org/10.1002/we.1508

Yates, J., Daiyan, R., Patterson, R., Egan, R., Amal, R., Ho-Baille, A., & Chang, N. L. (2020). Techno-economic analysis of hydrogen electrolysis from off-grid stand-alone photovoltaics incorporating uncertainty analysis. *Cell Reports Physical Science*, *1*(10), 100209. https://doi.org/10.1016/j.xcrp.2020.100209

Yin, S., Tseng, K. J., Tong, C. F., Simanjorang, R., Gajanayake, C. J., & Gupta, A. K. (2016). A 99% efficiency sic three-phase inverter using synchronous rectification.

Zaaijer, M., Viré, A., Balbino, R., Santos, D., Amir, P., Andres, D., Fonseca, L., & Marquis, D. (2017). *Introduction to wind turbines: Physics and technology*.

A

Overview of LCOH estimates in literature

The meanings of the abbreviations in the table below are as follows:

- OW: energy produced by utilising Offshore Wind turbines
- PEM: hydrogen produced through the PEM electrolyser
- OC: Offshore Conversion occurs, indicating that power is converted to hydrogen offshore
- DE: the W2H systems are in a Decentralised Configuration

Where the text in the cells indicate either a '✓' for "Yes" and a '✘' for "No".

Table A.1: Overview of W2H systems LCOH's from literature

Year	LCOH [€/kg H_2]	Scope	OW	PEM	OC	DC	REF
2018	3.5 - 9.1	Production of hydrogen from offshore wind by energy ships or sailing wind turbines	✓	✘	✓	✓	Babarit et al.
2019	3.23	Production of hydrogen from a hybrid energy system integrating wind and solar with a power-to-gas facility	✘	✓	✘	✘	Glenk and Reichel-stein
2020	4	Production of hydrogen from an offshore windfarm located in Germany	✓	✓	✘	✘	McDonagh et al.
2020	11.01 - 11.61	Techno-economic assessment of dynamic hydrogen production using PV and wind electricity for electrolyzers in northwest Germany	✘	✓	✘	✘	Schnuelle et al.
2020	6.88	Technological and market assessment of hydrogen production using far off-shore wind energy	✓	✓	✓	✘	Woznicki et al.

Table A.1 – Continued from previous page

Year	LCOH [€/kg H_2]	Scope	OW	PEM	OC	DE	REF
2021	2.48 - 6.16	Evaluation of different pathways to produce and transport hydrogen or hydrogen carriers from offshore to shore	✓	✓	✓	✘	Franco et al.
2021	5.35	Production of hydrogen from a hybrid energy system integrating offshore wind	✓	✓	✓	✘	Singlitico et al.
2021	5	Production of compressed hydrogen from a hypothetical offshore wind farm considering the size of the storage tank and decommissioning expenditure	✓	✓	✓	✘	Dinh et al.
2021	4.63	Production of compressed hydrogen from a hypothetical offshore wind farm considering the size of the storage tank and decommissioning expenditure	✘	✘	✘	✘	Papadias et al.
2022	4.25 - 8.25	Production of hydrogen and oxygen from the WindFloat Atlantic offshore wind farm	✓	✓	✓	✘	Lucas et al.
2022	4.9	Production of hydrogen from an offshore wind farm located in North Germany	✓	✓	✘	✘	Scolaro and Kittner
2022	2.09	Techno-economic analysis of offshore wind-driven PEM water electrolysis for hydrogen production, including cost comparisons and system design evaluations	✓	✓	✓	✓	Groenemans et al.
2023	8.45	Techno-economic assessment of offshore wind-to-hydrogen production scenarios in the UK, evaluating hydrogen production, storage, and transport options	✓	✓	✓	✘	Giampieri et al.
2023	13.81	Analysing green hydrogen production via renewable energy-linked alkaline and PEM electrolysis systems	✓	✓	✘	✘	Shin et al.
2023	4.53 - 5.18	Green H2 production from real world wind data and various configuration sizes including with and without battery	✓	✓	✓	✓	Egeland-Eriksen et al.

Note: this analysis of these several academic works is not with 100% certainty, as some assumptions are not explicitly named but have been estimated by the author of this research.

B

Overview of offshore hydrogen projects

Table B.1: Table of (offshore) hydrogen projects

Project title	Scope	Scale	Exp. date
Aberdeen Bay – Vattenfall (Uk)	Offshore wind to hydrogen demo at Vattenfall's wind farm in Aberdeen Bay, with an 8MW offshore hydrogen electrolyser.	8 MW	2025
Aker Offshore Wind/ Northern Horizons	Targeting offshore wind projects and the potential to reuse existing facilities at the Valhall oil field for power and energy islands, potentially for hydrogen or ammonia production.	5 GW	2030
Amphytrite	Feasibility study of AmpHytrite – a centralized offshore wind production project for green hydrogen, with a demonstrator planned for Port of Rotterdam	1 MW	2023
Aquasector	Large-scale offshore hydrogen park in the German North Sea	300 MW pilot, 10 GW scaled up	2028 (pilot), 2035 (full scale)
Aquaventus	Plans to install 10GW of offshore wind-based hydrogen electrolysis in the German North Sea, with AquaDuctus pipeline for transport.	10 GW	2035
Asturias	Naturgy and Enagas's feasibility study for green hydrogen production from floating wind power off the coast of Asturias, Spain.	150 MW	2026
Atlantic Shores	Developing 10 offshore wind facilities and a pilot for green hydrogen production using excess electricity in New Jersey, USA. Shell	1.5 GW	2032
Avedøre/H2Res	Ørsted and partners are constructing a 2MW electrolysis plant powered by wind turbines at Avedøre, Denmark.	2MW	2022

Continued on next page

Table B.1 – *Continued from previous page*

Project title	Scope	Scale	Exp. date
Bantry Bay Green Energy Facility	A joint venture between Zenith Energy and EI-H2 to develop a 3.2 GW energy offshore wind facility at Bantry Bay in Ireland to produce green hydrogen and green ammonia.	3.2 GW	2028
Belgian Offshore Platform	Tractebel (Engie) is developing a 400MW offshore platform for converting offshore wind power into green hydrogen in Belgium.	400MW	2028
Base Load Power Hub	Shell and Eneco's Hollandse Kust (noord) project with technology demonstrations including 'green hydrogen' production.	Not specified	Not specified
Deep Purple	TechnipFMC's concept for stable power to offshore installations using large-scale hydrogen storage, including offshore hydrogen production and storage for ports.	10 MW	2025
Dolphyn (Uk)	Production of hydrogen at scale from offshore floating wind in deep water locations.	1 GW (pilot) - 10 GW (full scale)	2025 - 2030
Donghae 1	Plans for a floating offshore wind farm including a green hydrogen plant in Korea's East Sea.	200 MW (wind), 100 MW (hydrogen)	2024 (wind), 2025 (hydrogen)
Esbjerg Offshore Wind-To-Hydrogen Project	Project will be commissioned in Denmark by Swiss energy company H2 Energy Europe, the second large-scale Power-to-X plant in Esbjerg region.	1 GW	2027
Gigastack Project	Ørsted and ITM Power's project to demonstrate bulk, low-cost, zero-carbon hydrogen integrated with offshore wind.	100 MW	2025
Green Ammonia	Ørsted and Yara's project to use green hydrogen for ammonia production, potentially operational by 2024/2025.	100 MW	2025
Green Energy Hub	Shell, MHI, Vattenfall, and Wärme Hamburg planning to produce hydrogen from wind and solar power at Hamburg-Moorburg, Germany.	320 MW	2026
Green Fuels For Denmark	A project in Copenhagen for hydrogen production with initial 10MW electrolyser, scaling to 1.3 GW facility.	10 MW - 1.3 GW	2023 (initial) - 2030 (scaled up)
H2Mare	German governments project to couple offshore wind turbines with electrolyzers for hydrogen and other power-to-X processes.	5 GW	2030
H2Opzee	Neptune Energy and RWE's project to build 300-500 MW electrolyser capacity in the North Sea for green hydrogen production.	400 MW	2030
H2Sea	HSM Offshore Energy and Enersea's project for offshore hydrogen development with platform concepts ranging from 50 to 400 MW.	50 to 400 MW	2028

Continued on next page

Table B.1 – *Continued from previous page*

Project title	Scope	Scale	Exp. date
Hydrogen Fpso	Korean consortium's proposal for a floating offshore plant using wind power to produce hydrogen, aiming for a full-scale unit by 2030.	1 MW (pilot) - 1 GW (full scale)]	2023 (pilot) - 2030 (full scale)
Lhyfe And Centrale Nantes - Sem-Rev	The world's first offshore green hydrogen production facility. The plant is powered by electricity from a nearby floating wind turbine, called Floatgen to be installed at the SEM-REV demonstration site, off the coast of Le Croisic in France.	50 MW	2024
Liivi Bay	Eesti Energia's 960MW Liivi Bay offshore wind project in Estonia, considering hydrogen production.	960MW	2030
Mid West Wind And Solar Project	A 1,100MW offshore wind project in Western Australia by Pilot Energy, focused on renewable hydrogen production.	1.1 GW	2030
Moneypoint	Joint project by Irish energy company and Equinor for a 1.4 GW floating offshore wind farm with potential hydrogen production.	1.4 GW	2030
North Of Scotland Hydrogen Scheme	Iberdrola's project with ScottishPower and UK distilleries for a green hydrogen hub in the Highlands, using electrolyzers powered by clean energy.	1 GW	2030
North Sea Port Hydrogen Plant	Ørsted plans a wind farm and adjacent 1-gigawatt hydrogen plant at the North Sea Port on the Dutch-Belgian border.	1GW	Not specified
North Sea Wind Power Hub	Concept for connecting wind farms and supplying power around the North Sea, with electricity conversion to hydrogen.	Not specified	2050
North2	Shell and Gasunie's project for green hydrogen from up to 10GW of offshore wind in the North Sea, Netherlands.	Up to 10GW	2027 (initial phase)
Oyster (Uk)	Development of a desalination, electrolysis, and hydrogen production system that is completely "marinized," or modified for marine use.	10 MW	2024
Poshydon	Three different energy systems will be integrated on one platform: offshore wind, offshore gas, and hydrogen. On a platform located 13 km from Scheveningen, the electrolysis system will be installed within a sea container.	1 MW (pilot) - 100 MW (full scale)	2025
Project Haldane	Lhyfe, Aquaterra Energy, and Borr Drilling developing offshore green hydrogen production in the North Sea.	1 GW	2027 (initial phase)
Holland Hydrogen One	Shell's development with Worley for a 200 MW electrolysis-based hydrogen plant in Rotterdam, Netherlands, powered by offshore wind.	200 MW	2025

Continued on next page

Table B.1 – *Continued from previous page*

Project title	Scope	Scale	Exp. date
Siemens Hydrogen Pilot	Siemens Gamesa is working on a wind-to-hydrogen project in Denmark with a 3 MW turbine and a GHS electrolyser.	3MW	2024
South Korean Offshore Project	Hyundai Heavy Industries' project with partners for a 1.2 GW green hydrogen plant in the Sea of Japan, powered by offshore wind.	1.2 GW	2028
The Agnes Project	Saipem's co-development in Italy for a wind farm with hydrogen production, including 620 MW of wind and solar.	50 MW	2023
The Salamander Project	A collaboration that uses the ERM DOLPHYN design in a location off Aberdeenshire.	100 MW	2028
Westküste 100	Aims to kick-start regional hydrogen economy in Schleswig-Holstein, Germany, producing green hydrogen from offshore wind energy.	30MW initially, 700MW planned	2020 (initial phase) ...

C

Wind turbine specifics

Table C.1: Characteristics for the IEA 15-MW Wind Turbine

Parameter	Units	Value
Power rating	MW	15
Turbine class	-	IEC Class 1B
Specific rating	W/m^2	332
Rotor orientation	-	Upwind
Number of blades	-	3
Control	-	Variable Speed Collective pitch
Cut-in wind speed	m/s	3
Rated wind speed	m/s	10.59
Cut-out wind speed	m/s	25
Design tip-speed ratio	-	9.0
Minimum rotor speed	rpm	5.0
Maximum rotor speed	rpm	7.56
Maximum tip speed	m/s	95
Rotor diameter	m	240
Airfoil series	-	FFA-W3
Hub height	m	150
Hub diameter	m	7.94
Hub overhang	m	11.35
Rotor precone angle	deg	-4.0
Blade prebend	m	4
Blade mass	t	65
Drivetrain	-	Direct drive
Shaft tilt angle	deg	6
Rotor nacelle assembly mass	t	1,017
Transition piece height	m	15
Monopile embedment depth	m	45
Monopile base diameter	m	10
Tower mass	t	860
Monopile mass	t	1,318

D

Electrolyser technology comparison

Table D.1: Comparison between an AEL electrolyser and a PEM electrolyser, adapted from Buttler and Spliethoff (2018) and Ibrahim et al. (2022)

Parameter	Unit	AEL	PEM
Operation parameters			
Cell temperature	°C	60-90	50-80
Typical pressure	bar	10-30	20-50
Current density	A/cm^2	0.25-0.45	1.0-2.0
Flexibility			
Load flexibility	% of nominal load	20-100	0-100
Cold start-up time	min	60-120	5-10
Warm start-up time	min	1-5	0.2
Efficiency			
Nominal stack efficiency (LHV)	%	63-71	60-68
... specific energy consumption	kWh/Nm^3	4.2-4.8	4.4-5.0
Nominal system efficiency (LHV)	%	51-60	46-60
... specific energy consumption	kWh/Nm^3	5.0-5.9	5.0-6.5
Available capacity			
Max. nominal power per stack	MW	6	2
H2 production per stack	Nm^3/h	1400	400
Cell area	m^2	<3.6	<0.13
Footprint	m^2/GW	95,000	48,000
Durability			
Life time	1,000 h	55-120	60-100
Efficiency degradation	%/year	0.25-1.5	0.5-2.5
Economic parameters			
CapEx	€/kW	800-1500	1400-2100
OpEx	% of CapEx	2-3	3-5

E

RAM model logic

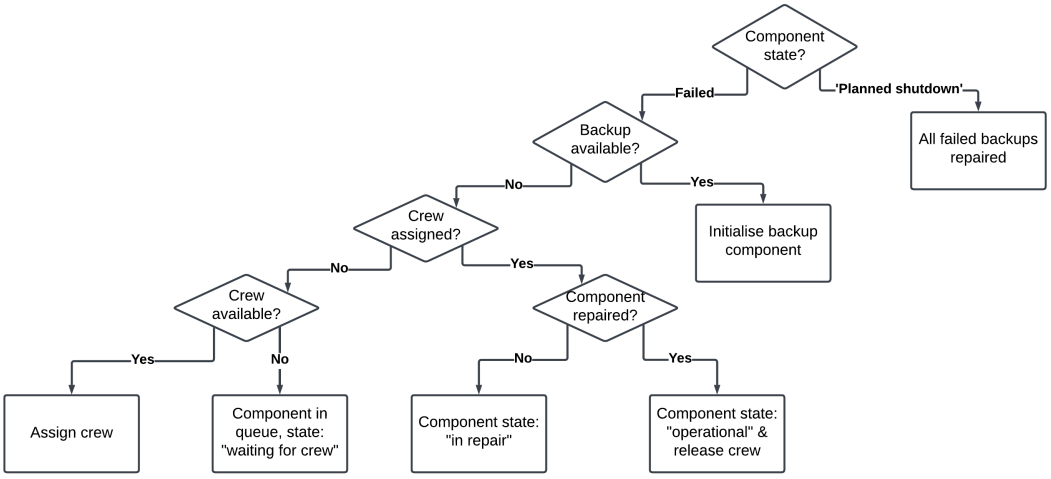

Figure E.1: Logic flow chart for the component part of the RAM model

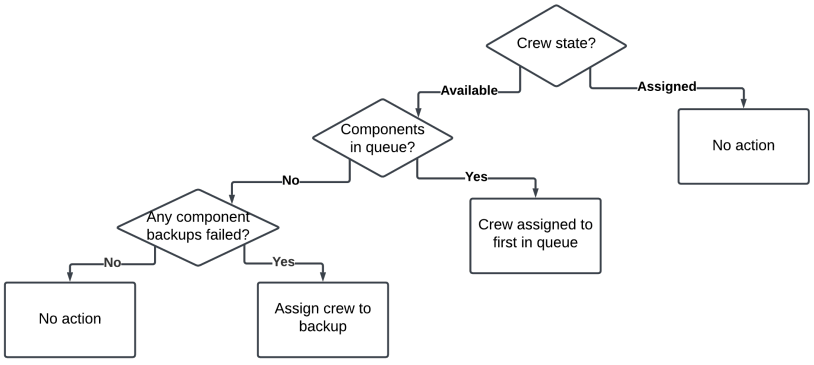

Figure E.2: Logic flow chart for the crew part of the RAM model

F

Other results

LCOH breakdown

This is the breakdown of the LCOH originating from the techno-economic calculating while not including RAM effects.

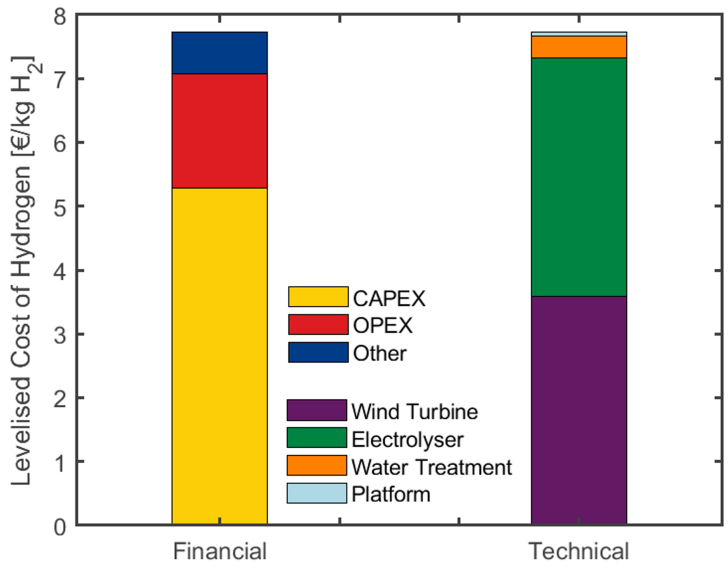

Figure F.1: LCOH breakdown into financial (left) and technical (right) components

Single system results

In Figure F.2, the LCOH as a function of the varying discount rate is shown. In this thesis, a discount rate of 7% was applied.

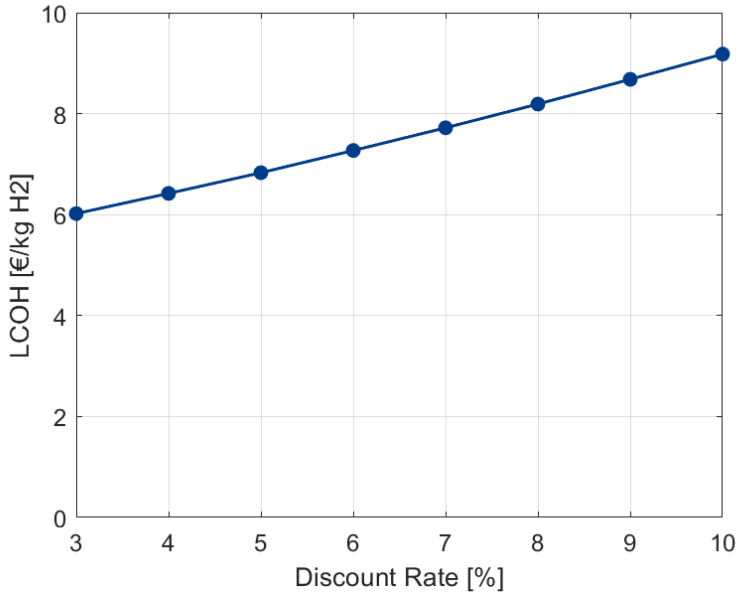

Figure F.2: LCOH as a function of the discount rate

RAM sensitivities

For the figures in this section, a consistent format is applied, which includes calculating the system availability for different RAM variables. This availability is then plotted on the y-axis in the figures, with dots indicating measurements and connecting lines enhancing readability. The variable being altered is shown on the x-axis. Additionally, the LCOH is plotted on the y-axis alongside availability. This represents the resulting LCOH when the optimal figure of €7.72 is multiplied by the availability to yield a consequential LCOH. Since a lower LCOH is typically desirable, it is found higher up on the y-axis, corresponding to greater availability. It should also be noted that the spacing between the LCOH figures is not proportional to the axis, so these should be viewed as indicative.

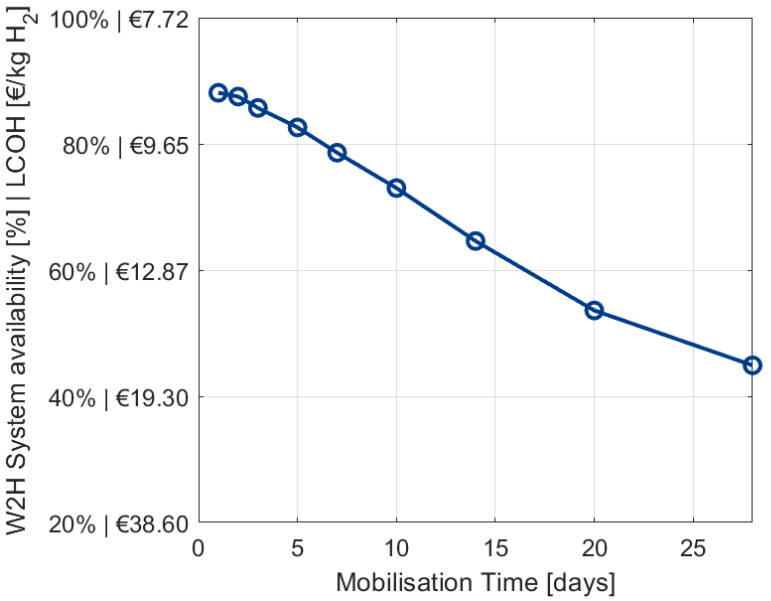

Figure F.3: Single W2H system availability (and LCOH) as a function of maintenance crew mobilisation time

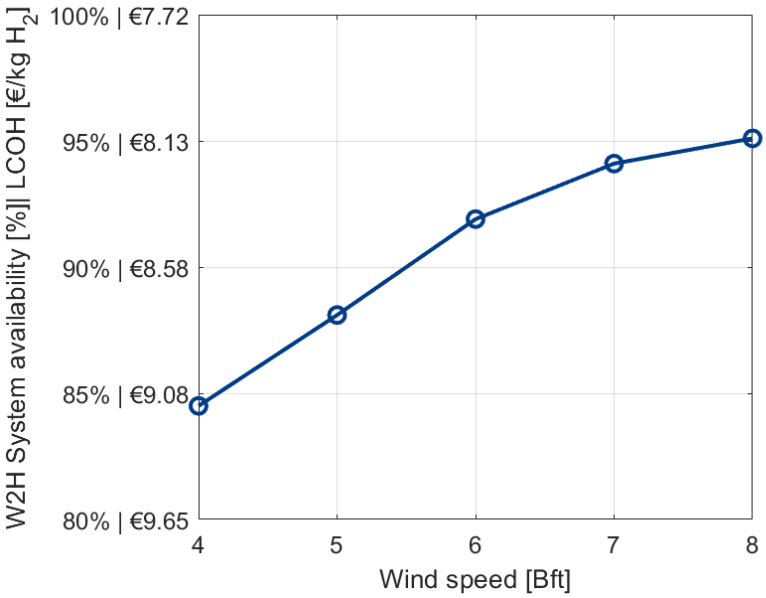

Figure F.4: Single W2H system availability (and LCOH) as a function of the maintenance crew's maximum wind speed working conditions

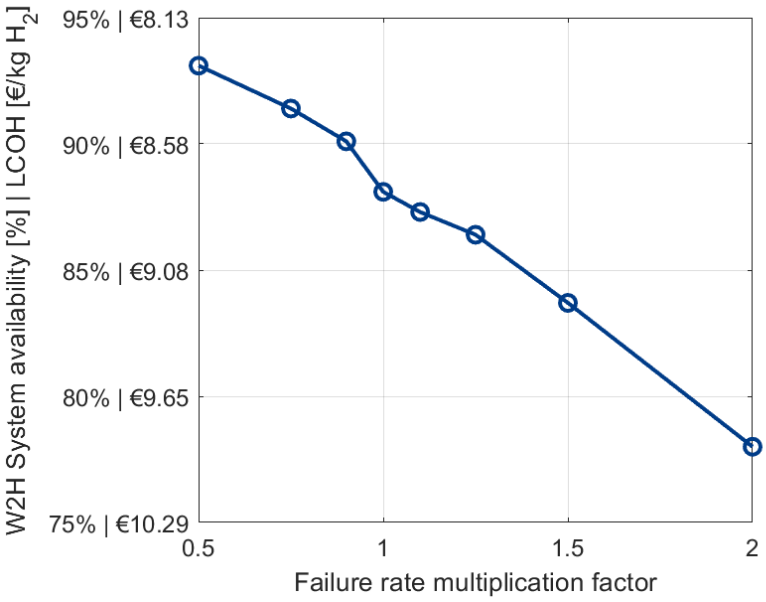

Figure F.5: Single W2H system availability (and LCOH) as a function of a failure rate multiplication factor

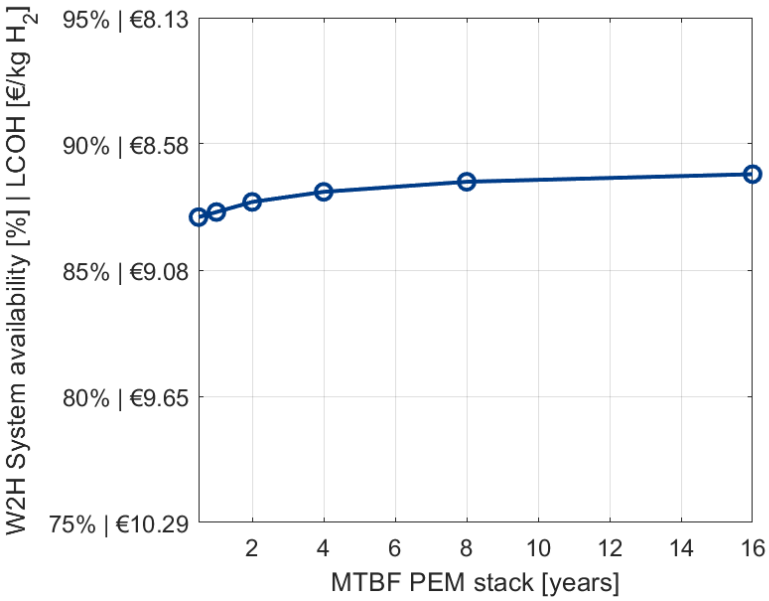

Figure F.6: Single W2H-system availability (and LCOH) as a function of the Mean Time Between Failure (MTBF) for the PEM electrolyser

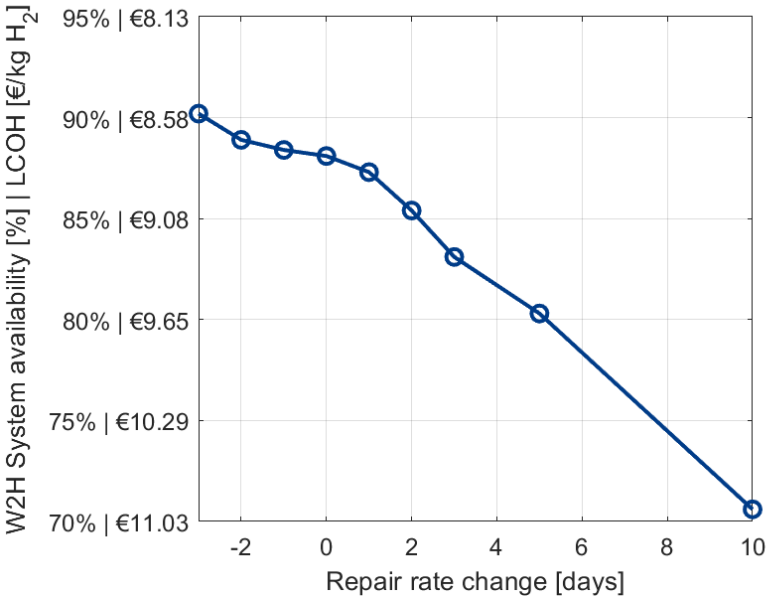

Figure F.7: Single W2H-system availability (and LCOH) as a function of the changing repair rate

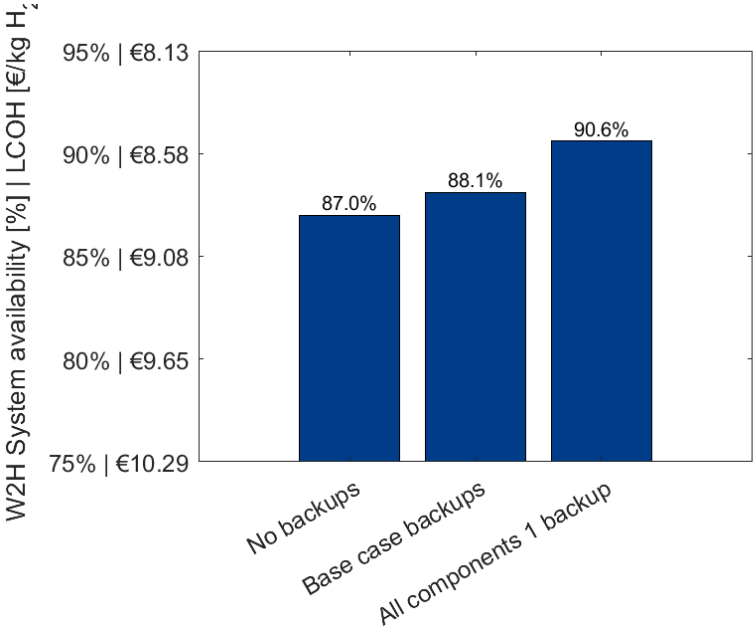

Figure F.8: Single W2H-system availability (and LCOH) for different back-up configuration scenarios

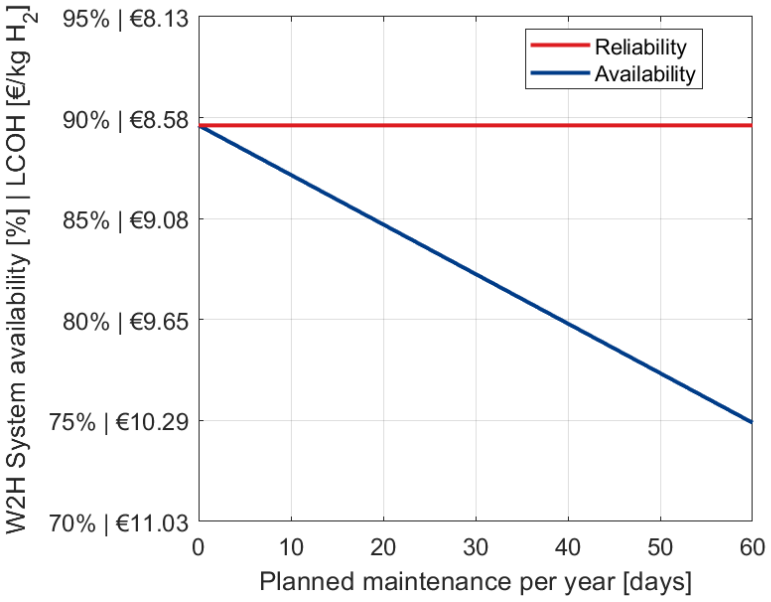

Figure F.9: Single W2H-system availability (and LCOH) as a function of the total yearly planned maintenance days

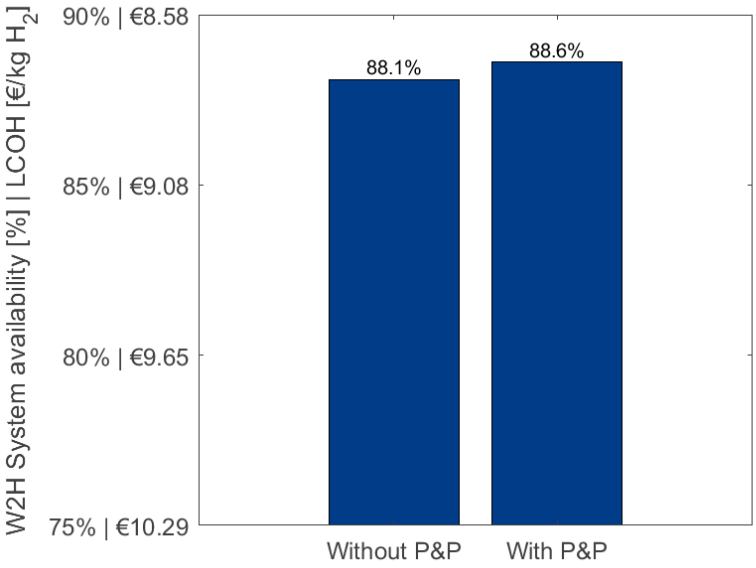

Figure F.10: Single W2H-system availability (and LCOH) for a plug&play versus the non plug&play scenario